NASA TECHNICAL TRANSLATION

NASA TT F-393

C.1

NASA TT F-393

THE FIRST PANORAMIC VIEWS OF THE LUNAR SURFACE

Izdatel'stvo "Nauka",
Moscow, 1966

NATIONAL AERONAUTICS AND SPACE ADMINISTRATION • WASHINGTON, D. C. • OCTOBER 1966

NASA TT F-393

THE FIRST PANORAMIC VIEWS OF THE LUNAR SURFACE

Presidium of the USSR
Academy of Sciences

Translation of "Pervyye panoramy lunnoy poverkhnosti"
Izdatel'stvo "Nauka," Moscow, 1966

NATIONAL AERONAUTICS AND SPACE ADMINISTRATION

For sale by the Clearinghouse for Federal Scientific and Technical Information
Springfield, Virginia 22151 – Price $3.00

CONTENTS

PREFACE

The soft landing of the Luna 9 automatic station[1] on the surface of the Moon was an outstanding scientific and engineering achievement. For the first time it was possible to investigate the microstructure of the lunar surface and to distinguish details measured in millimeters.

Soviet astronautics has progressed greatly. On 4 October 1957, the flight of the first artificial Earth satellite opened the era of space investigation, and on 12 April 1961, Man flew in space for the first time. Three lunar rockets solved new problems in 1959. The first artificial planet of the solar system was constructed, the magnetic field and cosmic rays were measured at great distances from Earth, the surface of the Moon was reached and the magnetic field and radiation patterns near the Moon were investigated, and a part of the side of the Moon never visible from Earth was photographed. Later, in 1965, the automatic interplanetary station Zond 3 photographed the remaining uninvestigated part of the far side of the Moon. Finally, on 3 February 1966, Luna 9 made a soft landing.

The panoramic photographs transmitted by Luna 9 provide material for direct scientific conclusions concerning the structure of the lunar surface. There is no noticeable layer of dust close to the station, which is inside a small crater. The ground is sufficiently hard to bear the weight of the station. On the surface there are linear structures, formed by a substance apparently stronger than the surrounding rock. Furthermore, near the station numerous individual stones can be seen which are not only free of dust, but seem to "grow" out of the surface of the soil as a result of its gradual disintegration.

Launching Luna 9 and achieving a soft landing on the Moon are the result of a great amount of work by Soviet scientists, engineers and the workers in production and experimental organizations who participated in this work.

In this book the USSR Academy of Sciences publishes panoramic photographs of Luna 9, reproduced with documented precision, the preliminary results of their processing and a description of the experiment itself. This has been done both to familiarize readers with this new and great success in the field of the conquest of space and to provide Soviet and foreign scientists with all possibilities for utilizing the data obtained here for the progress of science.

Presidium of the USSR Academy of Sciences

---

[1]Throughout this translation the Russian terminology "Luna 9 automatic station" is abbreviated to "Luna 9."

PART I. DESCRIPTION OF APPARATUS AND FLIGHT CONDITIONS

Introduction

The Moon's proximity to Earth and its many years of observations, carried out by many methods, have permitted Man to study it in more detail than any other planet. /9*

At the same time, a series of factors limit the possibilities for studying the Moon by terrestrial means. The well-known peculiarities of its movement around the Earth make 41 percent of the Moon's surface completely inaccessible to terrestrial observers.

The Earth's atmosphere, which interferes with optical observations and limits the resolving power of modern telescopes and radio apparatus, sets a limit to possibilities for studying the physical characteristics of our natural satellite and its surface from the Earth. Photographic and visual observations conducted with the aid of telescopes cannot distinguish details less than 300-500 m across on the surface of the Moon. Nevertheless, it has been possible to establish the pitted microrelief of both the maria and the highland regions by photometric analysis.

Investigation of lunar infrared radiation indicates a great temperature drop from day to night and extremely low heat conductivity of the surface layer, which can be explained only by low density and porosity. Radar investigations provide evidence that the lunar surface is quite smooth for centimeter and decimeter band waves, the irregularities, comparable with wavelength, occupying a small part of the area and having gentle slopes. Radioastronomic investigations made it possible to obtain thermophysical and dielectric characteristics of lunar rocks, averaged over sections measured in hundreds of kilometers; they indicate significant porosity of the external rock layer. Different authors estimate the dimensions of the particles composing this porous mass by various methods over wide limits. There is no information on the chemical composition of the external layer of the Moon and only very scanty data on processes taking place in it. /10

The flights of the American Ranger space vehicles made an important contribution to the study of the lunar surface. Up to the time of impact on the Moon's surface, each of them sent several thousand pictures to the Earth, which made it possible for the first time to obtain reliable information on details of the relief, measuring on the order of one meter. However, even

---

*Numbers given in margin indicate pagination in original foreign text.

these observations did not provide data on the microstructure and strength of the lunar surface.

The lack of information hampered the solution of a number of technical problems connected with soft landing on the Moon by spacecraft.

In particular, due to lack of knowledge of the lunar ground, it was necessary to design the Luna 9 to accommodate its landing on ground with the most varied characteristics--from dust to rock.

Another difficulty was the lack of atmosphere on the Moon. It was therefore necessary to orient the rocket with high accuracy relative to the lunar vertical before landing, and then to decelerate it with the aid of retro-rockets. In this case the speed had to be reduced from 2.6 km/sec to a few meters per second.

To achieve soft landing, the automatic station had to descend to the lunar surface in a precisely preassigned region. This required correcting the trajectory.

This part of the work provides a brief description of the lunar rocket, Luna 9 and its television system, and sets forth the basic principles of the dynamics and guidance of the flight, together with a log of the flight and the performance of the station.

CHAPTER 1. DESIGN AND ONBOARD SYSTEMS

1. The Lunar Rocket

The lunar rocket was designed to take the Luna 9 to the Moon and to ensure the station's soft landing on the lunar surface. /11

The composition of the instruments on board and the design of the lunar rocket were determined by the objectives to be achieved by the rocket and station from the time of entering the flight trajectory to the Moon up to completing transmission of the televised image of the lunar landscape and the results of scientific measurements.

These objectives were

--determining true flight trajectory after completion of the operation of the last stage of the launching rocket, determining flight adjustment data based on measurements of the flight trajectory (taken from Earth) and transmitting them to the rocket for correction;

--obtaining telemetric information on the functioning of the systems from the rocket and, if necessary, changing the mode of operation of these systems by radio command;

--correcting the trajectory, in which the rocket is oriented in space with high accuracy, activating the rocket apparatus, stabilizing the rocket during engine operation, switching it off after correction and restoring the necessary orientation in space;

--determining the true flight trajectory after correction, calculating /12 flight adjustment data on Earth and transmitting them to the rocket in order to achieve deceleration near the surface of the Moon;

--decelerating and landing on the surface of the Moon;

--ensuring two-way radio communication with Luna 9 after landing and transmission to Earth of televised images of the lunar landscape and the microrelief of the surface, as well as results of scientific measurements.

To solve these problems the following complex of systems was developed for the lunar rocket: the engine system, the orientation system, the radiotelemetry system, the engine control system and the system for stabilizing the rocket

during engine operation, the radioaltimeter, the antenna and feeder system, the thermoregulatory system, the power supply and onboard automatic devices.

Design of the lunar rocket

The design system of the lunar rocket and design realizations for its individual systems and equipment were selected on the basis of the need for ensuring maximum reliability of a soft landing, while retaining a lunar station of the greatest possible weight.

The lunar rocket (fig. 1) consists of the Luna 9 automatic station (ALS) 1, the engine system, the control system compartment 2 and various instruments 3 and 4, installed on the rocket body.

To reduce fuel consumption for deceleration near the Moon and, consequently, achieve the maximum weight of Luna 9, all equipment and units needed only for flight to the Moon were installed in compartments which would be separated before deceleration. The expediency of this procedure is obvious, since a considerable amount of fuel would be required for full deceleration.

To ensure minimum weight of the compartments to be jettisoned, their sealed hulls were designed for a pressure drop of only 100 mm Hg. On the ground, before launching, the compartment pressure is close to that of the atmosphere. After launching, the pressure in both compartments drops as the /13
rocket rises, due to a valve especially opened for this purpose. When the pressure reaches 100 mm Hg, the valves close, and this pressure is maintained for the rest of the flight. At this time, the pressure ensures adequate heat transfer from the instruments to the container walls.

Pressure is far higher, about 1.2 atm, in Luna 9 and in the control system compartment, where more intense heat transfer from the operating units by convective heat exchange is required.

The engine system of the lunar rocket consists of a liquid-propellant rocket engine 5, control engines 6 and fuel tanks.

The tank unit of the engine system consists of a spherical tank 7 containing the oxidizer and a toroidal fuel tank 8 of aluminum alloy. Designing the tanks in this form offered minimum weight of the engine system and minimum moments of inertia for the entire lunar rocket.

Two operations are required to land on the Moon: correction of trajectory and deceleration near the surface with the aid of the retrorocket. The lunar station reaches maximum weight when trajectory correction and deceleration are performed by the retrorocket arrangement.

The engine and the fuel delivery system ensure double activation during weightlessness and two modes of operation--correction with constant thrust and deceleration with a wide range of thrust control. Low-thrust rocket engines serve as control engines. These engines are intended to set up controlling moments, while maintaining the given orientation of the rocket in space.

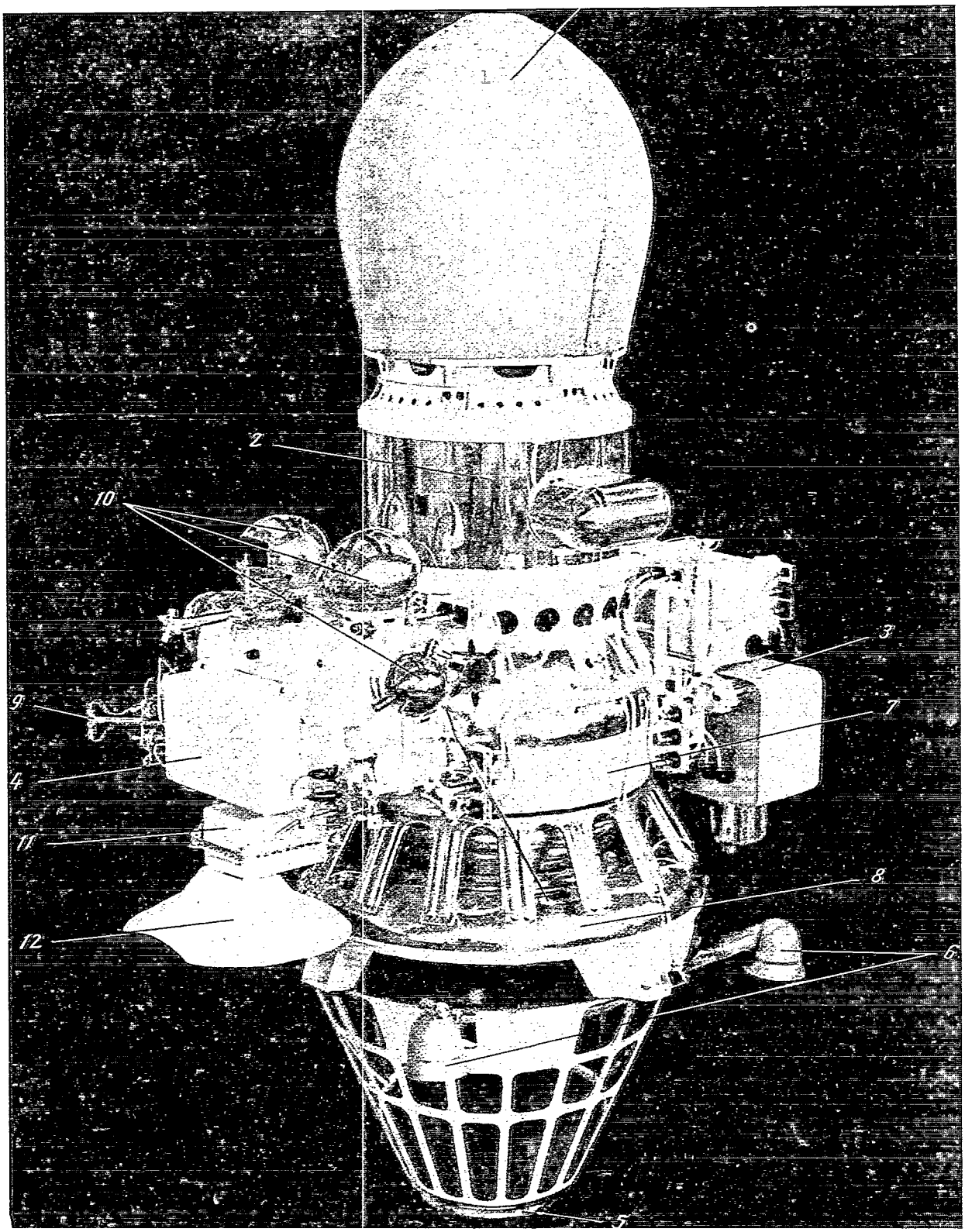

Figure 1. Lunar rocket

The spherical oxidizer tank 7 of the engine system is the principal structural power unit of the entire lunar rocket. The engine and all systems are installed on this tank. This will permit the adjustment of the directions of their mutual installation with an accuracy up to several minutes of the arc and retention of this accuracy during the entire flight, despite fluctuations of pressure in the tank due to temperature changes.

Moreover, this design minimizes the number of structural connecting elements and, consequently, provides a decrease in the weight of the Moon rocket.

Systems in the lunar rocket

The orientation system is intended to orient the engine in the direction given from Earth when effecting the correction and for alignment along the lunar vertical before decelerating near the Moon. The orientation system /14 consists of an optical unit, angular velocity sensors and computers.

The actuating devices of the orientation systems consist of microengines 9, operating with compressed gas, and gas cylinders 10. The radioaltimeter 11 has its own highly directional parabolic antenna 12.

As previously stated, the celestial orientation system provides the rocket the preassigned position before the engine starts correction and deceleration. The celestial orientation system is switched off when the command to switch on the engine is given. Later, throughout the period of engine operation, rocket control and stabilization are ensured by a special system consisting of gyroscopic devices. There is also a device for regulating engine thrust during deceleration.

Thermal control of the rocket and of all other systems is ensured during flight to the Moon by imparting specific optical properties to the structural elements. This is achieved by painting with suitable colors and by establishing a specific rotation mode of the rocket relative to the Sun.

During flight, the rocket is controlled both by radio command from Earth and by time-programmed and logic devices on board. Control of these processes, fundamental for delivery of the station to the Moon and functioning quite rapidly, e.g., for such maneuvers as correction and deceleration, is conducted autonomously. Only the initial data for these processes are supplied from Earth, because they depend on the parameters of the actual trajectory. On the other hand, control of many processes (in particular, all radio communication periods during flight intended for changes in the trajectory, transmission of telemetered information and reception of adjusting data on the rocket) is carried out by command from Earth. In a number of cases (e.g., radio communication sessions after landing) control may be achieved either by command from Earth or by programmed devices on board.

The radiotelemetry systems of the lunar rocket and the Luna 9 ensure not only transmission of scientific information, but also control over operation of the equipment and the state of various structural elements.

Temperature and pressure are measured in all sealed compartments. Temperature is also measured at different points of the shell and inside many /15
instruments. Power supply voltages are controlled directly, as are transformed voltages from different converters. Telemetered signals are also transmitted to confirm performance of various operations, such as opening of antennas, separation of various parts and the operation of mechanisms.

Such painstaking testing of the entire apparatus (in particular Luna 9 itself) was essential, because one of the most important scientific objectives of the experiment was to study the functioning of the equipment under the entirely new and complex conditions on the Moon. For example, soil temperatures in the vicinity of the station would vary during its operation by 150° as the elevation of the Sun increased.

Electric power is supplied to the rocket and Luna 9 by chemical batteries. This type system is more advantageous with respect to weight for operating 3-5 days than a power supply dependent on solar batteries. In addition, it is simpler and more reliable, which is particularly important for the first experiment of landing on the Moon.

Most electrical power sources are in the jettisoned compartments, and only those sources which ensure operation of the equipment for the decelerating stage of the flight and operation of the automatic station after landing were installed in control system compartment 2 and in Luna 9, respectively.

2. Luna 9

The basic systems of Luna 9 are in a hermetically sealed container of almost spherical shape. The body of the lunar station consists of two half-shells.

The frame with the receiving and transmitting apparatus, the instruments of the radio command circuits, the electronic time-programmed devices, the chemical batteries and the instruments belonging to the automatic, scientific and telemetry apparatus is installed inside the body. The blower, electric valve and radiator for the heat control system are installed in the lower half-shell, and the television system and cosmic ray particle counters are in the upper one.

Figure 2 shows four lobe antennas 1, four rod antennas 2 with brightness standards 3 suspended from them, and three dihedral mirrors 4 are mounted /16
externally on the body. The lobe and rod antennas and the mirrors remain folded during landing. The dihedral mirrors transmit stereoscopic images of six narrow sections of the lunar surface, and the brightness standards, having different colors with known reflection coefficients, are designed to estimate the albedo of lunar rocks in the vicinity of the landing.

The lunar station and landing devices are fastened to the control system compartment of the rocket.

The folded lobe antennas give Luna 9 an egg-shaped form; its center of gravity is closer to the base. Due to this, the station takes a certain position on the lunar surface (lobes up) after separation of the landing devices. The lobes also protect the television camera, the rod antennas, the mechanisms and the mirrors from accidental dust and damage.

The mechanism for opening the lobes is triggered about 4 min after landing, on command from a time programmed device or from a clockwork (the command for opening the lobes can also be given from Earth). When the lobe antennas open, the station itself, the rod antennas and the mirrors are placed into the operating position.

The weight of Luna 9 after landing corresponded to 100 kg. wt on Earth.

Station dimensions are: from the base to the center of the lens of the television camera - 58 cm, height with rod antennas included - 112 cm and the diameter of the circle described by the opened lobes - 160 cm.

During flight and after landing, until the time Luna 9 is in operating position, the folded lobes serve as the receiving and transmitting antennas in the meter range. The shape of the lobes was selected so that the radiation pattern of the antenna system would be almost circular.

After landing, when the station is in operating position, the opened lobes serve only as transmitting antennas, and four rod antennas, which open out after the lobes open, are used as receiving antennas. This scheme for arranging and utilizing antennas ensures communication with the station after landing, if the lobes fail to open for some reason or if the station does not assume a normal position on the Moon.

To maintain the temperature state of the station after landing, the temperature control was selected to insulate the station as much as possible /17
from external heat fluxes and to conduct the heat liberated by the instruments to the outside. Special heat insulation on the body protected Luna 9 from heat fluxes radiated by the lunar surface and the Sun.

The temperature control consists of radiators (small water tanks) and an automatic unit, a blower and an electrically operated valve.

The blower ensures heat transfer from the instruments to a gas and from the gas to the radiators. The automatic unit issues commands for opening or closing the electrovalve in accordance with the actual gas temperature. When the valve is opened, the tanks are connected with the external medium and water is evaporated into the vacuum, which ensures removal of heat from the radiators, and the temperatures of the gas and the instruments are then reduced. When the valve is closed, water evaporation and heat removal to the outside cease.

The temperature control system can function normally with the station in any position relative to the Moon. The external surface of the camera is gilded to maintain the thermal regime of the television camera, which protrudes beyond the sealed body of the station. This excludes heating of the camera by

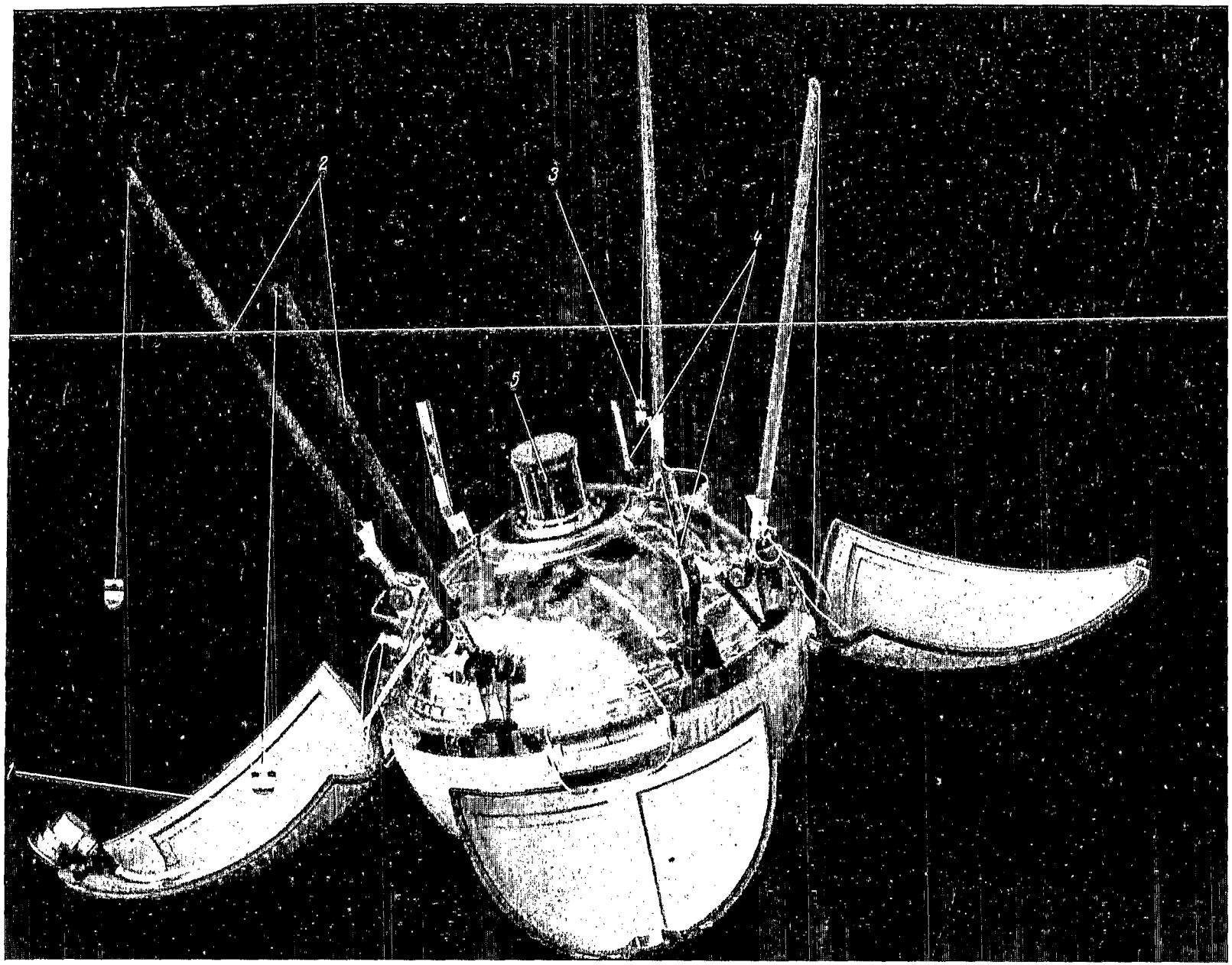

Figure 2. Luna 9 automatic station

lunar surface radiation and by the Sun. In addition, a heat-insulating screen was installed to prevent sunlight from directly striking the upper part of the television camera.

3. Television System

The image of the lunar landscape was transmitted from Luna 9 by a special panoramic television camera installed in the center of the upper part of the station.

As an object for television transmission, the lunar panorama is distinguished by a number of special features which had to be taken into account when the camera was developed.

A characteristic feature of the lunar landscape is its immobility. Only the shadows from irregularities on the surface change in length, depending on the height of the Sun, but this takes place comparatively slowly, as the lunar day lasts almost 15 Earth days. Thus, the altitude of the Sun changes only 0.5° per hour. Thus, practically speaking, a fixed image is transmitted.

Lighting conditions on the Moon are well known, for in the absence of an atmosphere the incident flux of sunlight reaches the lunar surface without /18 absorption. However, the wide range of possible brightness of details on the Moon's surface, the lack of knowledge of the characteristics of light reflection, determined by the microrelief, and the possibility of the station landing in different surroundings create considerable uncertainty. Furthermore, the light flux reflected from the surface of the Moon strongly depends on the altitude of the Sun and the direction of observation.

According to astronomical data, the characteristics of reflection of the Moon's surface (indicatrices of scattering) have a unique form, elongated in the direction of solar rays (fig. 3). Such indicatrices are characteristic of strongly pitted surfaces. They have been obtained by observing from Earth areas of the Moon's surface of considerable size--many kilometers. Although extension of these data to the microrelief, previously not investigated, seemed disputable, it was necessary to depend on them for orientation. The published materials obtained by the Ranger vehicles did not add any new information to this question.

When evaluating illumination, it was also necessary to consider instrument performance under the transitional conditions of the early lunar morning, when the Sun is very low. Moreover, we could not discount the possibility of the station landing in a depression on the lunar surface, where very low illumination could be expected.

The Luna 9 television camera is a mechanically scanned optical system the design of which is similar to that used in mechanical television or facsimile devices.

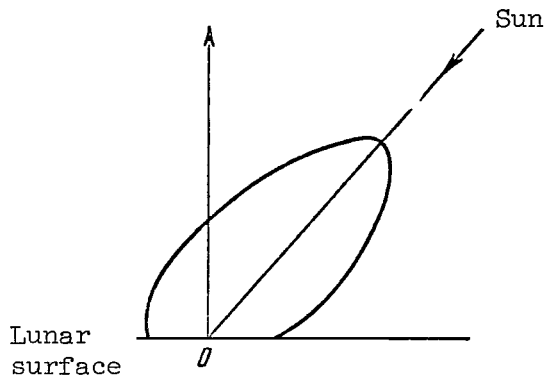

Figure 3. Indicatrix of light scattering by lunar surface from Earth observations.

This opticomechanical system for transmitting images from the surface of the Moon was selected after careful analysis and comparative tests of different systems for transmitting images. Unlike electronic television sys- /19
tems, the slow-acting opticomechanical system is not capable of transmitting a dynamic image. However, this fact is not a disadvantage.

When an image is transmitted slowly, the frequency band of the video signal is very narrow, and the signal can be transmitted through an economical radio communication channel, making use of low-power transmitters and nondirectional antennas on board.

It should be noted that the opticomechanical system best satisfies the rigid requirements in respect to weight, overall size, power consumption and operational reliability specified for the instrumentation of Luna 9.

Images are transmitted in this camera by a device consisting of mirror 1, cam 2 and objective lens 3 (fig. 4). The mirror here performs two types of motion: vertical rocking (line scanning) and slow rotation in the horizontal plane (panoramic scanning).

Both mirror displacements are accomplished by a motor 4, with a stabilized rotation rate. The profile of the cam, which causes the mirror to rock vertically, ensures linear angular displacement of the mirror during the period of line scanning and rapid return to its initial position in a time amounting to about 10 percent of the period. Use of a mechanical system yielded high, time-stable linearity of scanning and allowed the device to be used for measuring /20
purposes.

Selection of the magnitude of the vertical angle of view of the camera is a compromise between having the necessary resolution and ensuring a survey of a sufficiently large part of the surface. These factors and a series of additional considerations determined the choice of a vertical angle of view of about 29°. This angle was established asymmetrically to the plane perpendicular

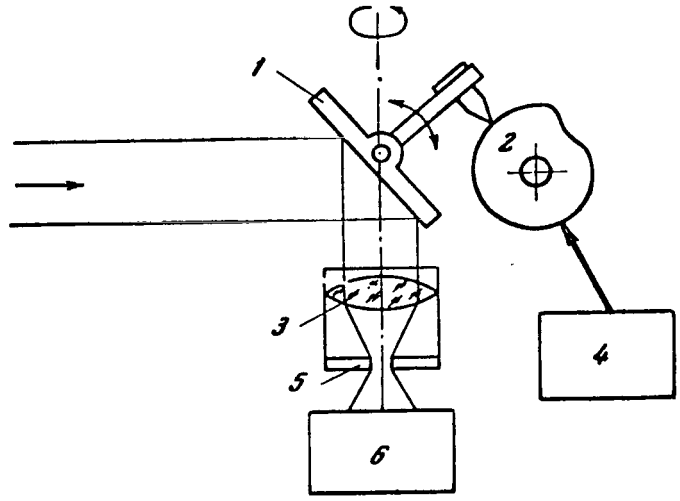

Figure 4. Television camera diagram.

to the axis of rotation of the camera (18° down, 11° up; fig. 5) primarily to ensure transmission of the image of the Moon's surface. With the selected vertical angle, a ratio of the sides of the circular panorama close to 1:12.5 was obtained.

A special feature of the station is a certain angle of inclination which was provided for in design. The base of the station and the mechanism of its antenna lobes were designed so that when the lobes are opened the axis of the station and, with it, the axis of the television camera are inclined approximately 16° to the local vertical, when the station stands on a sufficiently even horizontal surface. This ensures that one of the neighboring sections of the lunar surface falls within the field of view of the camera and creates favorable conditions for transmitting images of the microrelief at a minimum distance from the camera. This section, with maximum resolution of the surface, is located in the eastern sector of the lunar surface section observed from Luna 9.

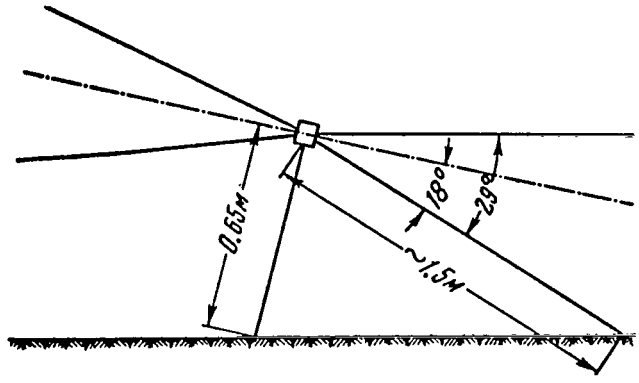

Figure 5. Field of view of television camera.

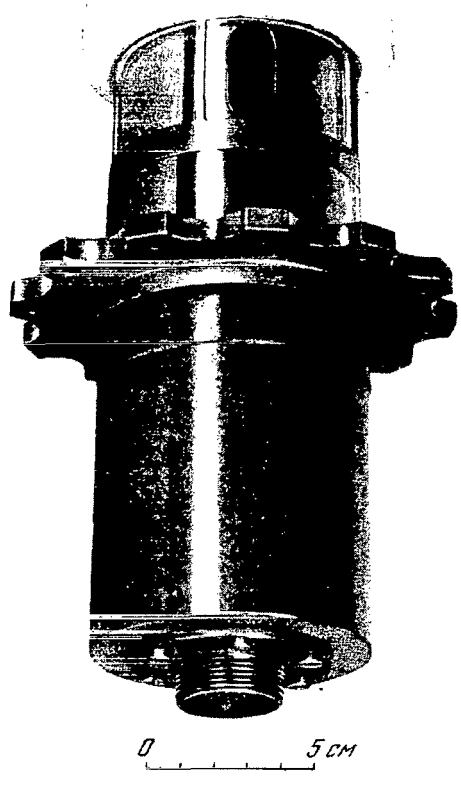

Figure 6. Television camera.

The pictures show that the selected vertical angle of view is close to optimal. The angle gives the necessary idea of the general structure of the landscape and ensures obtaining high-quality, well-defined pictures in which details of the microrelief measured in millimeters can be distinguished.

The Luna 9 television camera is made in the form of a small metal cyl- /21
inder with all essential units and assemblies located inside the cylinder (fig. 6). It is partially pressed down into the body of the station. Measures to ensure its thermal state have been discussed previously.

It was necessary to provide for flexible operational control of the camera for two reasons: the difficulty in making accurate and complete predictions of the camera's operating conditions on the Moon, and the limited power resources of Luna 9.

With this in mind, the camera was designed to operate in different modes on command from Earth.

The camera scanning mechanism provides for the following operating modes:

(1) image transmission at the rate of one line per second while scanning clockwise. Time for transmitting a complete panorama is 100 min;

(2) image transmission at the same rate while scanning in the opposite direction;

(3) accelerated mode of transmission with rapid rotation forward or reverse, the time required for a complete turn being about 20 min.

The availability of different operating modes allows for control of the instrument and examination of the most interesting places in the pictures with minimum loss of time. The third mode is an auxiliary one and is not intended for obtaining pictures, but for effective selection of the necessary sector of the panorama by observation of the video signal. This operating mode can also be switched on when there is transmission of telemetered information. In /22 this case there is generally no loss of time in selecting places in the panorama of interest to us. This property is of definite value.

As can be seen from the optical diagram of the camera (fig. 4), the light flux from the transmitted object strikes mirror 1, and passing through objective lens 3 to diaphragm 5 forms an element of the image.

The diaphragm dimensions determine the resolution of the instrument, which amounts to 500 elements per line in Luna 9, or approximately 0.06° per television element, which was checked during ground tests of the instrument by a special testing chart--a target with black and white lines. Errors in the mechanical scanning device did not exceed 1/3 of the television element. The camera distinguished details measuring 1.5-2 mm at a distance of 1.5 m. With the available relationship of the sides of the panorama for obtaining the same resolution in the line and vertical directions, 6000 lines are transmitted for each complete circular panorama.

When Luna 9 is oriented normally, the nearest sections of the lunar surface will be about 1.5 m from the camera. Thus, the camera objective was focused to ensure transmission of sharp images at distances from 1.5 m to infinity. As can be seen from the pictures obtained, even closer objects--structural elements of the lunar station itself--were transmitted with sufficient clarity.

After passing through the diaphragm located in the focal plane of the objective lens, the light flux from the object is registered by light receiver 6 (fig. 4), which converts it to an electrical signal. This signal, which is determined by the brightness of the object, undergoes a number of transformations, passes to the Luna 9 transmitter and is then transmitted to Earth.

Transmission was carried at a frequency of 183.538 Mc/sec by frequency modification of the radio signal. The degree of frequency modulation can be varied on Earth command for best adjustment of the communication channel.

Radio signals from Luna 9 were received by a special space communication center, where the video signal was separated and then recorded on photographic film and magnetic tape. The records on photographic film in the form of images of the panorama were produced on drum-type facsimile apparatus, in which one turn of the cylindrical drum on which the film was wound corresponded /23 to a line of the picture and displacement of the optical writing head along the drum corresponded to panoramic scanning.

Special devices ensured synchronous and in-phase operation of the recording apparatus on Earth and the television camera in Luna 9. Errors in recording (associated with geometric distortions and resolutions) were negligibly small when the image was received.

The uncertain light conditions for operation of the instrument made it necessary to develop a system for Automatic Sensitivity Control (ASC) for the camera. A photoresistor with a limiting diaphragm placed in front of it served as the sensor for the ASC system. The photoresistor is in the upper part of the opticomechanical scanning device and turns with it. It responds to the mean illumination in a field of view measuring $10^{\circ} \times 10^{\circ}$, approximately coinciding with the lower part of the panorama. The need to reduce exposure meter errors caused limitation of the field of view. The most important sources of these errors are the "black" lunar sky and flashes of sunlight.

Because the ASC system was adjusted under terrestrial conditions, which naturally differ from lunar conditions, provisions were made for controlling the operating mode of the ASC by command from Earth to eliminate possible mistakes and to enhance the reliability of the instrument. One command increases the instrument sensitivity relative to nominal sensitivity and the other reduces sensitivity.

The camera and the ASC system ensure transmission of good quality pictures with a range of illumination from 80 to 150,000 lux.

The ASC system has justified itself in practice. This can be seen from the pictures that were received, which are distinguished by uniform density over the entire panorama. At the same time, the influence of the properties of reflection of the strongly pitted surface is clearly noticeable in the darkening of sections located on the horizon as compared with the foreground.

While the Luna 9 camera was transmitting pictures, there was no need to interfere with the operation of the ASC system. Commands to increase sensitivity were transmitted for a limited time in the first session merely for experimental purposes--the section $\gamma = 69\text{-}133^{\circ}$, which was shaded with the Sun at an altitude of 7°, was transmitted in the first panorama with increased sensitivity.

CHAPTER 2. DYNAMICS AND FLIGHT CONTROL

1. Flight Trajectory

The overall flight plan consists of several basic stages. In the /24
first, the lunar rocket and booster stage are lifted to orbit close to the Earth by a carrier rocket. After engine shutdown the rocket circles the Earth as a satellite. The control system activates during orbit. The booster stage is activated at a predetermined time. At the end of the period when the rocket reaches required velocity, the engine is shut off and the lunar rocket is separated from the booster stage.

This begins free flight to the Moon. The missile-borne systems are guided by telemetry from the ground radio communication centers, which also measures the rocket flight parameters. Measured data are fed to computation centers, where parameters of the actual flight path are determined by mathematical processing of trajectory measurements.

The magnitude and direction of the correcting impulse are calculated after the flight path has been determined with a fair degree of accuracy. The lunar rocket control system is tuned by the command guidance system. The flight path is corrected at a predetermined time: the engine is activated and the flight parameters are changed.

Following the corrected flight path, the rocket hits the preselected area on the Moon. Measurements are made of the flight path after correction, and the actual flight parameters resulting from the correction are further /25
elaborated. The missile-borne control system is prepared for deceleration on approach to the Moon. The flight ends with deceleration of the rocket and landing of an automatic station on the lunar surface.

The design of the lunar rocket involved the solution of entirely new space problems: deceleration near the surface of the Moon and a soft landing. The use of retrorocket deceleration was, of course, obvious since there is no atmosphere on the Moon.

Analysis of different deceleration methods revealed that vertical deceleration was most reliable, and therefore preferable for the first experiment. In this case the relative velocity of the missile approaching the Moon had to be directed approximately to the center of the Moon. This made it possible to simplify the landing system.

Selection of the optimum flight trajectory based on energy considerations

The distance between Earth and Moon in its various positions in the orbit ranges from 360,000 to 407,000 km. A rocket in free flight can negotiate these distances, if its velocity on reaching flight trajectory to the Moon is above a certain minimum value.

If the velocity exceeds that limit, the rocket's trajectory will intersect a sphere extending from the center of the Earth with a radius equal to the distance to the Moon. A change in the starting time of the carrier rocket from Earth will shift the intersection point parallel to the plane of Earth's equator, because in this case the trajectory, as a rigid line, will rotate together with Earth around its axis. On the other hand, a change in the launch time, from the orbit of the artificial satellite, causes the trajectory to turn in the plane of this orbit. Here the point of intersection of the sphere by the trajectory is shifted along the arc of the great circle, forming angle i with the plane of the equator, which is equal to the angle of inclination of the artificial satellite's orbital plane to the equator.

Conditions required for landing a missile on the Moon can be achieved by selecting the starting time of the carrier rocket from Earth's surface and the starting time of the booster rocket from the satellite's orbit. In this way a trajectory with different flight times to the Moon can be achieved by changing the initial velocity. Selection of flight time is determined primarily on the basis of optimization of power consumption.

In the ordinary single-stage rocket the fuel consumption increases ex- /26
ponentially with increase in velocity v which the engine imparts to the rocket. In the case of multistage rocket systems, the correlation between initial and final weights is more difficult to define, but the space-flight difficulties related to power can always be estimated by the total velocity the engines must impart to the payload in all stages of the flight.

In the problem under consideration, the engines impart velocity to the rocket several times: when placing the artificial Earth satellite in orbit, leaving the orbit, correcting the trajectory and decelerating before landing.

Table 1 illustrates the corresponding velocities v at the beginning of free flight near Earth and deceleration v_D near the Moon depending on flying time T to the Moon.

TABLE 1.

T, 24-hr days	v, m/sec	v_D, m/sec	$\Delta d, \frac{km}{m/sec}$
2	10,995	2900	380
3	10,920	2625	1000
4	10,907	2540	1800

Both v and v_D increase with decreasing time of flight. If the flight correction did not have to be taken into account, the trajectory with the longest possible time of flight would require a minimum of fuel consumption. But the effect of the errors made when placing the missile in orbit increases with the increasing time of flight to the Moon. The misses of the mark near the Moon Δd produced by 1 m/sec error in the initial rocket velocity are shown in the last column of the table. Fuel consumed in the operation designed to correct the error committed when placing the rocket in its trajectory revealed that a trajectory involving a three to four day flight to the Moon is most profitable from the point of view of energy consumption.

The final selection of the flight path also considered the good visibility of the Moon from certain points in the Soviet Union during deceleration of the rocket and immediately after the landing of the station.

Lunar landing area and launch data

The trajectory of Luna 9 and the section of the lunar orbit are represented in a projection on the plane of Earth's equator in figure 7. The positions of the rocket and the Moon during the same instants of time are connected by dash lines. The latter coincide approximately with the direction in which the rocket approached the Moon, i.e., with the direction of relative velocity v_{rel}. At great distances from Earth the rocket is displaced approxi- /28

mately along a radius extending from the center of Earth. The angle formed by the relative velocity with this radius depends primarily on both rocket velocity v_r and velocity of the Moon v_m which is approximately 1 km/sec and is per-

pendicular to the radius extending from Earth to the approach point. However, rocket velocity v_r on the approach to the Moon's sphere of influence, where the

Moon's gravitational attraction is only beginning to be felt, is determined by initial velocity. For a trajectory with flight time to the Moon of about three and a half days, such velocity is ~ 0.5 km/sec. The relative approach velocity for such trajectories is therefore directed at an angle of about 60-70° to the Earth-rocket direction.

In almost vertical landing, the relative velocity vector on approach to the Moon should be directed approximately to the center of the Moon. Under such conditions the gravitational attraction of the Moon will change the relative velocity but will hardly affect the direction. Final approach to the Moon will therefore also take place at $\sim$ 60-70° angle to the Earth-Moon line.

It follows that for a trajectory involving a flight time to the Moon of about three and a half days, the almost vertical deceleration will form a 60-70° angle between the directions from the center of the Moon to the landing point and to Earth, i.e., an observer on Earth should see the landing point in the western part of the visible lunar disk. Depending on the position of the Moon in its orbit, as determined by its libration and orbital eccentricity, the

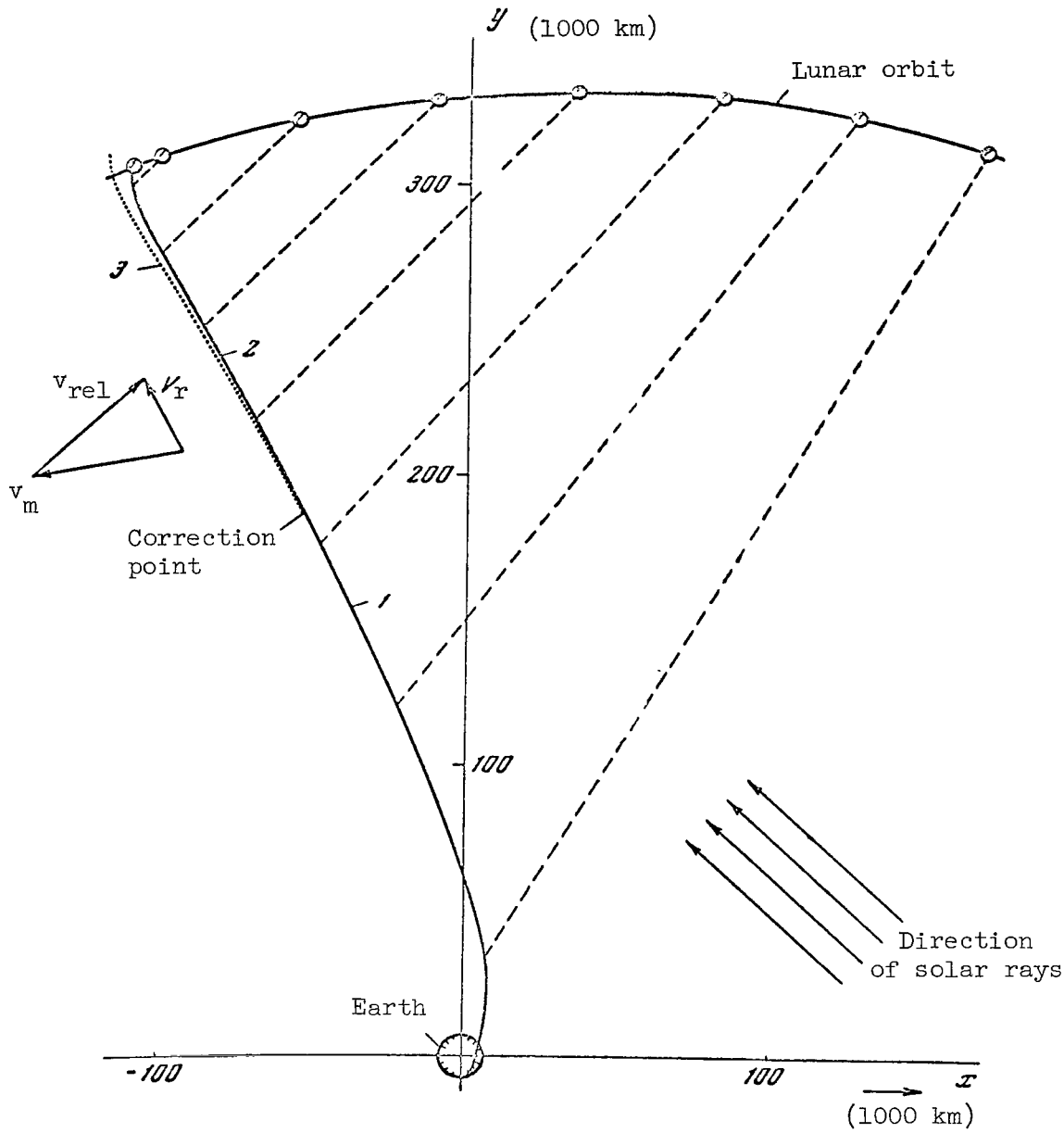

Figure 7. Projection of Luna 9 trajectory on the plane of Earth's equator.

landing point will shift (even in the case of a strictly vertical deceleration), but will remain in the region with selenographic coordinates 50-70° W longitude and 0-16° N latitude. An inclined deceleration may result in other landing point coordinates.

The landing had been planned in the area of the morning terminator to ensure the most favorable conditions for photographing the lunar surface and securing the proper temperature for the station.

Thus the angle between the radii extending from the center of the Moon to the landing area and to the Sun should be close to 90°, and in the landing area the Sun should be in the east. Consequently, the angle between the directions from the center of the Moon to Earth and the Sun should be about 20-30°. /29 This, in turn, will determine the Moon's position in its orbit during the given month at the time of the rocket's approach and also therefore the date of reaching the Moon and the launching date of the carrier rocket.

The relative location of the Earth, Moon and Sun recurs at periods equivalent to the synodical month, i.e., approximately every 29.5 days. The launching dates calculated to satisfy these conditions are therefore determined by the same periodicity.

2. Flight Control

General organization

The rocket contained time-programming, logic and computing devices designed to perform a series of operations required for solution of flight problems. Performance of the automatic devices was coordinated with ground control of the lunar rocket and Luna 9 by a command radio link.

Individual communication links were established by radio command from the control point according to a preset program. The command guidance system made it possible to telemeter the rocket-borne instrumentation and check the functioning of the automatic devices.

The command guidance system also made it possible to connect separate automatic control systems for the performance of prescribed operations. The radio-frequency link was also used for tuning the rocket-borne systems. With such an arrangement it was possible to interfere with performance of rocket-borne instrumentation whenever necessary.

Trajectory measurements and orbit determination

Accurate determination of the actual flight trajectory after the vehicle has been placed in trajectory is a problem which has been under constant solution since the launching of the first artificial Earth satellite. This is usually required for precise rocket-orbiting purposes, for predicting further flight or relating the scientific measurements to a particular place in space.

This problem was an element of the flight control concerned with the landing of an automatic station on the Moon. The trajectory, determined with greater precision after the orbiting operation, was also used to determine the magnitude and direction of the correcting impulse, which was to change the flight path in such a way as to ensure the prescribed approach of the rocket to the Moon. The automatic devices carried were adjusted according to flight parameters determined by the accurate trajectory. The time for the rocket's /30

deceleration near the Moon had been preset according to the trajectory defined after correction.

The refinement of the trajectory, after the rocket had been placed on trajectory and the correction made, was based primarily on radio measurements. Special hookups with ground control centers in the Soviet Union were used to measure the distances to the rocket, the velocity of the radial motion in relation to the control center and the rocket's angular coordinates in relation to a certain coordinate system associated with the particular control center. These data were automatically telegraphed to computation centers. The measurements were included in the mathematical processing by electronic computers.

Parameters measured visually were used in addition to radio measurements for determining the flight path. Photographing the lunar rocket against the stellar background made it possible to determine independently the rocket's angular coordinates.

3. Correction

The first flights of the Soviet rockets to the Moon took place with no trajectory correction. The orbiting precision required to hit the Moon with the second space vehicle and to encircle the Moon and photograph its surface was adequate for such experiments.

Landing in a predetermined area on the Moon after an almost vertical descent to its surface required considerably higher degree of precision. It was found to be inexpedient to make too many demands on the control system when launching the rocket from the ground; the actual flight path was to be determined by measurements in the initial section of the flight, and the orientation and propulsion systems would then be used to make the required trajectory correction, i.e., to correct the orbiting errors.

Trajectory correction may be considered an abrupt change in the velocity vector. The three vector components of the correction rate are three control parameters, which can be used to accomplish a predetermined approach to the Moon. One correcting impulse (three free parameters) can be used not only to /31 insure the rocket's approach to a preselected area on the Moon, but also to change the duration of flight to the Moon. The latter eventuality had not been provided for, because the possible differences in the flight duration due to the launching errors on the ground are not very large.

Analysis of the problem revealed that the optimum vector of the correcting impulse should be close to the plane perpendicular to the Moon-rocket beam. This characteristic was found to be convenient for instrument orientation of the engine during correction.

Selection of correction time

In accordance with the flight program, the trajectory was corrected on 1 February 1966, at 22:29 Moscow time, when the vehicle (station) was 233,000 km from Earth and 190,000 km from the Moon.

Selection of a particular trajectory correction point is determined from several considerations. The actual trajectory must be accurately and reliably determined after the vehicle has been orbited. The trajectory parameters must be measured and processed by computers, and the necessary correction calculated and transmitted to the rocket-borne instruments. The accuracy of defining the trajectory increases with an increase in the section along which the flight parameters are measured.

Even in the case of an ideal correction, accuracy in approach to the Moon cannot be higher than the exact knowledge of the actual trajectory. Another factor, which makes a later correction preferable, is the impossibility of calculating an ideally accurate correction. The effect of correction errors (errors in changing the magnitude as well as direction of the velocity) on a miss near the Moon diminishes as the rocket approaches the Moon.

The optimum energy requirements for the correcting impulse pose a different problem. Table 2 illustrates the values of the vector modulus designed to correct a 10,000 km miss near the Moon, depending on the distance between the correction point and the Moon.

TABLE 2.

Distance to the Moon, 1000 km	Correction rate for 10,000 km miss, m/sec
300	28
200	46
100	140
50	200

The table reveals that the energy used in correcting the same orbiting errors increases substantially with approach to the Moon.

Corrections made 190,000 km from the Moon were due to a compromise so- /32
lution, which took into account other causes than those indicated.

Engine orientation

An astronavigation system was installed in the rocket to ensure preselected direction of the engine in space during correction and at the

end of flight before deceleration. The system included optical sighting devices, logic and computing devices, angular velocity sensors and micro-engines operating on compressed gas and producing the moments of force for the required orientation and stabilization of the rocket in relation to its center of mass.

Sun, Moon and Earth were selected as reference luminaries. Until now the Sun and the star Canopus, i.e., fairly remote objects, have been used as reference luminaries in the flights of Soviet and American space rockets to Venus and Mars. Orientation to closer luminaries, such as Earth and Moon, has certain advantages. Their greater brightness provides greater reliability in the search for luminaries. Furthermore, the astronavigation system with functions with close celestial bodies facilitates not only necessary engine orientation, but also permits measurement of the rocket coordinates in relation to the planet to which the rocket is flying.

Preparation for correction began with automatic orientation of one of the rocket axes to the Sun. Signals from the system of sensors in the rocket were fed to a computer which controlled the operation of the microengines.

Rough orientation made it possible to put the Sun in the optical sighting device of the accurate solar orientation. When one rocket axis was stabilized by the Sun, a turn of the rocket around that axis initiated the search for the Moon.

Adjusting the orientation systems

Telescopes of optical sensors have a rather small field of vision, from one to several degrees. The required angle between the solar and lunar sighting devices must be achieved beforehand, so that the Moon can enter the field of view of the lunar transducer by rotating around its axis directed to the Sun.

Preliminary tuning of the astronavigation system occurs on Earth. Actual arrangement of the luminaries is determined by the estimated trajectory for /33 the planned orientation moments, and the telescopes are adjusted on the basis of these estimates.

Final adjustment of the system occurs during flight. The characteristic features of the orientation system's operation are such that some parameters always require readjustment, while others are merely subject to possible readjustment. New calculations are made after the actual flight path has been determined by measurements. If the rocket position in relation to reference celestial bodies is substantially different from that expected when adjusting the system on Earth, it is corrected by the use of the command guidance system.

The required rotation of the telescope axis, determined by calculation, is coded on Earth in the form of a binary number. The latter is transmitted to the rocket and memorized by its counter. This is followed by a command from Earth (or through a computer) which causes the rocket-borne telescope to rotate.

The flight of the Luna 9 rocket, in particular, did not require any changes in the angle between the lunar and solar sighting devices established on Earth, because the correction had been made in preplanned time and the launching of the rocket from Earth was fairly accurate. However, the celestial navigation system could be readjusted, and this made it possible to introduce corrections, if necessary, in the case of a rough launching or at a different instant.

When the Moon enters the field of view of the sensor and the rocket is stabilized, the rocket-borne system permits the measurement of the actual angle between the Moon and Sun. That angle is transmitted to Earth in code. The coincidence of this magnitude with the precalculated value makes it possible to check both the performance of the astronavigation system and the correct determination of the actual flight path.

The telescope orientation to the Moon and Sun, whose position relative to the rocket is known, makes it possible to lock the rocket's axes onto an absolute coordinate system at any time. The astronavigation system was installed in the rocket in such a way that when the Sun and Moon came into the field of view of the appropriate sighting devices, the engine was approximately perpendicular to the direction to the Moon.

To put the correcting engine in space in the desired direction, it was necessary to rotate it in relation to the rocket-Moon axis. The magnitude of rotation had been determined on Earth on the basis of the accurately defined flight path, and transmitted to the rocket.

Engine control

Microengines are required to provide insignificant moments of force for /34
the orientation of the rocket relative to its center of mass in free flight. Perturbations accompanying the engine operation are due to the impossibility of an ideal coincidence of engine thrust line and the rocket's center of mass. The astronavigation system therefore transfers the stabilization functions to another system before the engine is turned on. The coordinate system and position of the rocket are memorized by gyro devices. The moments of force required to maintain the desired rocket orientation are produced by special small rocket engines.

A device designed to integrate the acceleration went into operation simultaneously with the engine. The engine was turned off when the integral accelerations (apparent velocity) along the rocket's axis reached the preselected magnitude. The estimated value of the apparent velocity had been determined on Earth by the actual flight path and transmitted to the rocket in code before the correction.

4. Deceleration

Correction was followed by several trajectory measurements. Mathematical processing of those measurements by computers made it possible to check the

accuracy of the correction and determine the flight parameters on the stage of the rocket approach to the Moon. The computers were used to calculate the parameters of the system adjustment for the eventual autonomous control of landing.

The appropriate adjustment data were transmitted to the automatic station by the command guidance system six hours before landing.

Preparation of the rocket for deceleration was initiated by the command guidance system about two hours before approach to the lunar surface. The sequence of operations that followed was determined by the automatic devices in the rocket. The first stage of the rocket orientation was similar to the orientation during the correction. The rocket was consequently stabilized in relation to the Moon and Sun.

A special optical sighting device then initiated a search for Earth. When Earth passed into the sighting device field of view, it was constantly tracked by a logic element of the system through that device during the prolonged flight.

These operations were completed about 10 min before the lunar rocket /35
passed through a point 8285 km from the center of the Moon.

The purpose of deceleration was to reduce the speed of the rocket's flight in relation to the Moon almost to zero (the approach speed was about 2600 m/sec). This, naturally, can be achieved only by orienting the engine along the direction of relative velocity.

Analysis revealed that if the engine in space had been oriented to the estimated flight path during deceleration, the lateral speed component at the end of deceleration would have been very great. It would have been approximately proportional to the deviation of the actual point of intersection of the trajectory and the lunar surface from the estimated point. A lateral speed on the order of 40 m/sec corresponds to 100 km deviation, which means that such a deceleration system would have required exact knowledge of the trajectory after correction.

The solution to that problem involves orientation of the engine to the lunar vertical during deceleration. Figure 8 shows a diagram of the Moon's surface with its center at point O. The straight line AMO represents the estimated trajectory, whose approach to the Moon is perpendicular to its surface. The curve SS' is the actual trajectory; the distance between its point of intersection with the lunar surface and the estimated point is l, which is equal to the length of the arc MN. The arrow NV indicates the direction of the relative velocity near the lunar surface.

Figure 8 shows a plane picture. However, point N may be shifted in /36
any direction from estimated point M. The total number of possible trajectories with various positions of point N produces a beam of trajectories possessing axial symmetry with the axis AM in the first approximation for small misses l.

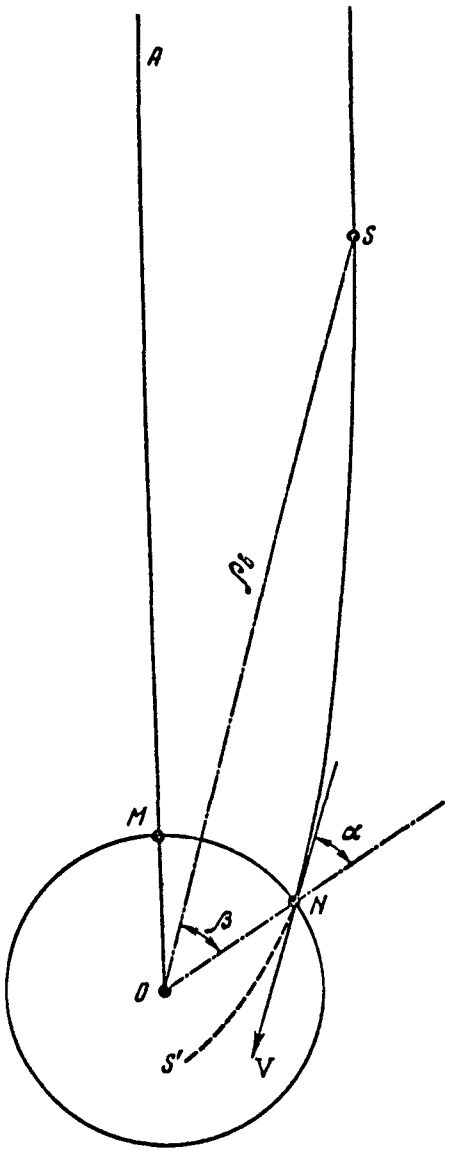

Figure 8. Explanation of deceleration diagram.

Analysis revealed that it was possible to indicate the special distance from the Moon ρ_b (depending on h) for a beam of trajectories with a definite selenocentric energy h. In the case of any trajectory of the beam and substantial miss ι, the direction from point S, located at distance ρ_b, to the lunar center values O would differ little from the direction NV of the relative approach velocity during flight along this trajectory. This feature was utilized for orienting the rocket during deceleration. The main idea is to orient the engine to the center of the Moon at precalculated distance ρ_b and maintain this

TABLE 3.

ι, km	α, degrees	α-β, degrees	v_σ, m/sec
60	1.1	0.006	0.3
100	2.2	0.012	0.5
200	4.5	0.026	1.1
300	6.9	0.054	2.5
500	11.4	0.103	4.7

orientation until deceleration. The following was adopted for the Luna 9 flight: ρ_b = 8285 km. Table 3 shows the angles α and α-β and lateral velocity v_σ at the end of deceleration, depending on the miss ι. The magnitudes were calculated for ρ_b = 8285 km.

After the preselected altitude ρ_b had been passed, the Moon tracking was discontinued and rocket orientation maintained by tracking Earth and Sun with the appropriate optical sensors.

Orientation had to be maintained in an absolute coordinate system at the time the lunar vertical was fixed in order to achieve the necessary orientation by the beginning of the deceleration. Since Earth had shifted within that coordinate system during flight before deceleration, it was found necessary to take this effect into account by making the necessary corrections in engine adjustment relative to the optical sighting devices.

It was necessary to know the exact altitude of the rocket above the lunar surface in the final section of the approach trajectory before turning on the engine to initiate deceleration on time.

This required installation in the rocket of a radar altimeter, whose /42 antenna axis was oriented parrallel with the engine axis.

The radar altimeter recorded the instant the preselected altitude of ~ 75 km above the landing point was passed. This measurement was a signal to initiate the deceleration cycle.

The engine was turned on at a specified time after the altimeter signal. Rocket stabilization during engine operation was controlled by a special gyro system, just as during correction. As soon as the engine was started, the devices no longer needed for continued flight were separated from the rocket, which reduced its weight by 300 kg. This made it possible to deliver a heavy vehicle to the Moon.

During correction, the system had to ensure only the preselected change in the magnitude and direction of velocity. Landing required not only achievement

of the estimated velocity at the end of deceleration--the acceleration integral--but also observance of the law governing the change of that velocity. This requirement stemmed from the necessity for reaching the preselected altitude above the lunar surface at the end of deceleration.

The sequence of operations performed by Luna 9 is listed in Table 4 and illustrated in figures 9 and 10.

TABLE 4.

No.	Date and duration	Operation /37
1	31 Jan 15 hrs 53 min 21 sec	The last stage of the carrier rocket completes its function and separates from the lunar rocket; the programming and timing system is switched on.
2	16 hrs 46 min-- 16 hrs 56 min	The first series of trajectory measurements are made on the trajectory to the Moon and telemetric data received. The receiving and transmitting radio devices, the ventilation system, and the telemetering units are switched on. Trajectory measurements (using radio engineering facilities to determine the distance, velocity and topocentric coordinates of the site angle and azimuth) of the lunar rocket and the transmission of telemetric data containing scientific information as well as information on the temperature and pressure in the different compartments of the lunar rocket, and the performance of its equipment.
3	17 hrs 57 min	Rotating the lunar rocket to maintain normal temperature for all its parts.
4	18 hrs 19 min-- 18 hrs 43 min	Trajectory measurements and reception of telemetric data; the astronavigation system is turned on and its performance controlled.
5	23 hrs 15 min-- 23 hrs 25 min	A series of trajectory measurements are made and telemetric data received.

(continued)

TABLE 4 (continued)

No.	Date and duration	Operation
	1 Feb	
6	4 hrs 41 min-- 4 hrs 56 min	Period of trajectory measurements and reception of telemetric data
7	15 hrs 36 min-- 15 hrs 52 min	Radio communication period in which the same program was carried out as in the first period, plus a check on the time in the rocket.
8	20 hrs 9 min-- 20 hrs 42 min	Radio communication period. Rocket-borne systems are adjusted for correction. Checking the proper flow of data into the programming and timing device of the rocket. Receiving telemetric information on the condition of the basic systems of the lunar rocket.
9	21 hrs 16 min-- 23 hrs 14 min	Period trajectory correction. Checking the time in the rocket. Measuring the radial velocity. First rough and then exact solar orientation. Opening the shutters of the lunar sensor and orientation to the Moon. Warming up the control system. Engine performance following correction. Engine is automatically turned off by command of acceleration integrator. /38 Radial velocity is measured after the engine has completed its operation. Performance and condition of the rocket-borne instrumentation are controlled in the course of the entire series. Lunar rocket made to rotate about longitudinal axis.
	2 Feb	
10	1 hr 36 min-- 1 hr 46 min	Period of trajectory measurements and reception of telemetric information.
11	16 hrs 16 min-- 16 hrs 31 min	Radio communication period, trajectory measurements, telemetric control and tests of the television devices in the automatic lunar station.

(continued)

TABLE 4 (continued)

No.	Date and duration	Operation
12	22 hrs 42 min-- 22 hrs 59 min	Period of trajectory measurements and reception of telemetered information.
	3 Feb	
13	1 hr 22 min-- 1 hr 28 min	Period of trajectory measurements and reception of telemetered information.
14	15 hrs 34 min-- 16 hrs 31 min	Period of adjustment of rocket-borne systems for deceleration purposes. Controlling the condition of the rocket-borne systems and the proper flow of data into programming and timing systems.
15	19 hrs 28 min	Begin final radio communication period before the landing--deceleration period. Equipment controlling lunar rocket during deceleration is turned on. Check of time in the rocket and the initial data transmitted in the preceding period. Trajectory measurements. Turn of the lunar rocket. Orienting one of the rocket axes to the Sun, and the other to the Moon. Orienting the optical sighting device to Earth. Construction of a lunar vertical at a distance of ~ 8300 km from center of the Moon, and switching on of the control gyro system. Continuous control of the operation of all rocket-borne systems by telemetry. Radar altimeter signals that the preselected altitude (~ 75 km) has been reached, and deceleration engine is switched on.
16	21 hrs 44 min 42 sec	The astronomical orientation system is turned off and the autonomous gyro system takes over. The engine is started. The system is prepared for a landing on the Moon.
17	21 hrs 45 min 30 sec	Luna 9, the automatic lunar station, makes a soft landing. /39
18	21 hrs 49 min 40 sec--22 hrs 6 min	First radio communication with automatic lunar station on the lunar surface.

(continued)

TABLE 4 (concluded)

No.	Date and duration	Operation
		Receiving and transmitting radio devices and ventilation system as well as scientific and service apparatus are connected. Transmission of scientific information and telemetric control of the station's systems. Temperature control system of the automatic lunar station is turned on. Opening of the lobe-type and rod antennas. Receivers change from lobe-type to rod antennas. Opening of the antennas is duplicated by mechanical timing device.
19	4 Feb 0 hr 00 min-- 0 hr 15 min	Second radio communication period.
20	4 hrs 50 min-- 6 hrs 37 min	First lunar panorama image televised and telemetric data transmitted. The television of the automatic lunar station is turned on. A view of the lunar landscape and the transmission of the panorama of the lunar surface to Earth. Receiving telemetered information on the condition and functioning of the systems and instrumentation.
21	17 hrs 00 min-- 19 hrs 54 min	Transmission of the second lunar panorama and telemetered information.
22	5 Feb 4 hrs 00 min-- 4 hrs 04 min	Third radio communication period.
23	19 hrs 00 min-- 20 hrs 41 min	Transmission of third lunar panorama and telemetered information.
24	21 hrs 47 min-- 21 hrs 56 min	Fourth radio communication period.
25	22 hrs 28 min-- 22 hrs 45 min	Fifth radio communication period.
26	6-7 Feb 23 hrs 37 min-- 1 hr 55 min	Additional transmission of individual sections of the lunar surface and telemetered information.

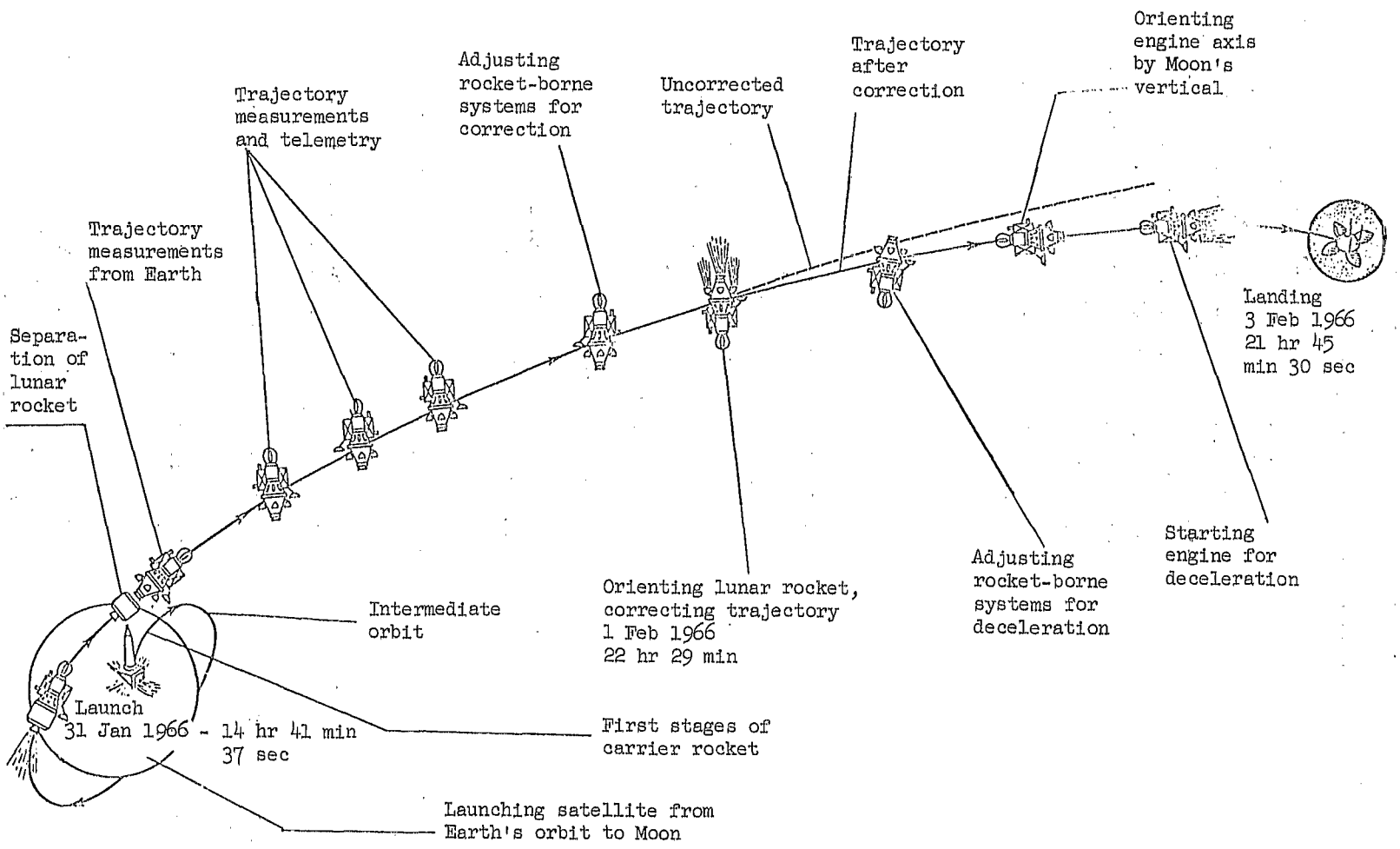

Figure 9. Flight diagram of lunar rocket.

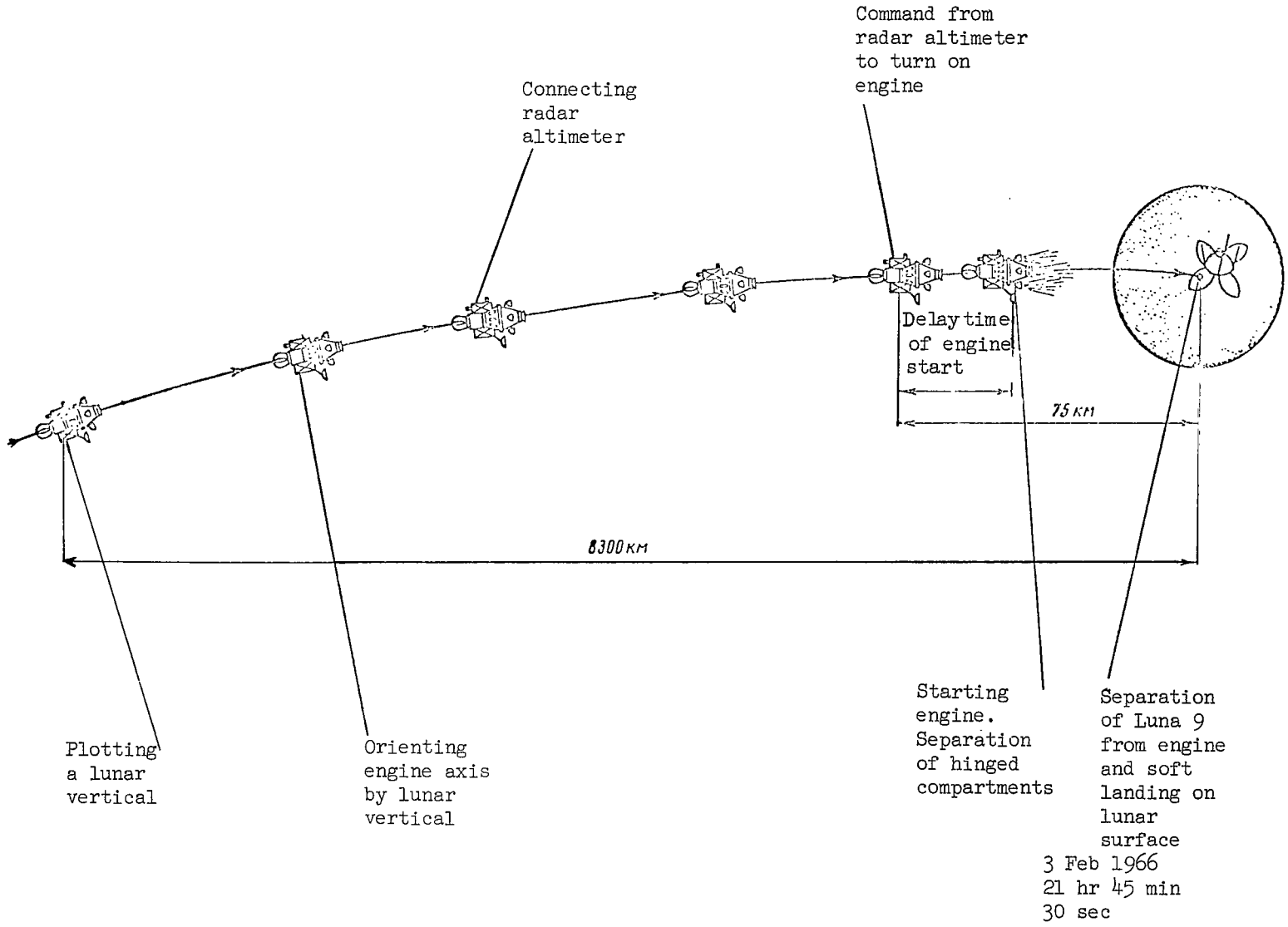

Figure 10. Trajectory of lunar rocket near Moon.

PART II. RESULTS OF STUDIES OF LUNAR PANORAMAS

Introduction

The landing area for Luna 9 was selected in the equatorial region near /45 the morning terminator on the illuminated part of the lunar surface, i.e., where the Sun has just risen and its elevation has increased approximately to 12° of the terrestrial day.

Selection of such a landing site provides favorable conditions for obtaining pictures of the lunar surface. During the morning hours all objects cast long shadows, which shorten with comparative rapidity as the Sun's elevation above the horizon increases. Due to this it was possible to obtain quickly many panoramas with shadow that changed almost in geometric progression. Actually, during the first two days of the station's operation the panoramas specified by the program were obtained with a solar elevation of 7°, 14° and 27°, and fragments A and B, which covered part of the panorama in the interval of values from 330° to 55°, were even obtained in days during the period of additional operation at a solar elevation of 41°. The pictures with shadows of quite varied lengths provide material for determining the forms of both depressions and projections.

Three full panoramas are included in the third part of the book, where they are also presented in the form of 22 fragments and 12 stereopairs reproduced by a phototype method which ensures the most precise documentary reproduction of the originals. Isolated impulse flaws resembling small white or black circles have been retouched on the panorama pictures. Fragments A and B are given in figure 27.

Indication of the location of details on the panoramas and their frag- /47 ments according to the axis of the abscissa was facilitated by a degree scale drawn plotting angle γ, which is read off on the plane of panorama compilation (Part 1, Chapter 1) from an arbitrary point located approximately north. The scale has not been drawn along the axis of the ordinates, but where necessary we will indicate angle $\xi = \beta - 18^{\circ}$, measured from the lower edge of the panorama to a scale of $1^{\circ} = 5.5$ mm (on the fragments).

The station landed near the western border of Oceanus Procellarum, near a point with coordinates 7° N and 64.5° W. Although this area is located within the limits of Oceanus Procellarum as accepted in selenography, it is obviously impossible to consider it strictly a region of maria. Several western and southern landing sites encompassed the great craters of Cavalerius (diameter 60 km) and Hevelius (diameter 120 km), which are encircled by a well-developed system of embankments and spurs resembling semisubmerged mountain systems. The distance from the landing site to the wall of the Crater of Cavalerius is

comparable to the diameter of the crater itself. This is essential for interpretation, if it is considered that secondary craters usually originate at distances comparable to the diameter of the primary crater. In the same region of the landing site there is a group of hills (the system of Cavalerius γ) with sloping sides (incline does not exceed 10-15°) and rising 500-800 m above the surrounding territory.

Apparently all the landing area is somewhat elevated above the area of Oceanus Procellarum, which is adjacent to it in the east. Figure 11 presents a map of the landing area to a scale of 1:1,000,000 (Lunar Chart US Air Force and NASA, N 56, May 1963), and figure 12 is a photographic map of the visible hemisphere of the Moon with the landing site indicated. Possibly Luna 9 landed in an area which, from its characteristics, is intermediate between purely maria and purely upland areas, similar in this respect to the area of the Mare Cognitum, large-scale pictures of which were obtained by Ranger 7.

In the area observed, the upland and maria regions are so intermingled that it is not possible to determine the similarity of the landing site to regions of one or the other type from data on flight and landing dynamics.

It is difficult to determine whether the landing site is in an upland or maria region by reference to the panoramas alone, because the area encompassed by the survey is very limited in comparison with details distinguishable from Earth. However, by detailed study of the pictures we can determine not only the microrelief characteristics, but also a number of macrocharacteristics of the landing site.

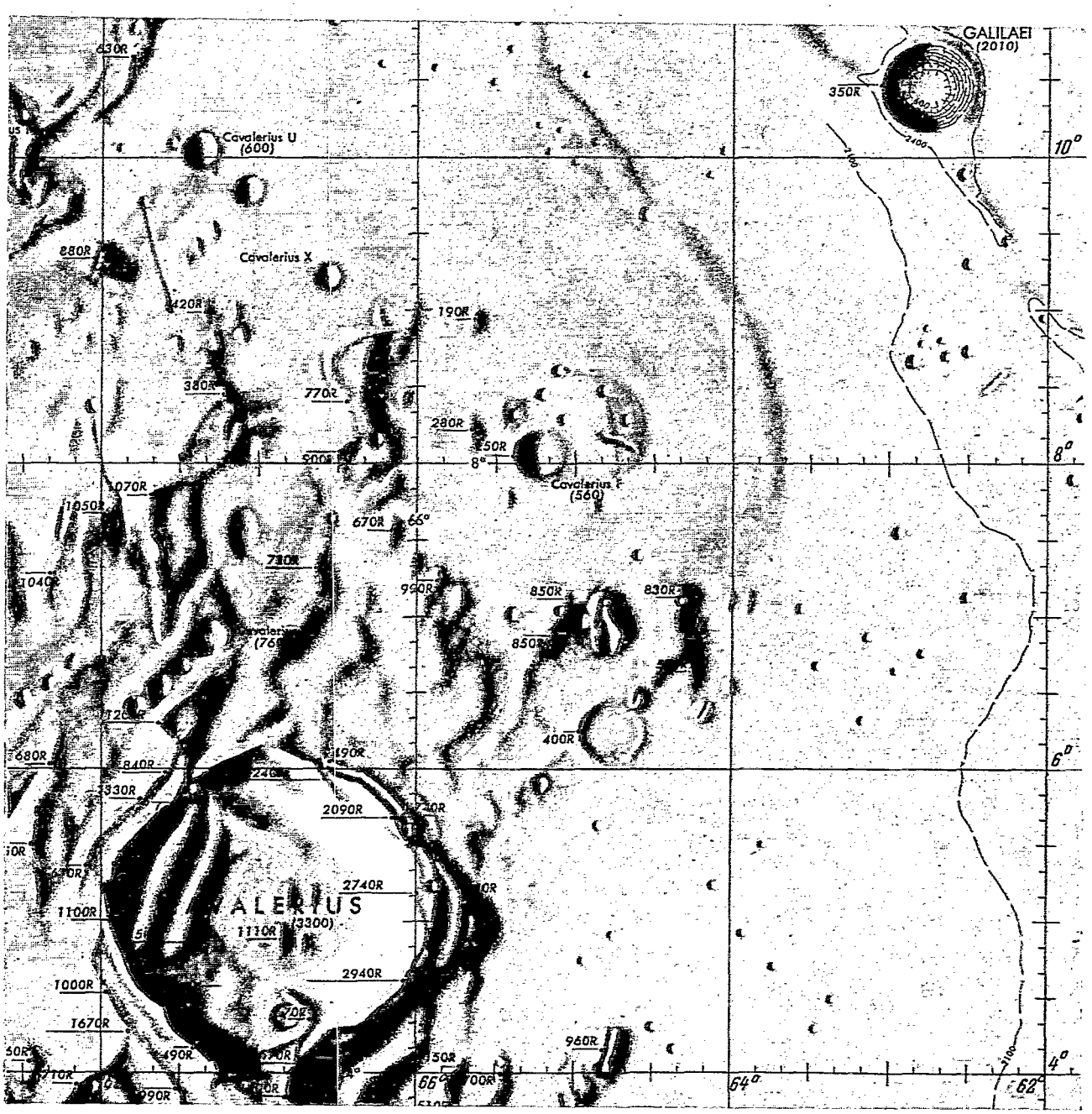

Figure 11. Map of the region of the landing site of Luna 9.

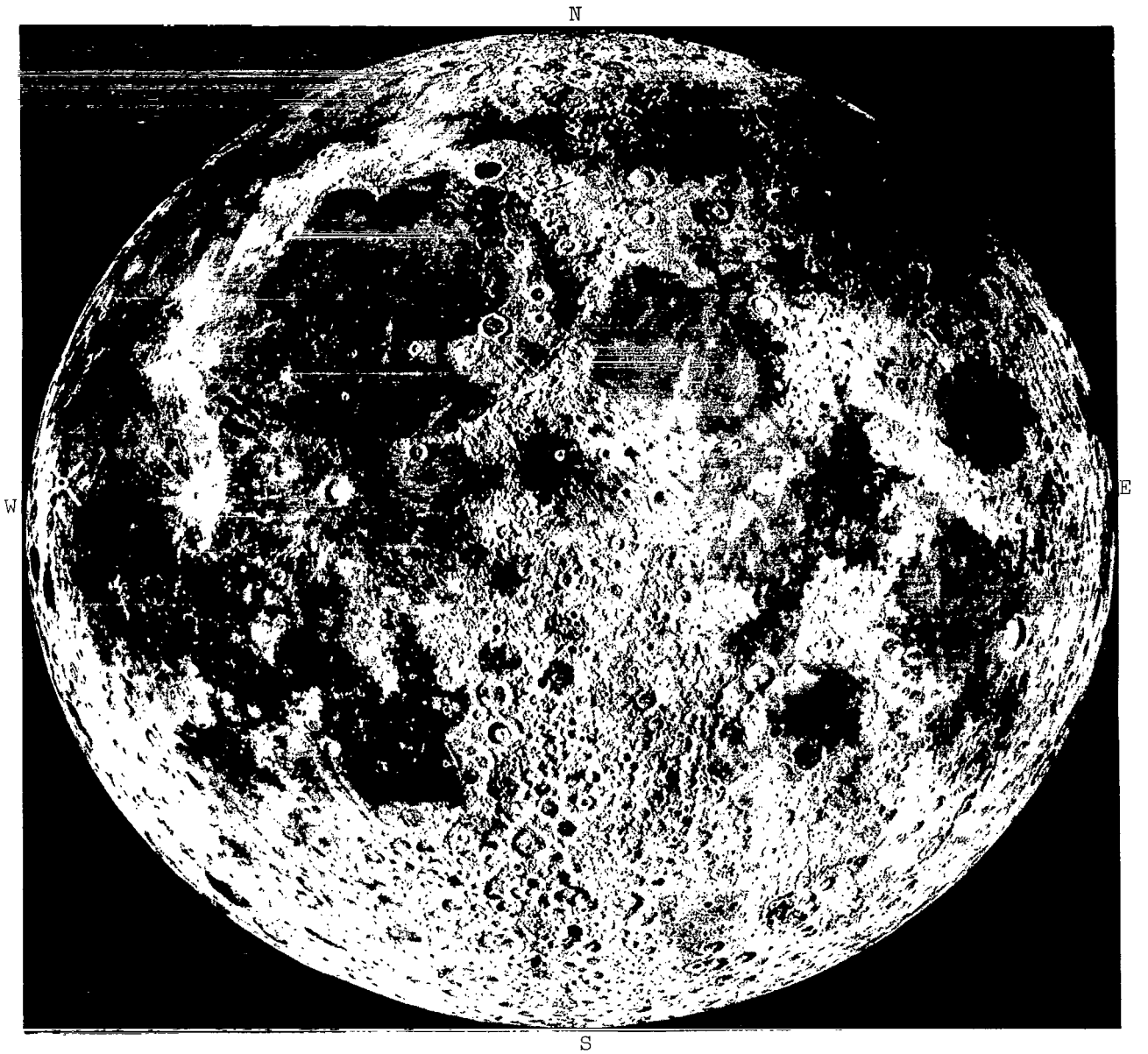

Figure 12. Photographic map of the Moon. The cross indicates the landing site of Luna 9.

CHAPTER 1. CONSTRUCTION OF THE LANDING SITE PLAN

1. Methods of Photogrammetric Processing of Panoramas

The picture surface on which the special panorama television camera /48
builds its image is a sphere (fig. 13). The television scanning beam makes two angular motions on mutually perpendicular planes rotating around the center of panorama compilation S, which is the point of reflection of the projecting beam on the scanning mirror surface.

One plane is the plane of panorama compilation (planning plane). It proceeds through point S perpendicular to the axis of panorama compilation Sc (the axis of rotation of the television camera head). The panorama compilation plane is rigid relative to Luna 9. The other plane is the scanning plane. It proceeds through the axis of panorama compilation and rotates around it (frame scanning). The scanning beam is inclined in this plane due to mirror oscillation (line scanning) within the limits of angle β_0, determining the transverse angle of the field of vision.

The position of the sighting beam relative to Luna 9 at each moment is characterized by angles γ and β. The former (γ) is considered in the plane of panorama compilation from a certain base direction to the foot of its intersection with the scanning plane. The direction toward any part of Luna 9 which falls within the television camera field of vision (e.g., the antenna) is taken as the origin of the reading. The second is determined in the scan- /49
ning plane from the foot of its intersection with the plane of panorama compilation to the sighting beam.

The center of panorama compilation, the plane of panorama compilation and the plane of scanning which coincides with the base direction, form a panoramic coordinate system. Angles β and γ are the panoramic latitude and longitude of terrain point M, designated in figure 13 by point m. In recording the panorama on the facsimile equipment, line scanning is obtained by drum rotation, so that one line corresponds to one revolution.

Frame scanning is accomplished by moving the recording photo-head along the generatrix drum. The distance read off on the photograph along a line is directly proportional to angle β and in a direction perpendicular to the lines proportional to angle γ. Knowing angle β_0, the length of the line on the film

and the spacing of the frame scanning, we easily determine the transverse and longitudinal coefficients of proportionality. Thus it is possible to take readings of β and γ from the photograph.

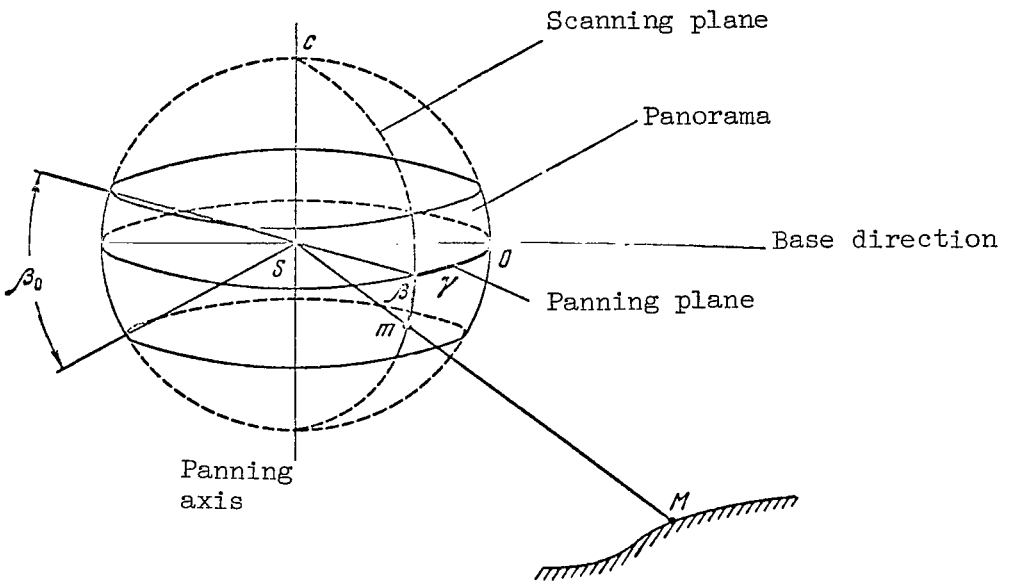

Figure 13. Panoramic projection.

One panorama gives the direction from the center of the panorama compilation to the terrain points, but does not permit determining their spatial position. Resolving this problem requires two panoramas obtained from various points in space and suitably oriented in relation to each other. Then, after finding directions β, γ to the same terrain point according to two panoramas and relocating the orientation of the latter, it is possible to solve the so-called spatial intersection. Figure 14 shows a diagram of the general case of the spatial panoramic intersection.

Figure 14 shows the following: X, Y, Z is some horizontal system of coordinates; S_1, S_2 are centers of panorama compilation of the first and second panoramas; C_1c_1, C_2c_2 are the axes of panorama compilation; S_1N_1, S_2N_2 are verticals; N_1, N_2, n_1, n_2 are nadir points on the terrain and on the panoramas; $S_1n_1c_1v_1$, $S_2n_2c_2v_2$ are the planes of the main vertical; S_1v_1, S_2v_2, N_1C_1, N_2C_2 are tracks of their intersection with the planes of panorama compilation and plane XY; S_1o_1, S_2o_2 are the base directions.

In figure 14 the heavy lines indicate the so-called elements of exterior orientation, limiting all degrees of freedom of the panoramas and determining their orientation relative to the system of coordinates X, Y, Z. Thus, X_{n_1}, Y_{n_1}, H_1 are coordinates of the main center of panorama compilation; α_1, α_2 are the angles of incline of the panoramas; $\varkappa_1$, $\varkappa_2$ are the angles between the base

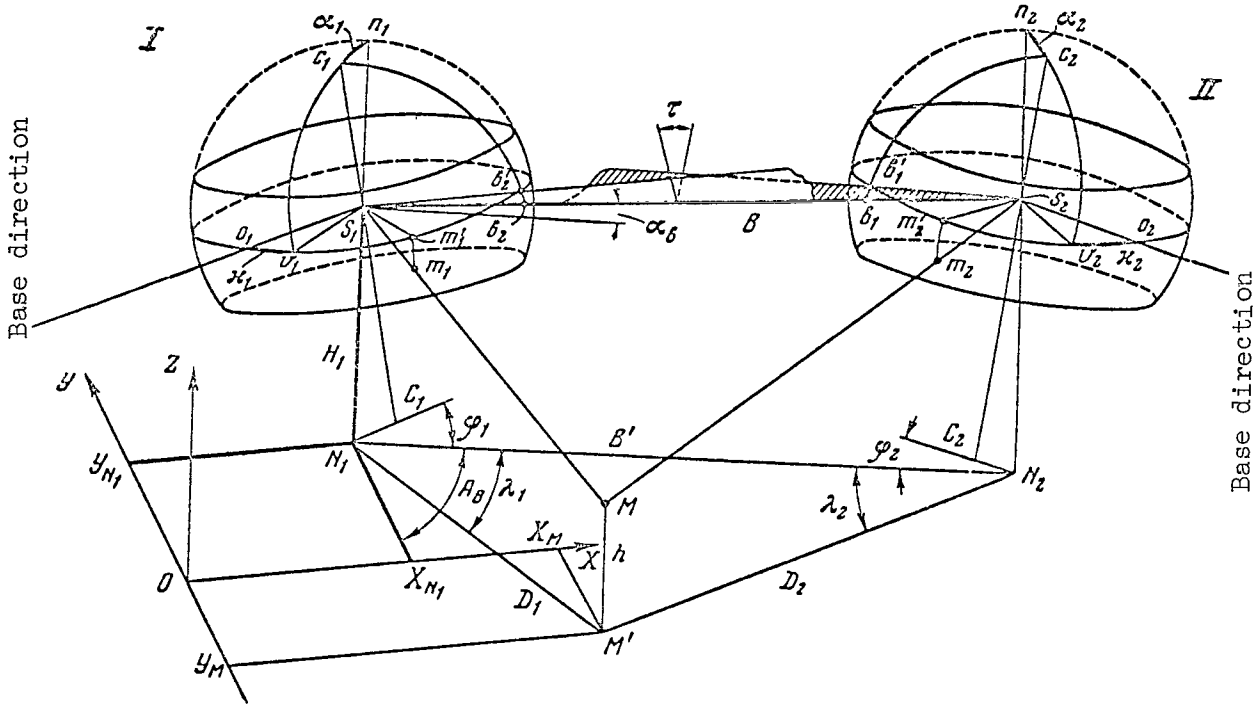

Figure 14. Spatial panoramic intersection.

directions and lines Sv of the panoramas; B is the base of panorama compilation; α_B is the angle of inclination of the base relative to the horizontal /51 plane; φ_1, φ_2 are the angles between lines N_1C_1, N_2C_2 and the projections of the base B' on plane XY; A_B is the azimuth of the base projection. If the elements of exterior orientation and the panorama coordinates for terrain point $o_1m'_1 = \gamma_1$, $m_1m_1 = \beta_1$, $o_2m_2 = \gamma_2$, $m'_2m_2 = \beta_2$ are given (fig. 14), coordinates X_M, Y_M, h of terrain point M are determined identically.

When exterior orientation of the panoramas is unknown, a nonoriented model of the region can be constructed. To achieve this, the elements of mutual orientation of the panoramas must be known. They are: $o_1b'_2 = \gamma_{b_2}$; /52 $b'_2b_2 = \beta_{b_2}$; $o_2b'_1 = \gamma_{b_1}$; $b'_1b_1 = \beta_{b_1}$; τ is the angle between base planes $S_1c_1b'_2b_2$ and $S_2c_2b'_1b_2$. Points b_1 and b_2 are images of the centers of panorama compilation of adjacent panoramas. Figure 14 also designates the following: D_1 and D_2 are the distances from nadir points N_1 and N_2 to point M'--

projections of the terrain point on the horizontal plane; λ_1, λ_2 are the angles between the base projection and directions N_1M', N_2M'.

The panoramas forming the spatial intersection make it possible to view the image of the area stereoscopically.

It is convenient to solve the spatial panoramic intersection in parts: /53 to determine separately the position of the terrain points on the plan and separately by elevation. To achieve this, it is necessary to reduce angles β and γ, which are measured according to the panorama, on vertical and horizontal planes.

Figure 15 shows a geometric diagram of such a reduction. The line of intersection of the plane of panorama compilation with the horizontal plane $\left(\varkappa = \frac{\pi}{2}\right)$ is adopted for simplicity for the base direction of the reading of the panorama longitudes. This is designated as follows: $m'm = \beta$, $Tm' = \gamma_T$ are the measured and $m''m = \beta'$, $Tm'' = \gamma'_T$ are the reduced panorama latitudes and longitudes of terrain point M. From the spherical triangle mnc is found

$$\sin\beta' = \cos\alpha \sin\beta + \sin\alpha \cos\beta \sin\gamma_T. \quad (1)$$

$$\cos\gamma'_T = \frac{\cos\beta \cos\gamma_T}{\cos\beta'}. \quad (2)$$

Knowing angle φ (fig. 14), it is easy to find angle λ /54

$$\lambda = \frac{\pi}{2} - \gamma'_T - \varphi.$$

Having thus found λ_1, λ_2 and keeping in mind that $B' = B \cos \alpha_B$, we solve the intersection on plane XY (triangle N_1N_2M' in fig. 14) and determine D_1, D_2, X_M, Y_M. Having found D_1, H_1, β'_1, it is easy to find h.

Three dihedral mirrors were installed on Luna 9 to obtain a spatial panoramic intersection. Figure 16 presents a diagram of the mirrors installation (seen from above). Thus, limited sections of terrain are viewed twice by the television camera--directly and after reflection in the mirrors. Thus in the first case panorama compilation proceeds from the actual center S_1 and in the second case, from the virtual center S_2. This forms the virtual base B_M. The mirrors are installed perpendicular to the plane of panorama compilation. Figure 16 presents the following: Q is the edge; $B_k = S_1Q$ is the adjusting

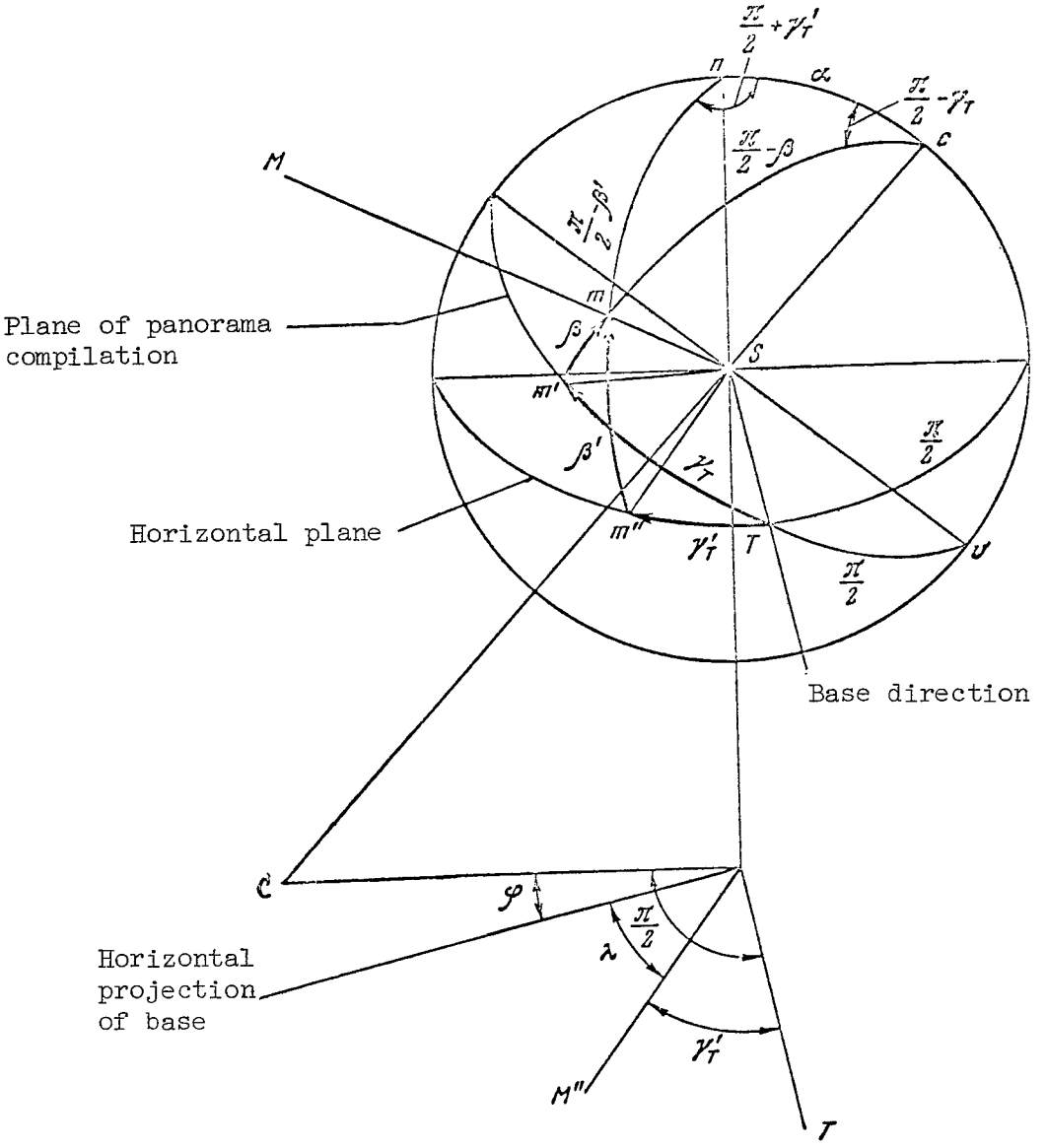

Figure 15. Diagram of reduction of panoramic latitudes and longitudes.

base of the mirror; δ is the angle between its edge and direction S_1Q; ψ is the angle between S_1Q and the virtual base. It is obvious that

$$B_M = 2B_k \sin\delta, \quad \psi = \frac{\pi}{2} - \delta.$$

Figure 17 presents a diagram of the construction of the panoramic intersection with the aid of a mirror. Terrain point M, taken for simplicity as lying in the plane of panorama compilation, is represented on the actual panorama at

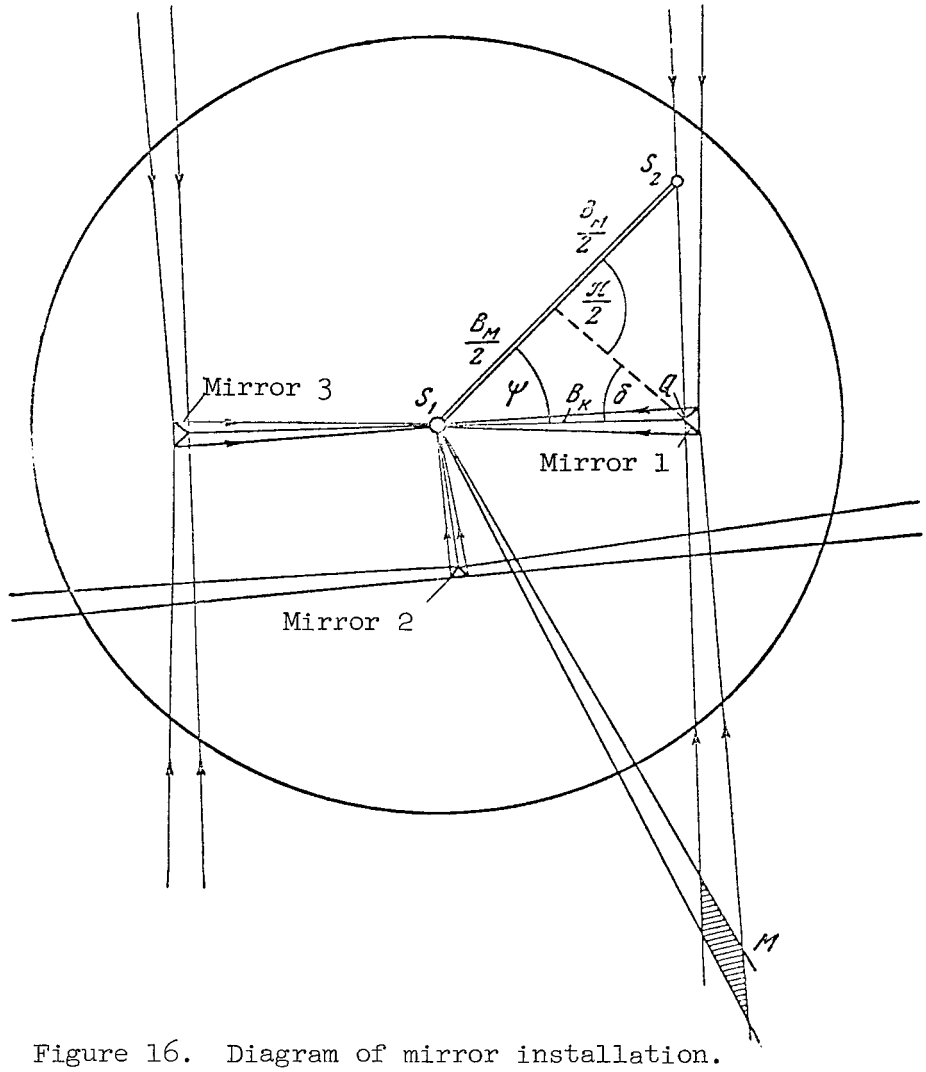

Figure 16. Diagram of mirror installation.

points m'_1 and m'_2. They have panoramic longitudes γ_{T_1} and γ_{T_2}, which are read from the axis of incline of the plane of panorama compilation S_1T_1. The panoramic longitude of the image m''_2 of point M" on the virtual panorama is read from its axis of inclination S_2T_2, which is parallel to S_1T_1, and is equal to

$$\gamma''_{T_2} = \pi + 2\gamma_{T_B} - \gamma_{T_1},$$

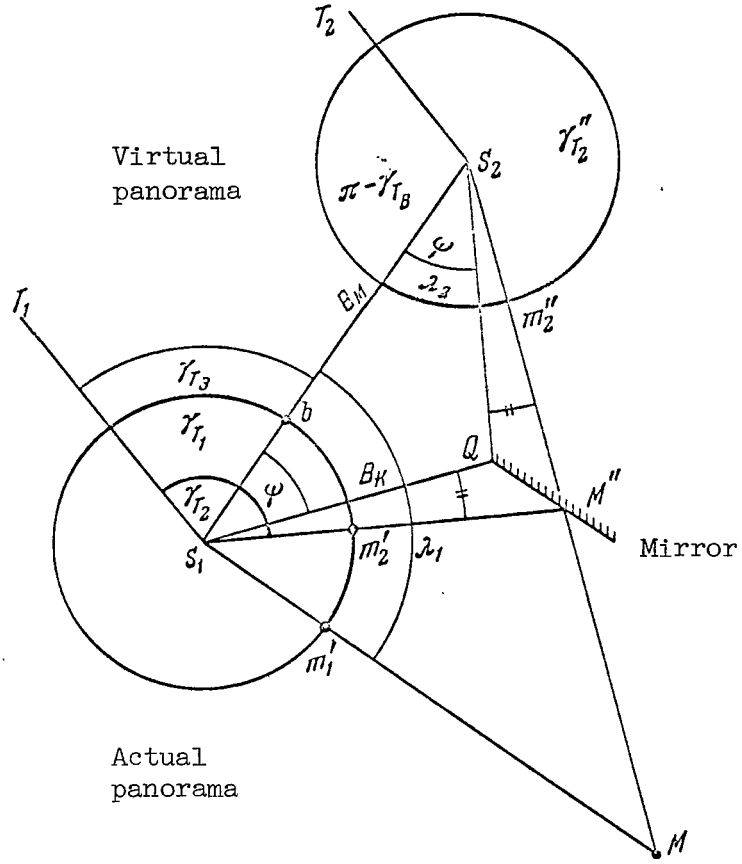

Figure 17. Diagram of construction of panoramic intersection with aid of mirror.

where γ_{T_B} is the longitude of point b on the actual panorama (base direction relative to line S_1T_1). Furthermore, we obtain angles of intersection

$$\lambda_1 = \gamma_{T_1} - \gamma_{T_B}, \quad \lambda_2 = \gamma_{T_2} - \gamma_{T_B},$$

with which we find the position of point M on the plane of panorama compilation.

If B_M, γ_{T_1}, γ_{T_2} are reduced on a horizontal plane, this problem can be solved in plane XY.

If the terrain point does not lie in the plane of panorama compilation, its panoramic latitude on the virtual panorama is equal to the latitude for the image of this point in the mirror on the actual panorama.

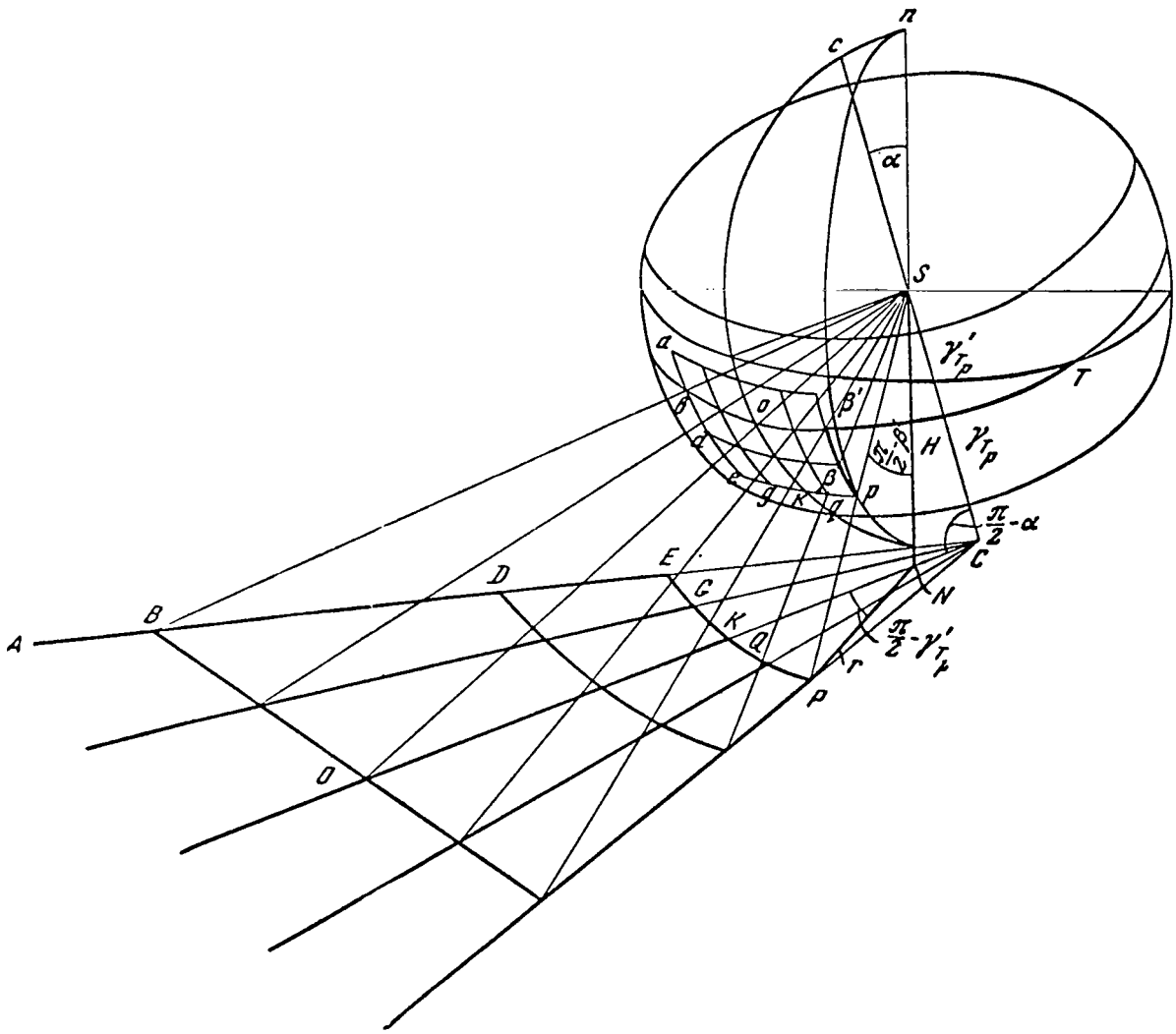

Figure 18. Perspective grid.

Another possibility results for constructing a spatial panoramic intersection according to the Luna 9 panoramas, because the panoramas, through station rotation, were obtained from various points of space. If two panoramas (e.g., the first and third) are used, they form a panoramic stereopair (fig. 14). /55

The directions near the base give the intersections at a very sharp angle. Such intersections are not precise. When the terrain is close to the plane, a contour plan can be constructed in zones with poor intersection by a perspective grid (fig. 18). A grid of various latitudes and longitudes is built on the panorama. The panorama coordinates of grid nodes are reduced on the horizontal plane according to formulas (1) and (2). The distance of the nodes from the nadir point N is found by the formula $r = H \cot \beta'$.

The position of nodes in the plan can be determined after construct- /56

ing directions $\frac{\pi}{2} - \gamma'_T$ (fig. 18) and after plotting interval r along them. The lines of the perspective grid corresponding to panoramic meridians in the plan are represented by straight lines and intersect at point C. The plane of panorama compilation is represented by a straight line, while other lines of various latitudes are represented by conical cross sections.

2. Panorama Orientation

The terrain section encompassed by the panoramas is small, so that the topographical plan of the Luna 9 landing site is constructed using a local rectangular horizontal system of coordinates. It is convenient to adopt as its origin the center of panorama compilation of one of the panoramas, while the axes of the abscissa and the z-axis are oriented according to the selenographic meridian and local vertical. The coordinates of one center of panorama compilation are thus given (fig. 14).

The line of visible horizon is used to determine inclination of the axis of panorama compilation. If the visible horizon line is identical to the true horizon line, the pivot axis of the plane of panorama compilation proceeds on the panorama through the intersection points of its track with the horizon line (fig. 19).

Let us take one of them as the origin for the reading. Here the point of greatest departure of the horizon from the track of the plane for panorama compilation has a longitude $\gamma_h = 90^\circ$. Obviously the reduced latitudes β'_h of all horizon points equal zero, because they lie on the horizontal plane which passes through the center of panorama compilation (the dipping of the horizon is disregarded due to small elevation of Luna 9 above the area). From expression (1) we find that $\alpha = -\beta_h$. In other words, inclination of the panorama occurs in the scanning plane where the panoramic latitudes of the horizon line β_h are extreme.

Since the lines of visible and true horizons differ due to the relief, /57 the greatest possible number of horizon points is used to determine α. This reflects clear projections and depressions. Equation (1) is transformed, keeping in mind that $\beta'_h = 0$ and is solved with reference to α_i for a number of horizon points

$$\tan \alpha_i = - \frac{\tan \beta_{h_i}}{\sin \gamma_{h_i}}. \qquad (3)$$

Thus, each time, γ_h is read from the intersection point of the visible horizon line with the track of the panorama compilation plane.

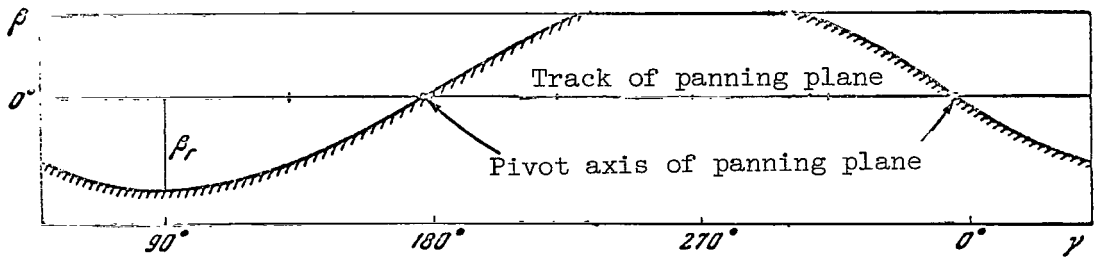

Figure 19. Image of horizon on panorama

The mean is found from the values obtained for α_i, and is taken for the initial approximation. Equation (3) is solved relative to γ_{h_i} for the same horizon points by substituting α'_m in it

$$\sin \gamma_{h_i} = - \frac{\tan \beta_{h_i}}{\tan \alpha'_m}.$$

After setting off on the panorama values γ_{h_i}, which correspond to various horizon points, a certain dispersion of the origins of the reading is obtained relative to that selected initially (at the intersection of the line of visible horizon and the track of the plane of panorama compilation). Mean derivation is found by the formula

$$\Delta\gamma'_h = \frac{\Sigma (\gamma_{h_i} - \gamma_h)}{n},$$

where n is the number of measurements. The origin of the reading of panoramic longitudes is transferred to the point with coordinates $\gamma_h + \Delta\gamma'_h$ and is taken as the new origin of the reading γ_{h_i}. Analogously, the subsequent approximations α''_m, α'''_m ... and $\Delta\gamma''_h$, $\Delta\gamma'''_h$ ... are continued until $\Delta\gamma_h$ differs from zero by not more than one order of magnitude for precise panorama measurements.

The final point of the reading of the longitudes of panorama compilation, found in this manner, lies on the pivot axis of the plane of panorama compilation relative to the horizontal plane, i.e., on line ST (fig. 15) and is identical to point T. The value α_m obtained from the last approximation is taken as the angle of incline of panorama α. However, because the horizon relief is unknown, the angle of inclination obtained should be related to a quasihorizontal plane.

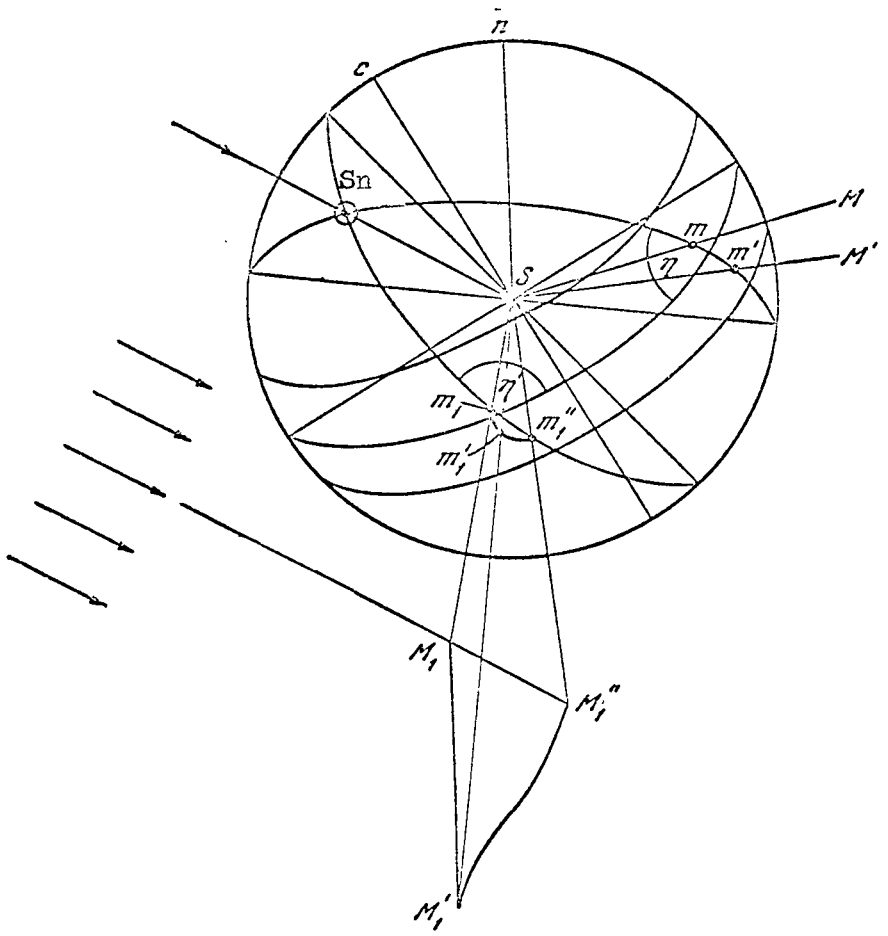

Figure 20. Constructing object and shadow images.

The azimuthal orientation of the panoramas is found from the shadows of local objects. Figures 20 and 21 depict a diagram of such a determination. /58 Figure 20 shows the following: M_1, M'_1 is a local object; $M'_1M''_1$ is its shadow[1]; $m_1m'_1$, $m'_1m''_1$ are images of the object and its shadow; M, M', m, m' are analogous points corresponding to another object; Sn is the image of the Sun on the panorama if it covered the whole sphere. Obviously, identical points of the object and its shadow lie on a straight line proceeding through the Sun and a parallel line SnS. Consequently, the projecting rays SM_1, SM" lie on the plane containing straight line SSn. This plane cuts the panorama along the arc of the large circle $m_1m''_1$, on which lie the images Sn of the Sun, points of object M_1, and shadow points M''_1.

[1]The shadow form depends on the relief of the area where the shadow falls.

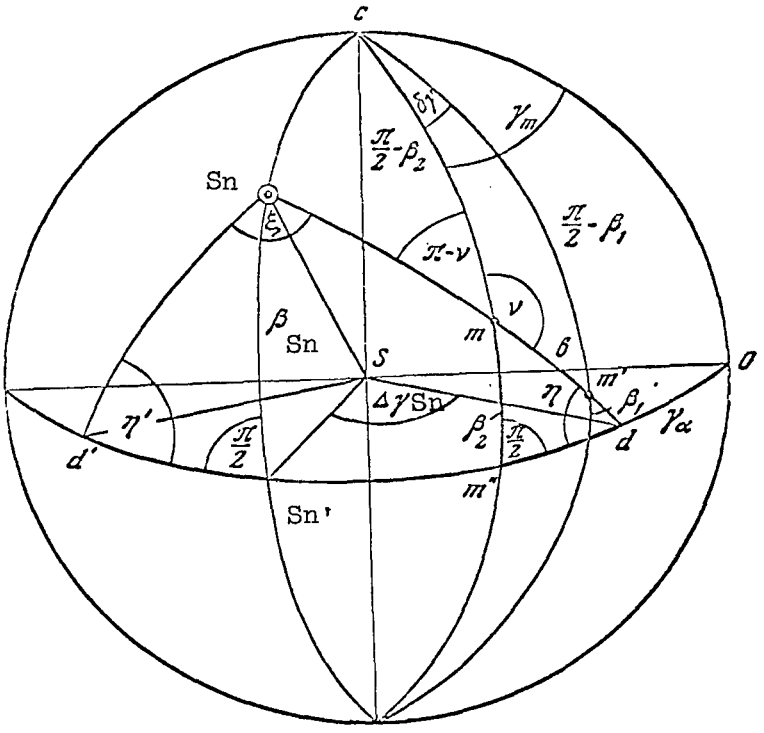

Figure 21. Diagram for determining panoramic latitudes and longitudes of the solar image on the panorama.

The arcs of the large circles uniting identical points of several objects and their shadows intersect at the image point Sn of the Sun. Consequently, after such arcs are found on the panorama, we determine the panoramic coordinates of the solar point in the following manner. /59

From the spherical triangle mcm' (fig. 21) we obtain

$$\cos b = \sin\beta_1 \sin\beta_2 + \cos\beta_1 \cos\beta_2 \cos\delta\gamma.$$

It is obvious that $\delta\gamma = \gamma_m - \gamma_{m'}$, where γ_m and $\gamma_{m'}$ are the longitudes of points m and m'

$$\cos\nu = \frac{\sin\beta_1 - \cos b \sin\beta_2}{\sin b \cos\beta_2}.$$

From the triangle mm"d we determine the angle of inclination of plane Snmm'd to the plane of panorama compilation

$$\cos\eta = \cos\beta_2 \sin\nu,$$

and also

$$\sin \delta'\gamma = \tan \beta_2 \cot \eta,$$

where $\delta'\gamma = dm''$. The longitude of the intersection line of the plane Snmm'd with the plane of panorama compilation is obtained by the formula

$$\gamma_d = \gamma_m - \delta'\gamma.$$

The values γ_m, $\gamma_{m'}$, β_1, β_2 are measured directly from the panorama. /60

Angle η and point d, having a longitude γ_d, determine on the panorama the position of the arc of the large circle which passes through the point of the Sun and the image of a certain object and its shadow. Angle η' and point d' for another object can be found analogously.

Thus, in the spherical triangle dSnd' (fig. 21) we know angles η, η' and side $dd' = \Delta\gamma$, which is equal to the difference of panoramic longitudes of points d' and d. Consequently,

$$\cos\xi = -\cos\eta \cos\eta' + \sin\eta \sin\eta' \cos \Delta\gamma.$$

From this triangle we obtain

$$\cos a = \frac{\cos\eta' + \cos\eta \cos\xi}{\sin\eta \sin\xi},$$

where a = Snd.

From the right triangle SndSn' we find

$$\tan \Delta\gamma_{Sn} = \cos \eta \tan \alpha,$$

$$\tan \beta_{Sn} = \sin \Delta\gamma_{Sn} \tan \eta.$$

The value β_{Sn} is the panoramic latitude of the Sun. The panoramic longitude of the Sun γ_{Sn} is determined after adding to the longitude of point d the value $\Delta\gamma_{Sn}$

$$\gamma_{Sn} = \gamma_d + \Delta\gamma_{Sn}.$$

Reducing γ_{Sn}, β_{Sn} on a horizontal plane, we find the elevation of the Sun above the horizon $\beta'_{Sn} = h'_{\odot}$ and the horizontal panoramic longitude γ'_{Sn}.

As soon as the landing site coordinates and panorama compilation times are known, the solar azimuth $A_{\odot}$ and its calculated elevation $h_{\odot}$ can be determined. The convergence $h'_{\odot}$ and $h_{\odot}$ is the control for determining the local vertical and constructions on the panorama. After $A_{\odot}$ is known, the azimuth of the axis of inclination of the panorama can be calculated as follows

$$A_T = A_{\odot} - \gamma'_{Sn}.$$

To construct the spatial intersection from stereopairs formed as a result of Luna 9 inclination, it is necessary to find the base--the distance between the centers of panorama compilation. This can be done graphically after constructing from the reduced panoramic longitudes plans of points formed in the mirrors of both panoramas. If these plans are placed one on the other and identical points are superimposed, the centers of panorama compilation on the plans will not coincide. The straight line uniting them is a projection of base B' of the panoramic stereopair on a horizontal plane. A vertical constituent of the base can be found by calculating, according to the reduced panoramic latitudes, the heights of elevation of terrain points represented in the mirrors of both panoramas. /61

Taking the mean of the differences of elevation increments of indentical points, the elevation height of one panorama compilation center above the other is obtained. This problem can be solved analytically by adopting the known formulas of inverse spatial intersection.

3. Construction of a Topographical Plan of the Terrain

The first and third panoramas were used to construct the plan. Identical terrain points depicted on the actual and virtual panoramas (reflected in the mirrors) were identified and labeled. Thus it was found that to a certain extent identical points were represented on both panoramas in the mirrors. The overlapping parts of the panoramas were then viewed under a stereoscope and characteristic formations were deciphered--craters, rocks, ridges and level sections of the terrain differing in structure. In stereoscopic analysis there appeared certain decipherable indications of the formations used to study those sections of the panoramas where the stereo effect is absent or inadequate.

The indications are as follows:

--for craters: an ellipsoidal nature of the contour, a shadow within the contour, a characteristic change in contrast relative to the surrounding

terrain (if contrast is understood as the ratio $K = D_1/D_2$, where D_1 is the photographic density of the diapositive image beyond the limits of the crater's contour and D_2 is the same within the contour, then $K > 1$ for the illuminated side of the crater and $K < 1$ for the shaded side);

--for rocks: irregularity of contour, deep shadows outside the contour, spots of light--sections with a very small photographic density of diapositive image (light, almost white spots on the side opposite the shadow);

--for ridges: elongation of contour, absence of deep shadow, a small density of the image on the side exposed to the Sun and a somewhat larger density on the opposite side, large structure within the contour; /62

--for level sections with fine structure: an overall low mean density of image due to absence of deep shadows from small roughnesses, absence of a noticeable splitting of the image;

--for level sections with coarse structure: a more or less uniform alternation of light spots on a dark background or a comparatively large mean-density of the image due to shadows from roughnesses, the presence of seperate impregnations noticeably distinguished in size from broken elements of the overall background.

These indications must not be considered absolute in view of the perspective nature of the image and the rapid decrease of the scale from the near edge of the panorama to the far edge. They need a logical interpretation for various sections of the panorama, taking into account their location and direction of illumination.

Reliability of deciphering is correspondingly unequal. It can be considered adequate for sections of the plan close to zones of good stereo effect, where fine elements of surface structure are examined by volume. As these zones recess, the deciphering takes on an even more hypothetical nature. (In figure 22 the results of the deciphering are described by panorama a.)

Over 200 stakings necessary for composing a topographical plane are selected and labeled at the same time as the deciphering at characteristic points of the relief and planimetry. The stakings were chosen on noticeable folds of the relief, on crater edges, at the base and, where possible, on the tops of rocks and ridges. In view of the deep shadows on the first panorama, stakings could be selected on the floor of craters in only a few cases.

Scales of panoramic latitudes and longitudes were laid out according to the constructional data on the panoramas, and the coordinates of all designated terrain points were determined according to them.

Orientation of the panoramas was determined from the horizon and shadows of terrain features by the method described in section 2 of this chapter. Table 5 presents the obtained solar elevations, angles of inclination of the panoramas and the azimuths of the axes of inclination.

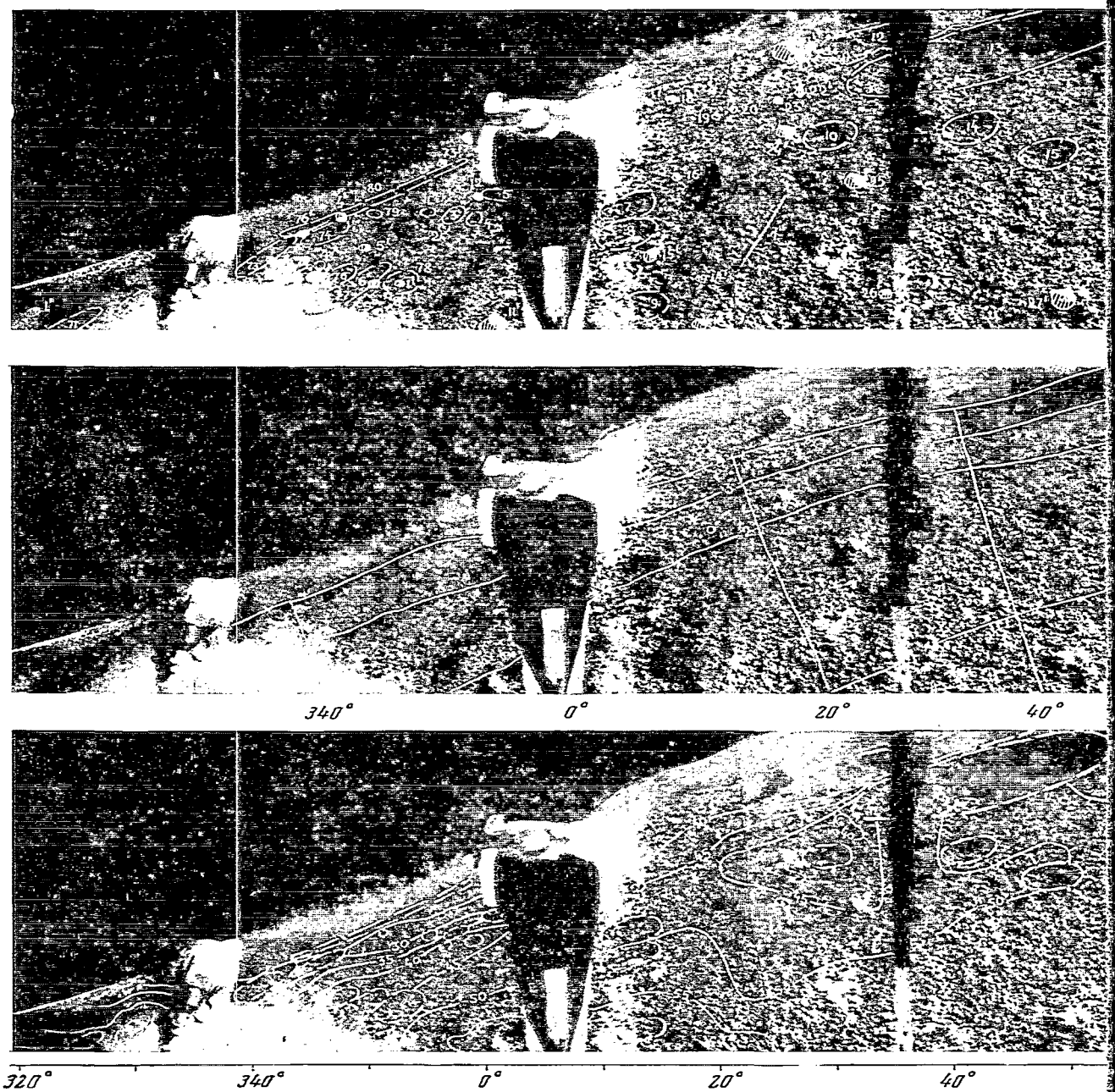
a
b
c
340°
0°
20°
40°
320°
340°
0°
20°
40°

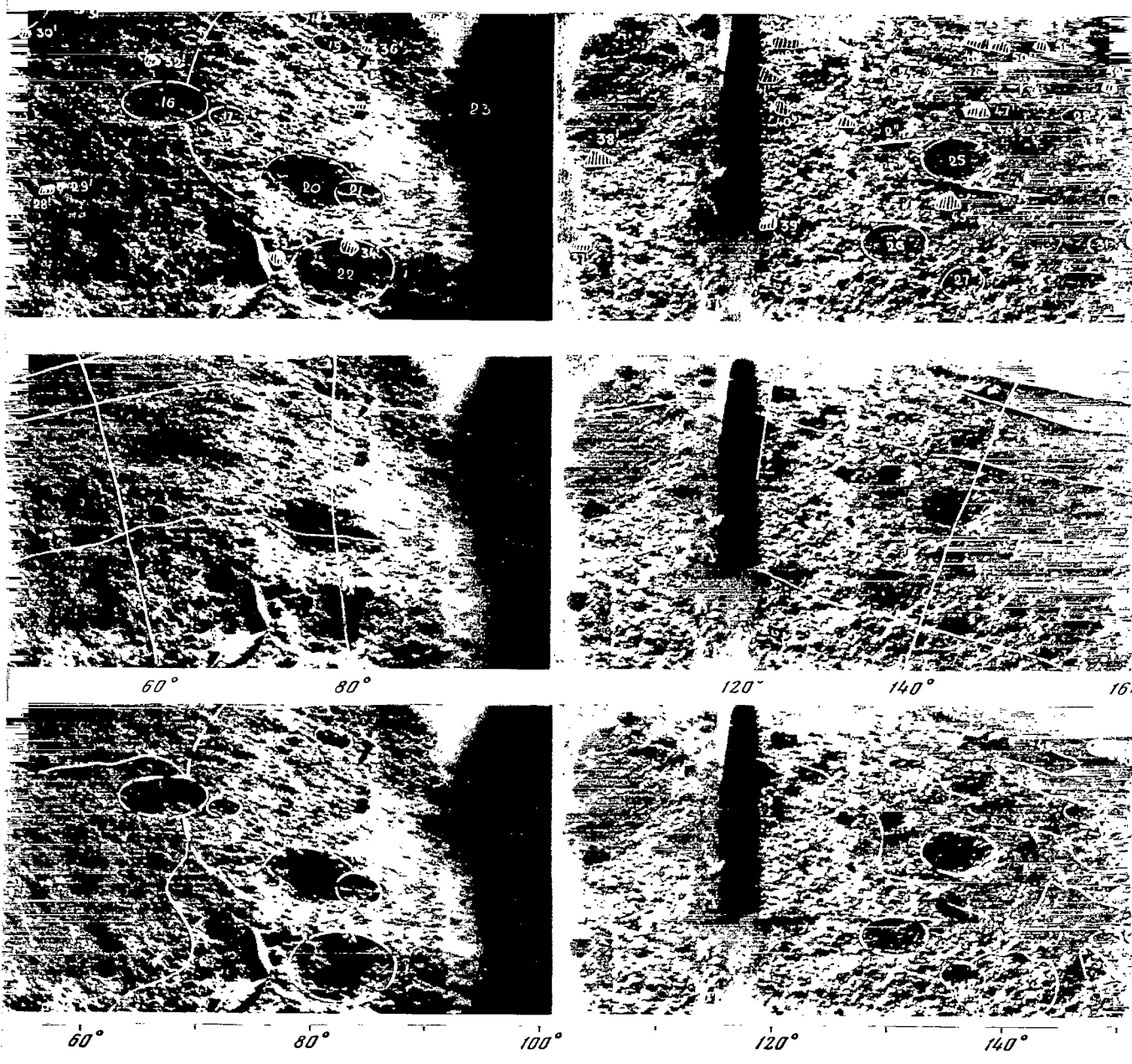
60°
80°
120°
140°
60°
80°
100°
120°
140°

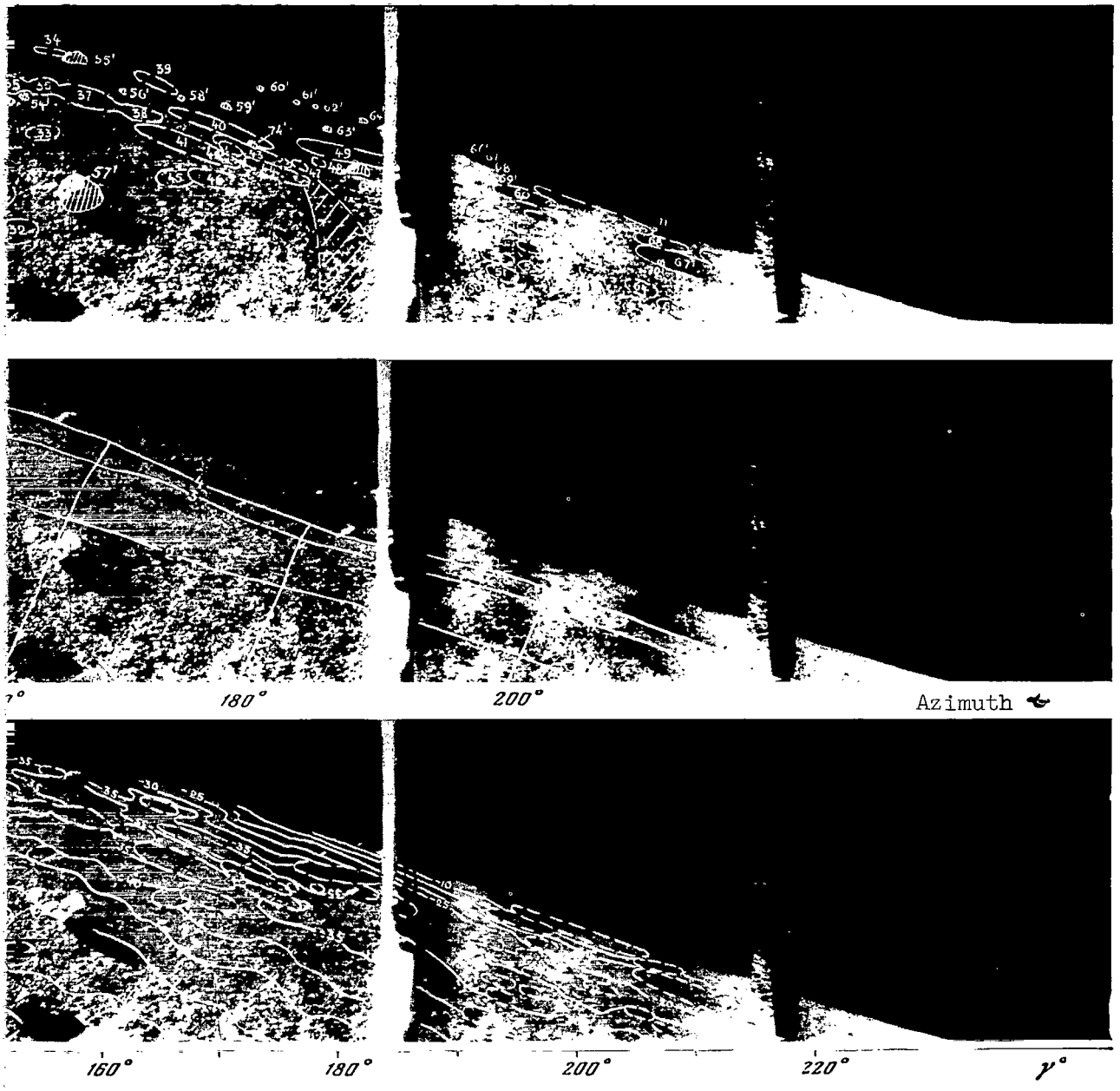

Figure 22.

a, Results of panorama deciphering; b, image of range lines; c, image of contour lines.

TABLE 5

No. of panorama	Date and time of exposure	Solar elevation	Absolute angle of inclination	Azimuth of inclination axis
1	4 Feb 4 hr 50 min 6 hr 37 min	7°30'	16°30'	169°
3	5 Feb 19 hr 00 min 20 hr 41 min	26°18'	22°40'	173°

Using these data, panoramic latitudes and longitudes of terrain features were reduced on vertical and horizontal planes. Necessary calculations were made on computers.

All measurements were made according to the original panoramas. The /63 scale of their image is such that one line has a width of about 0.4 mm. This predetermined the expediency of making the panorama measurements graphically. (As is known, 0.08 mm constitutes the precision of graphic measurements.) For this reason the stakings were plotted on the plan by a graphic-mechanical method with the aid of a device which constructs the intersection mechanically. The sequence of tasks is as follows:

The actual and virtual centers of panorama compilation for the third panorama were plotted on the chart board to a scale of 1:10 (1 cm on the plan corresponds to 10 cm on the terrain). The meridian was designated, and we drew the axes of incline of the plane of panorama compilation relative to the horizontal plane, which correspond to the actual and simulated centers of panorama compilation. From them we plotted the reduced panoramic longitudes of identical terrain points which were represented on the actual panorama, and the plane intersections were constructed in the mirrors. The plan position of these points was found by the method described in section 1 of this chapter.

The distances from the centers of panorama compilation to all points were taken from the plan, and the excess elevations of terrain points over the quasihorizontal plane passing through the actual center of panorama compilation on the third panorama were determined by means of the reduced panorama latitudes (vertical angles). This plane is adopted as the one for the plan to which the excess elevations of all remaining terrain points were referred. The elevations of the virtual centers of panorama compilation relative to the actual center (elevations were found by reducing the virtual bases on the quasihorizontal plane), were considered in determining the elevation excesses.

The construction was performed for images reflected by one side of the first mirror, two sides of the second mirror and one side of the third mirror.

Two sides were not used in the process, since they were found to reflect the sky.

Thus, four direction point lines were obtained on the plan (fig. 23). Internal control was maintained in constructing the lines of direction. /64 For each line of direction the elevation excess of the points is determined twice--relative to the actual and virtual centers of panorama compilation. The divergence of the elevation excesses did not exceed 4 cm and had a root mean square value of ±1.5 cm. Furthermore, the first and second mirrors were oriented so that two lines of direction in the plan intersected. Several identical points were identified in the intersection zone. This permitted control of the position of such points on the plan and by elevation also. The divergences in the plan did not exceed 1 cm on the terrain (1 mm in the plan); divergences in elevation have the same order as within one line of direction. Since the construction principle for all direction lines is the same, the other two lines of direction obviously have the same precision.

The direction lines described were adopted as the geometric framework for constructing the plan of the terrain as a whole.

Furthermore, the positions of the center of panorama compilation of the first panorama and the base of the panoramic stereopair were found by the method described in section 2 of this chapter, the axis of inclination of the first panorama was plotted on the plan, the plan intersections of stakings were laid out according to reduced panoramic longitudes, plan distances to stakings from the first and third panorama compilation centers were taken, and the elevation excess of corresponding terrain points on the quasihorizontal plane was found according to the reduced latitudes of the stakings. The magnitude of base B (in nature) proved to be equal to 9 cm, the angle of inclination of base $\alpha_B = 6^\circ 20'$, and the excess elevation of the center of panorama compilation of the first panorama above the quasihorizontal plane is 1 cm.

Convergence of elevation excesses found from one or another center of panorama compilation was the internal control. The order of divergences proved to be the same for the lines of directions.

Because the intersection of stakings in the plan took place at a very sharp angle (for near points about 5°, for distant points up to 10'), the correlation of stakings according to a position relative to the points of lines of direction was made where necessary.

Certain stakings for control were constructed twice: by the graphic-mechanical method already described and by an analytical method. A convergence of the same order as above was obtained.

Stereo-intersections obtained were inadequate in the sector near 60°, which is located on the continuation of the base to the east from the center of panorama compilation. In this zone (fig. 23) the layout was plotted on the plan according to the perspective grid. Construction of the plan was not successful in the sector around 100° from the western side, because the terrain was not obtained on this part of the panoramas (the television camera was aimed

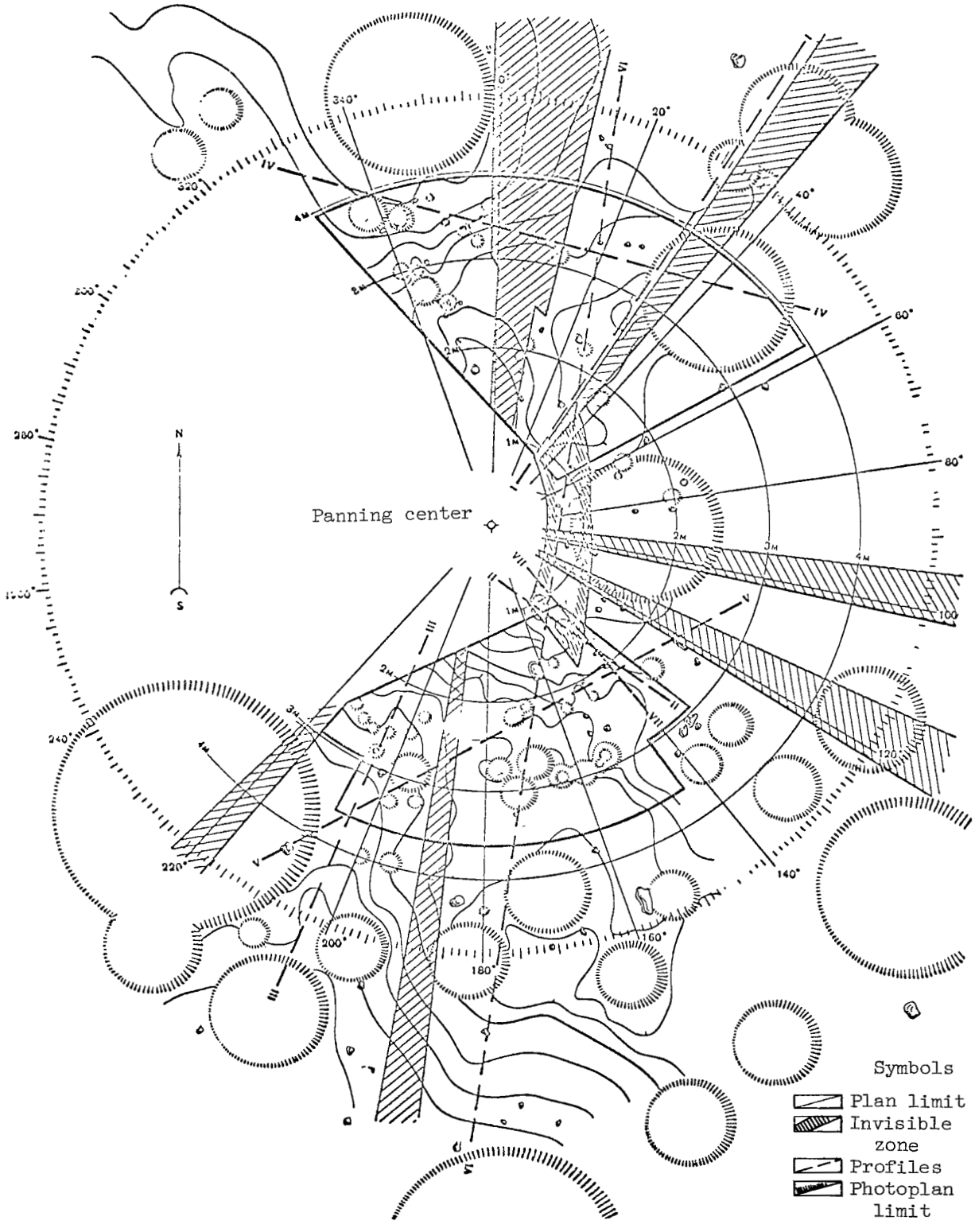

Figure 33. Dispositions of linear structures in the panorama.

into space). Furthermore, there are seven narrow sectors in which details /66
of the station (lock, antenna, mirrors) screened the terrain. These sectors actually did not interfere with composing the plan, since the layout hidden by them is easily interpolated from adjacent sections.

The horizontal lines were then drawn on the plan, by interpolation between stakings, at intervals of 5 cm in elevation. The layout of horizontal lines was corrected by stereoscopic observation of the photographs.

The topographical plan obtained was quite uneven in precision for various sections, both because of the rapid diminution of the intersection angle and because of the perspective, which hinders reliable determination of image contours. In the final view it is therefore presented in two variants. The first includes the central part of the section encompassed by the panoramas. This section is given to a 1:20 scale and is characterized by a root mean square error of point positions in the plan of the order of ±10 percent and ±2-5 cm in elevation.

The second variant embraces the whole section treated photogrammetrically. It is given to a scale of ~ 1:40 and should be considered a diagram. It is not possible to evaluate its accuracy. Both variants are presented in the third part.

In comparison with the plan, the diagram is somewhat generalized. In particular, the smallest craters are not indicated.

A mosaic photoplan of the terrain to a 1:6 scale, composed of separate reconstituted photographs, was prepared for a limited section shown on the diagram (fig. 23). Fragments of the three panoramas were used. Small sections delineated by lines of equal latitude and longitude forming the rectangle grid were laid out on the panorama for this purpose.

By the method described in section 1 of this chapter, this grid was reduced on several intermediate planes inclined with reference to the plane of panorama compilation at various angles. Separate sections of the panoramas were reconstituted on the phototransformer so that the section boundaries coincided with the lines corresponding to them on the first grid established on the transformer screen.

The photographs obtained in each such operation were reconstituted by the following grid, etc., until the image again became a plan image. The mosaic thus created is installed on the survey plot containing the plan perspective grid, which is identical to the grid laid out on the panorama. Thus /67
each element of the mosaic was established on the grid in a corresponding fashion. Because the section of terrain on which the photoplan is composed has an insignificant relief, a satisfactory convergence of contours according to the cuts was obtained (divergences do not exceed 1.0 mm).

In reviewing the reconstituted photographs included in the third part, it should be remembered that the angles of inclination of panorama sections relative to the plan range from 54 to 70°. Therefore, separate microelements of

the relief actually appearing on the lunar surface create "dead" (opaque) sections on the panoramas. When these elements are reconstituted on the plan, they appear to be lying on their sides, resulting in distortion of their form. This is particularly noticeable on the edges of the photoplan.

4. Topographical Features of Luna 9 Landing Site

Panoramas with range grids and horizontals and the previously described plan and diagram and profiles of the terrain serve as initial material for topographical analysis.

The range grids and horizontals were transferred to the panorama (fig. 22, b and c) from the plan according to the stakings by comparing their position on the plan and on the panorama. The range lines correspond to the circles located every 1 m on the plan concentric to the projection of the center of panorama compilation of the third panorama.

The profiles of the terrain (fig. 24) are constructed with the aid of the topographical plan. Three profiles correspond to the lines of direction described previously and three others are laid out along the directions which are the most interesting from the viewpoint of surface morphology. Profile placement in the plan is indicated on a diagram (fig. 23). For greater clarity the vertical scale of the profiles is twice that of the horizontal.

The landing site is a quite level surface with a well-defined relief with hills noticeable on the line of apparent horizon.

The most characteristic forms of mesorelief are craterlets and craters, i.e., rounded depressions-small holes of various dimensions. No system is observed in the location of these depressions. Some are isolated, others are /68 grouped and still others overlap. Small craterlets are encountered within and on the slopes of the larger. Small mounds are noted in the center of some small recesses.

The nature of the horizontals allows the supposition that Luna 9 lies on the western slope of a large depression, possibly a lunar crater which, due to its dimensions and the limitations of the field of vision, is only partially viewed on the panoramas. By stereoscopic examination, the "edge" of this crater is observed as the limit of surface rise, beyond which proceed the depression in the northern section of the panorama and the terrace-like surface in the southern section. If the crater edge is extrapolated on the plan and the circumference is considered, its diameter proves to be approximately 14-15 m. By analyzing the profile, it is possible to establish that the crater depth is $\sim$ 60-70 cm. All craters and craterlets visible on the panorama have smaller dimensions, from 3 to 10 cm in diameter and from 20 to 2 cm in depth.

Sharp folds and surface cracks, which impede movement under terrestrial conditions, are completely absent in the surveyed zone. On the whole the

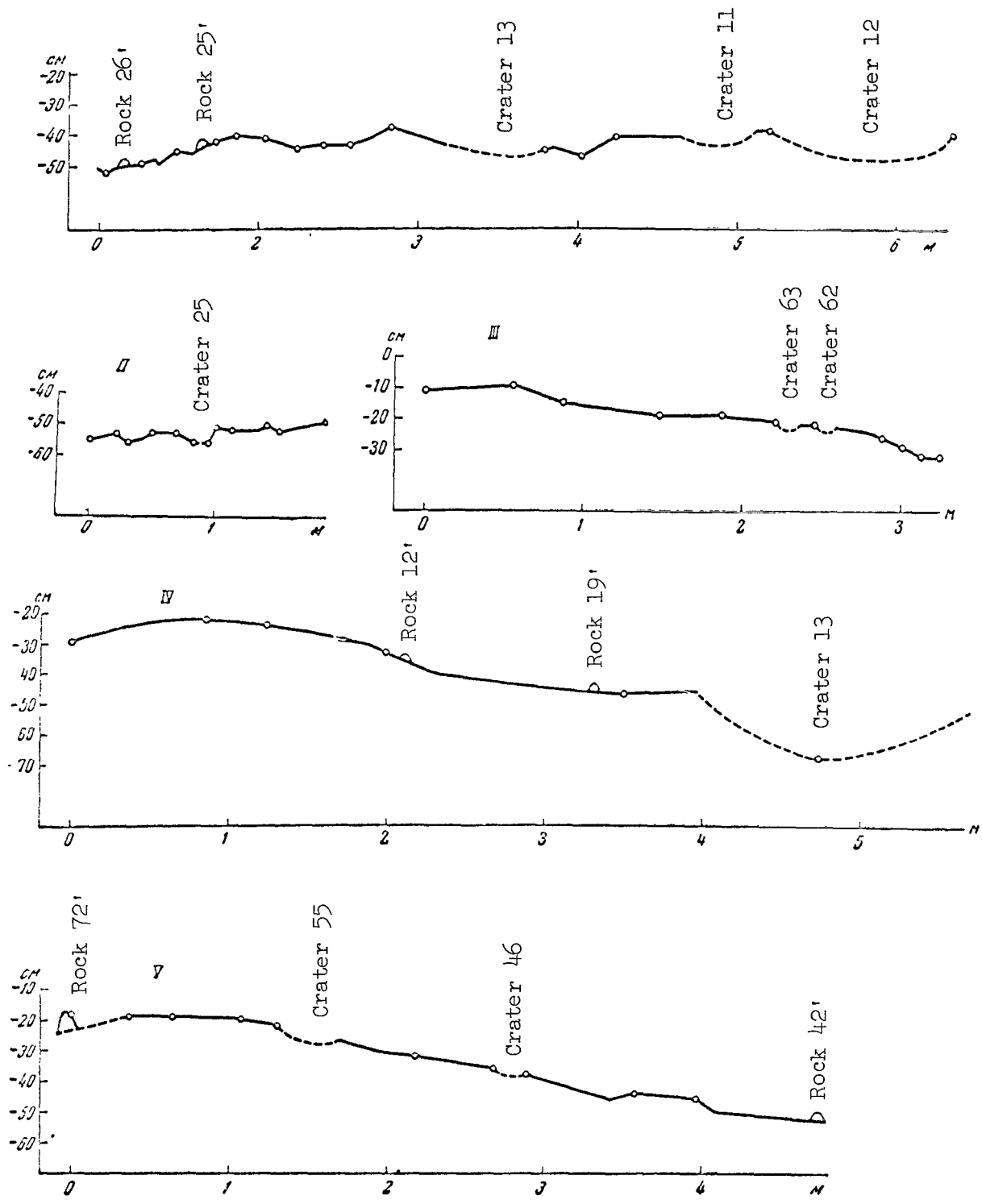

Figure 24. Profiles of selected directions.

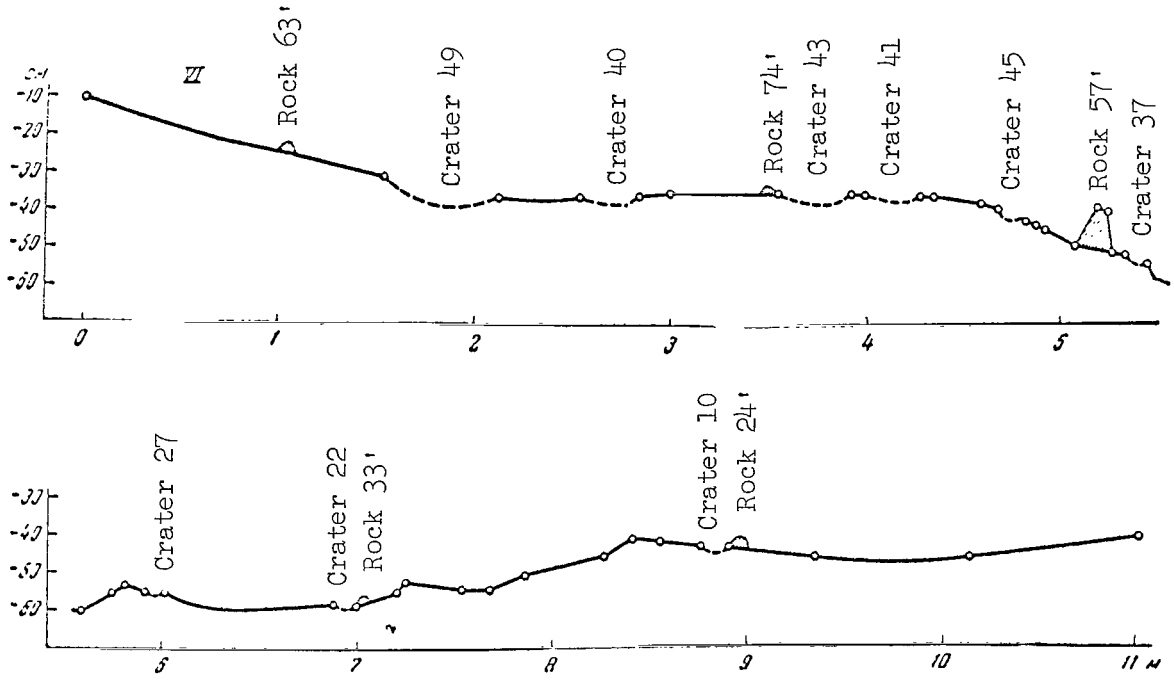

Figure 24 (continued).

relief is comparatively smooth, though its structure is quite complex, a fact testified to by the winding nature of the horizontals. Gently sloping hillocks, depressions, ravines and anticlines are encountered on the slopes of the large crater. /70

Because elevation heights are given relative to the quasihorizontal plane, it is not possible to determine the overall grade of the terrain. The local grade of the slopes of the large crater is approximately 0.09 (5°).

As shown in section 3 of this chapter, in view of the deep shadows and perspective of the image, the internal parts of craters cannot be shown by horizontals. Therefore it is not possible to judge their cross section and actual distribution of gradients on the basis of the same stereophotogrammetric data. Distribution of gradients within the large crater can be traced along the profile.

Another widespread element of the landscape is clod-like or rock-like objects above the topographical surface, which for brevity in the future will simply be called rocks. In their seemingly chaotic distribution a certain orderliness is observed, due to the fact that the rocks are frequently seen close to crater edges. The dimensions of the rocks vary from several centimeters to several decimeters both in the plan and in height.

Small ridge-like projections and sections of ground possessing different microsculpture should also be related to the images creating the topographical

layout. The wrinkles of the ground with dimensions on the order of 1 cm and less are designated here and below as microsculpture.

The ridge extending in the meridian direction is identified on the plan. Other ridges possibly exist, oriented otherwise and remaining unnoticed because of the absence of contrast in the illumination of their slopes.

The microsculpture of the ground surface has essentially a "pitted" porous nature. Dimensions of individual roughnesses noticed in the pictures are of several mm. This can be judged by comparison with the dimensions of the belt appearing in the detail of the station, seen on the third panorama near $\gamma \approx 75^{\circ}$ and having a 13 mm width. The roughnesses are combined in local groups measured in centimeters. They appear variegated due to a combination of clearly illuminated and shaded sections.

Sections on which groups have an almost linear location with an extension to several decimeters stand out on the background of such a structure. /71 Some are recorded on the plan.

In evaluating the terrain in the Luna 9 landing area we note that it is quite complex for orientation purposes. This is due to an extreme monotony in the landscape, an absence of noticeable orientation points, a masking of the layout by the relief and a limited field of vision for observation from depressions. In this regard the terrain resembles terrestrial rocky deserts.

CHAPTER 2. MORPHOLOGICAL FEATURES OF LUNAR SURFACE

The panoramas obtained by Luna 9 contain much material for studying /72
the morphological and geological features of the landing site. Details show a number of characteristic types of formations appearing repeatedly in the panoramas. The uniformity of the structure of widely separated details excludes the possibility that the forms observed are created by random lighting effects or random arrangement of unrelated elements. This is true of very small formations in particular.

Investigation of the landscape surrounding the station may yield important information on processes occurring on the lunar surface and on properties of the lunar substance.

In this chapter, we shall stress the elucidation and phenomenological description of the observed forms. References to the nature of the surface and formative processes will be limited to the most obvious aspects.

Comparison of the lunar landscape features with the forms of various familiar terrestrial landscapes is based on visual comparisons to a considerable extent. This comparison involves some difficulty due to inclination of the axis of the television system to the lunar vertical, with the result that a panorama of the lunar surface acquires an unfamiliar form, as the inclination of the horizon line to the frame of the panorama varies in its different parts. It is essential to attempt to eliminate the visual impression of an iso- /73
lated hill with comparatively steep slopes. Therefore, to obtain a more accurate idea of the lunar landscape shown in figure 25, we have presented a panorama with a corrected horizon line, i.e., oriented parallel to the frame of the picture.

For the transformation performed with the aid of a rectifier, panorama I was divided into sections bounded by vertical lines separated by 12° intervals. Each section was rectified separately, on the assumption that the image could be replaced within its bounds by a plane photograph constructed according to the laws of central projection. This did not introduce important errors. The divergence of details of the image at the joints, which was greatest in the lower part of the panorama, did not exceed 0.5°.

The lunar landscape appears to be generally flat in the panorama with the corrected horizon line. The most outstanding positive relief forms, i.e., elevations, are visible in the southwestern-western part of panorama I ($230-270^{\circ}$). These are two hills with slopes of $12-14^{\circ}$.

From examination of the pictures, morphologic comparison of similar details in different regions of the panorama and comparison of panoramas taken with different altitudes of the Sun above the horizon, we distinguish the following characteristic types of details in the surface structure: /74

1. "Depressions" or "craters"--circular holes of small dimension having as a rule no embankment or a scarcely noticeable embankment. In the text these are often called craters, as is the accepted practice for known lunar formations; these terms are used synonymously.

2. Linear structures with individual elements arranged along a line. These structures intersect in various directions, at times forming characteristic rayed and forked formations.

3. Stones.

There are many interesting sections with a complex relief that permit various interpretations. As an example, we shall show some in a much enlarged form (fig. 26).

In addition to the clear-cut forms, the panoramas show intermediate, mixed or ambiguous details, apparently caused by the repeated action of various processes of endogenic and exogenic nature. The latter appear as the result of impacts of meteorites and stones, as well as the action of solar wind particles.

Negative forms having the appearance of circular holes or craters (sinks), which are characteristic of the entire surface of the Moon, constitute the dominant type of relief of the section under study.

We shall now give a description of the formations seen in the panoramas.

a

b

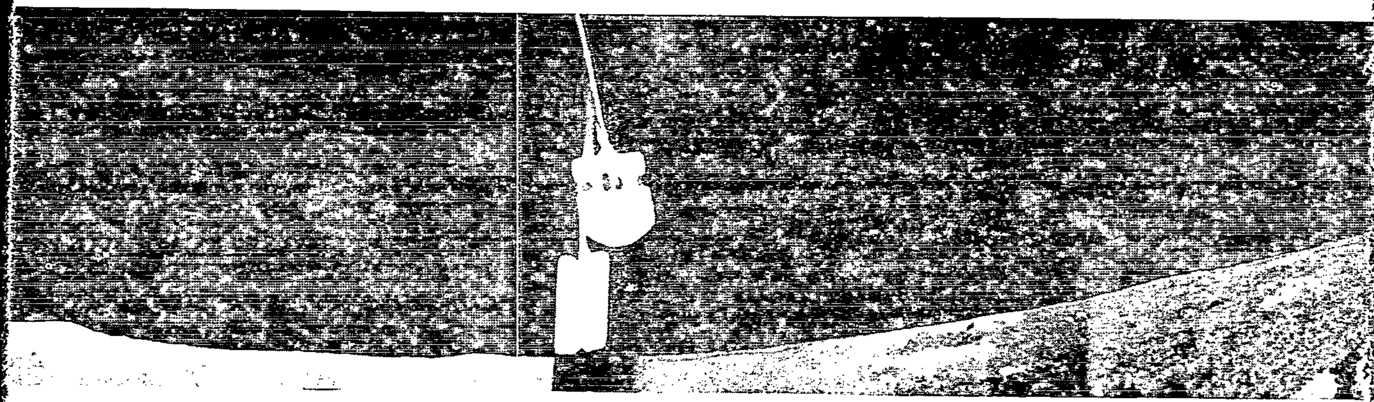

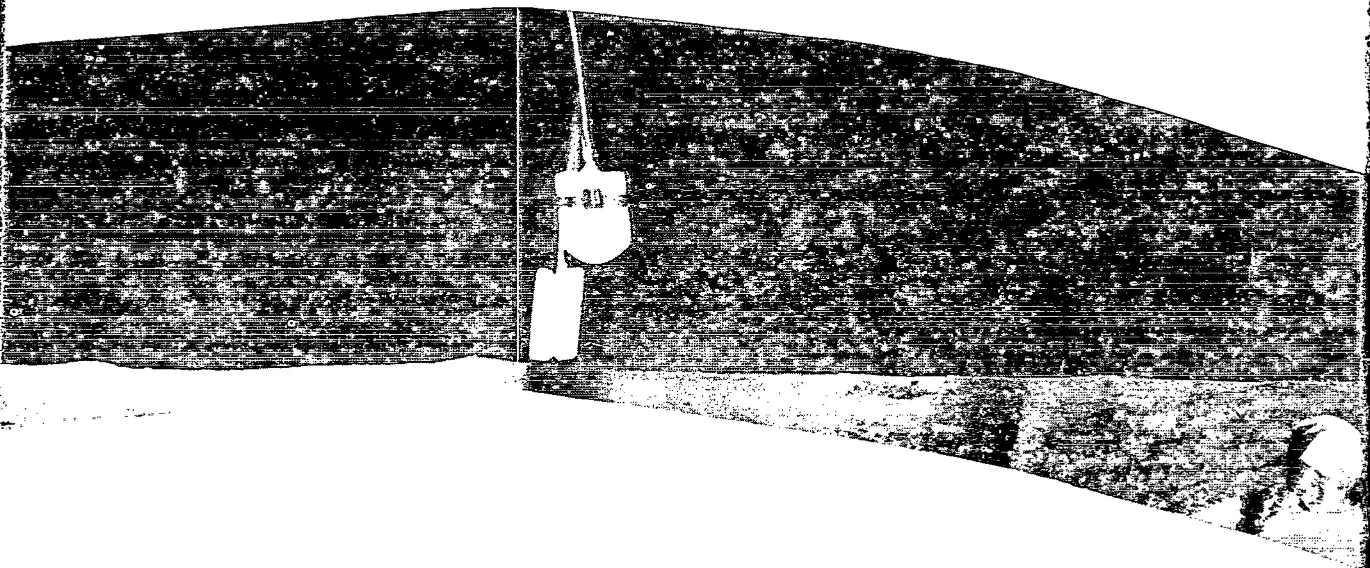

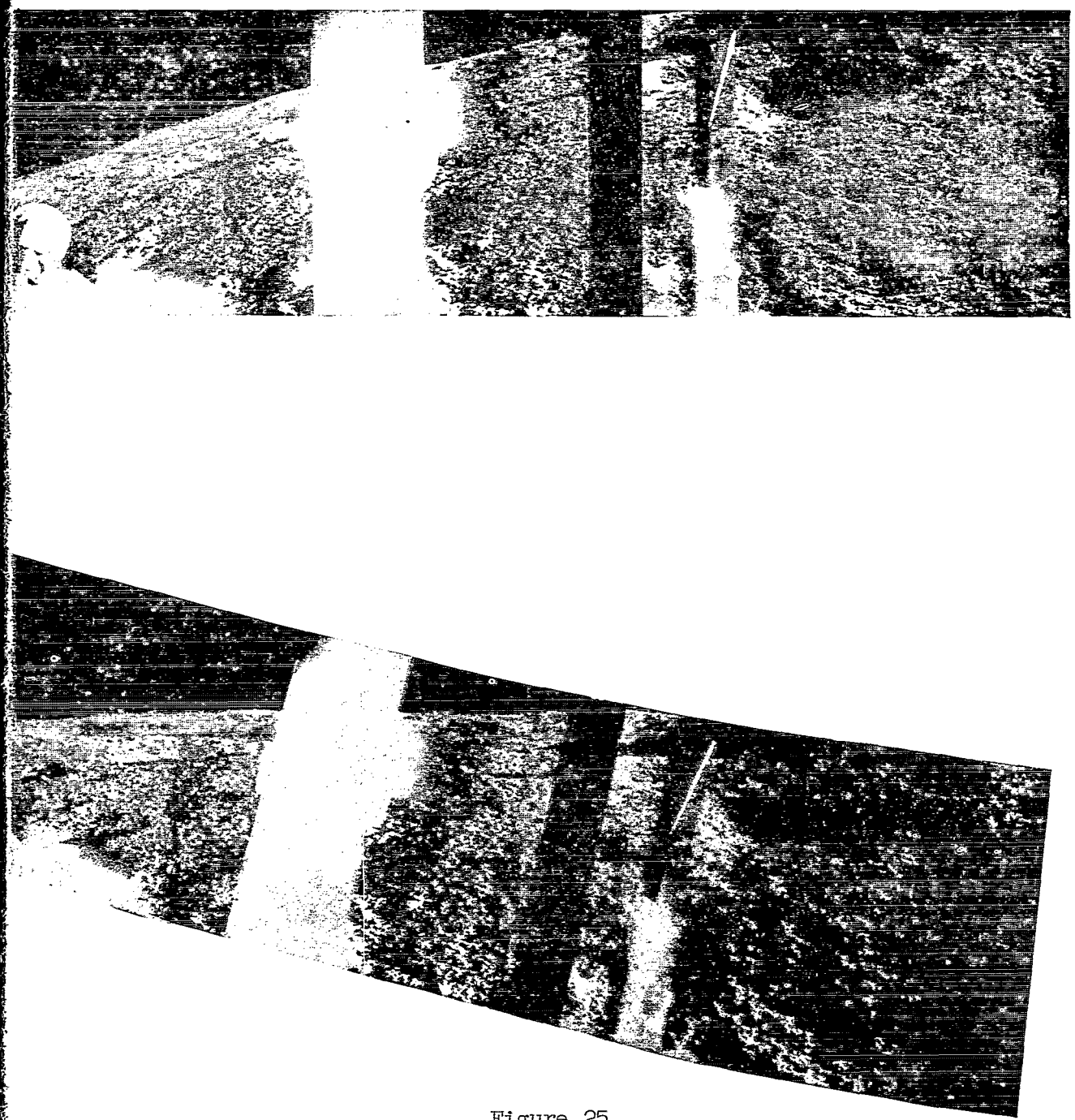

Figure 25.

Sweep and transformation of panoramic photographs. a, Panorama I, obtained at 16° camera inclination; b, panorama I, transformed to the view at zero inclination.

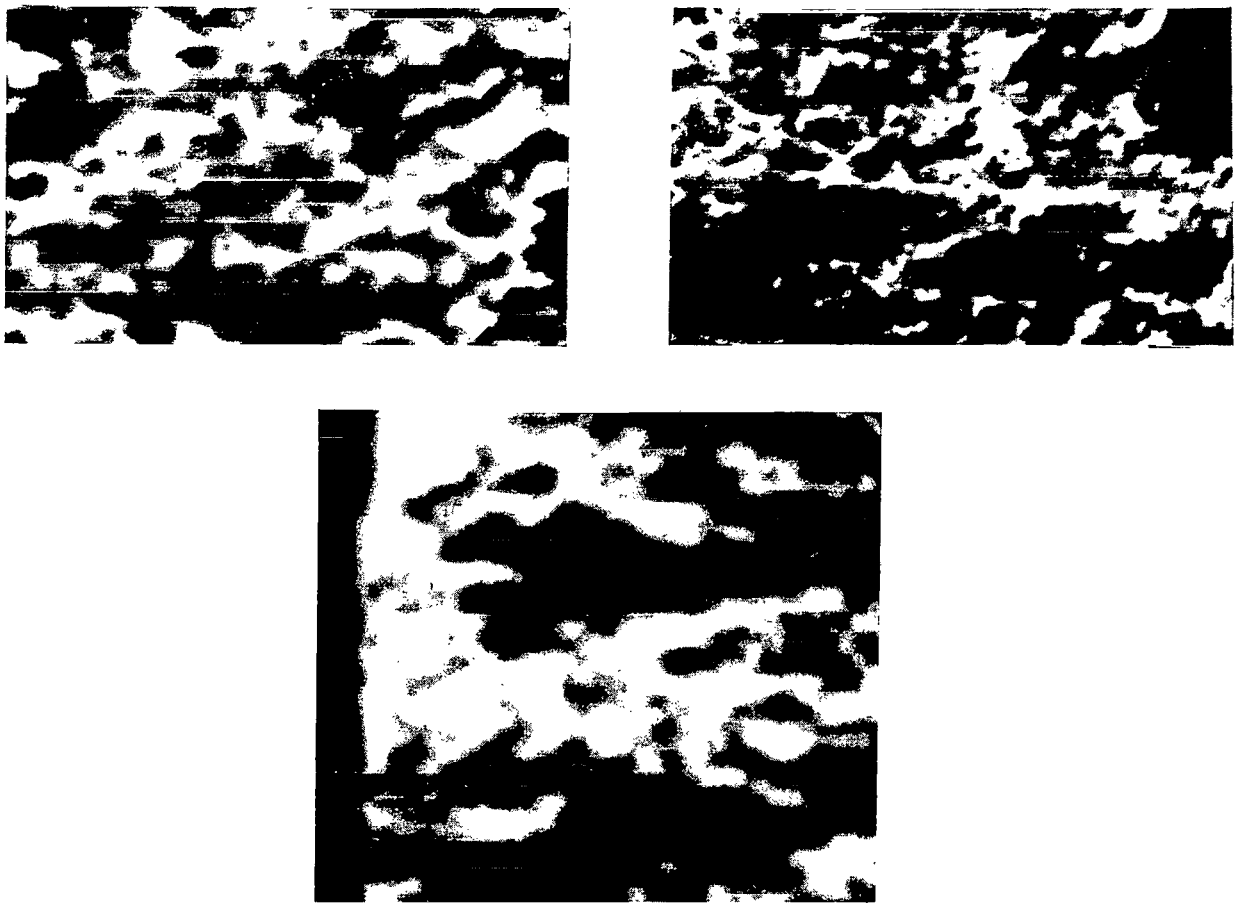

Figure 26. Details of images with complex structure.

1. Depressions

The largest depression in the right part of the panorama (panorama I, 200-230°) has a diameter of about 2.8 m. The smallest of the depressions, which are clearly noticeable and shown in the plan, have a diameter of about 10 cm.

Table 6 gives the statistical size distribution of depressions shown in the central section of the plan.

Here, D is the depression diameter, N is the number of depressions noted in the plan, and S is the area in which the depressions are counted, that is, 15 m^2. The size distribution of depressions can be approximated by the /75 power function $N' = cD^{-n}$. The values computed by this formula with $n = 3.5$ are given in the third column.

TABLE 6.

D, cm	N	N'	$\frac{N}{S}$, m^{-2}
6-9	6		
10-12	11		
13-15	14	11.7	0.93
16-18	8	8.9	0.53
19-21	6	5.4	0.40
22-24	3	3.2	0.20
25-27	2	2.1	0.13
28-30	2	1.5	0.13
31-33	2	1.1	0.13
34-36	1		0.06
37-39	2		0.13
40-45	2		0.13

Table 6 does not include depressions (holes) located far from the station. A total of 88 depressions were counted in an area of 50 m^2 in the topographical layout.

In addition to the small amount, the cited statistical data have two other important shortcomings. In the first place, small depressions are not clearly visible on the slopes of larger formations or far from the station. In the second place, the plan does not show all depressions, but only those whose distances were determined sufficiently reliably by the stereoscopic effect, that is, the sample of depressions is not complete.

The minimum size of the clearly observed depressions is about 5 cm. It is comparable to the sizes of the structural formations of the porous lunar surface, which is the background against which the circular form of the depressions is lost and the edges acquire ragged, irregular outlines. It is possible that this corresponds to continuous overlaying of depressions. Only in rare cases is it possible to distinguish circular depressions with a diameter of less than 5 cm.

Individual depressions are encountered everywhere in the panorama, both on the slopes of larger depressions and possibly on the surfaces of a number of stones having areas similar to conchoidal fractures and shallow surface pitting. Small depressions are often closely grouped. In such cases they form raggedly cellular sections. Individual cells within groups usually have irregular edges and sometimes acquire a honeycomb structure.

Judging by shadows, the steepness of the interior slopes of depressions measuring more than 10 cm at times exceeds 41°, which is clear in figure 27, showing the fragments A and B obtained during an additional television transmission during the night of 6 and 7 February. All sorts of slopes, possibly

including negative angles of interior cavities in the soil, are encountered /78 in the smaller depressions which merge into cells of the terrain.

In the plan based on stereoscopic determinations of distances, it was possible to measure the depth of five depressions measuring 10-20 cm, which had a diameter-to-depth ratio of 6:4, and one depression with a diameter of 1.6 m having a similar ratio of 9:6. In this case, the slope is as steep as 55° in one instance, if we approximate the depression by a cone, because it lies on the steep edge of another larger formation. In fact, many depressions are cup-shaped, thus the limiting slope may be still larger, which is evidence of sufficient cohesion of the terrain.

Schematic cross sections of these depressions are shown in figure 28. The following are shown for each cross section: M - scale, D - diameter, D/h - diameter-to-depth ratio of the crater. It was possible to construct profiles of seven depressions by changes in the position of the edges of shadows as the Sun rose above the horizon. In this case, only the plane of the solar vertical passing through the center of the crater was considered. A drawing was made for this plane in which the points of the beginning and end of shadows were plotted in accordance with three panoramas. The diagram in figure 29 shows how the position and size of its shadow depends on the crater form.

Moreover, taking the diameter of the depression on the plan as the initial dimension and assuming it to be axisymmetric, this drawing was made to coincide with its mirror image and the missing sections of the contour were filled in. When a crater is asymmetric, a mismatch may result, as was apparently the case for depression No. 15. Results are given in figure 30. The points correspond to actually determined values and are joined by solid lines. The remaining part of the profiles constructed on the assumption of the symmetry of depressions is filled in with dashed lines.

Stereoscopic examination of the panoramas shows that the interior edges of a part of the depressions and sinks do not have a cup-shaped or conical form, but are flared out above and resemble the shape of a phonograph loudspeaker. This can be seen in craters Nos. 13 and 16 in figure 30. This property is partially reflected in the topographical plan as their inclination to a trough-like shape denoted by horizontal lines. Clarification of the true nature of sinks with bell-mouth openings, also noted in photographs by Ranger 7, is of great interest. This type of crater is formed, in particular, by an explo- /80 sion in soil with a sharp increase in strength with depth. There is an important change in the strength of the soil at the level where the slope of the crater changes sharply. The depth of this level differs for various craters, but lies within a range of several centimeters.

The following comments can be made about the individual features of the depressions. As a rule, no scattered material is noticeable in the depressions, possibly because not all depressions have been thoroughly examined. However, both individual stones or pellets apparently fallen there (fig. 31f) and accumulations of particles (fig. 31a and 31b) are occasionally seen. The /82 fine spongy structure of the lighted part of a depression at the resolution limit is quite evident in figure 31c and can be contrasted with the coarsely

Fragment A

TO

Fragment B

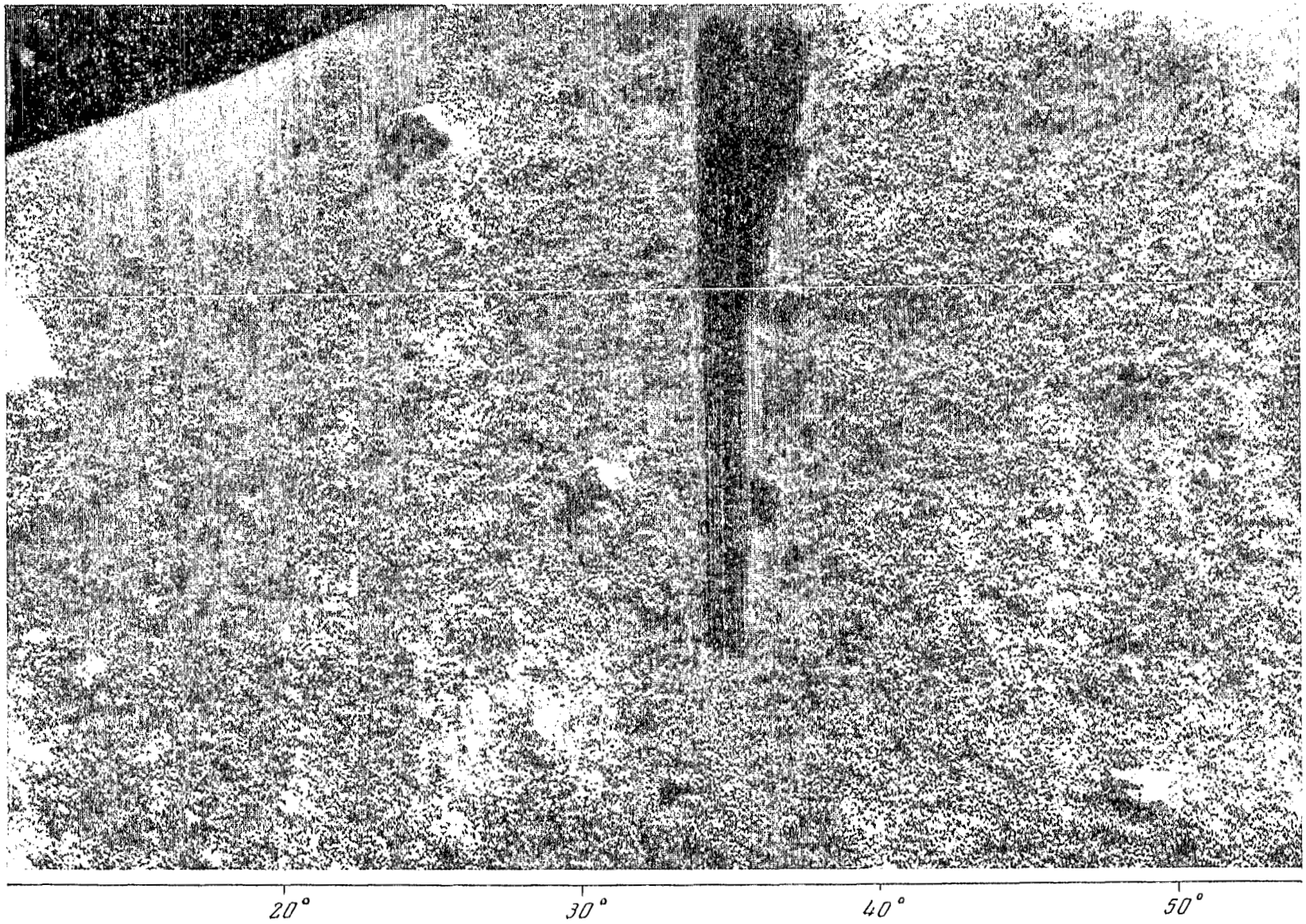

Figure 27. Panorama fragments obtained during additional television transmission.

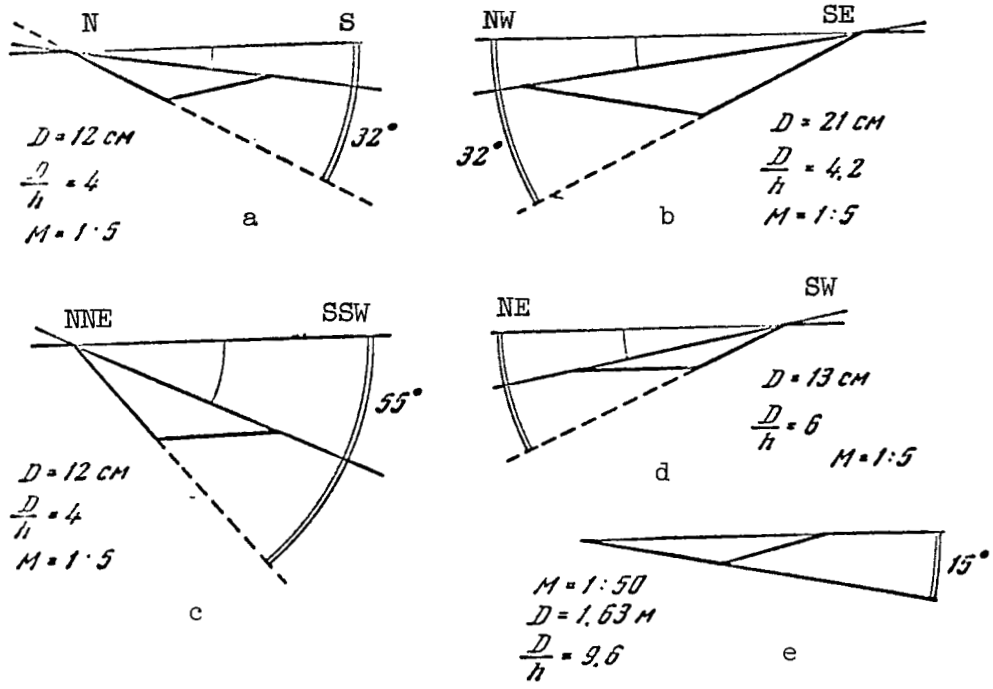

Figure 28. Cross sections of depressions from topographical plan data. Cross sections of craters Nos. 15(a), 25(b), 33(c), 54(d) and (13(e).

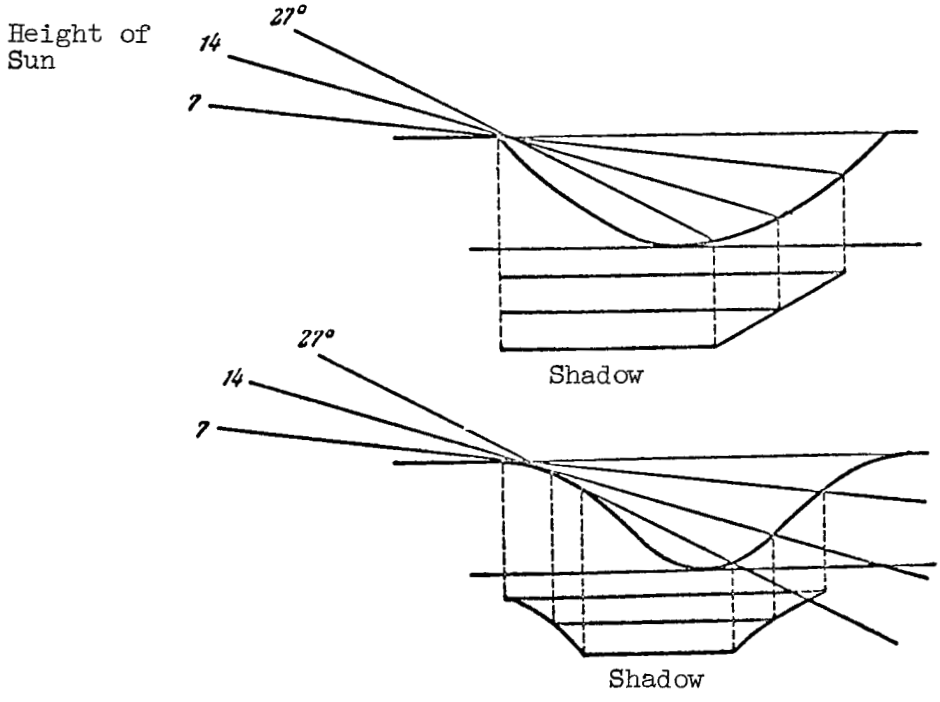

Figure 29. Nature of change in shaded part of crater, depending on lighting conditions for different crater profiles.

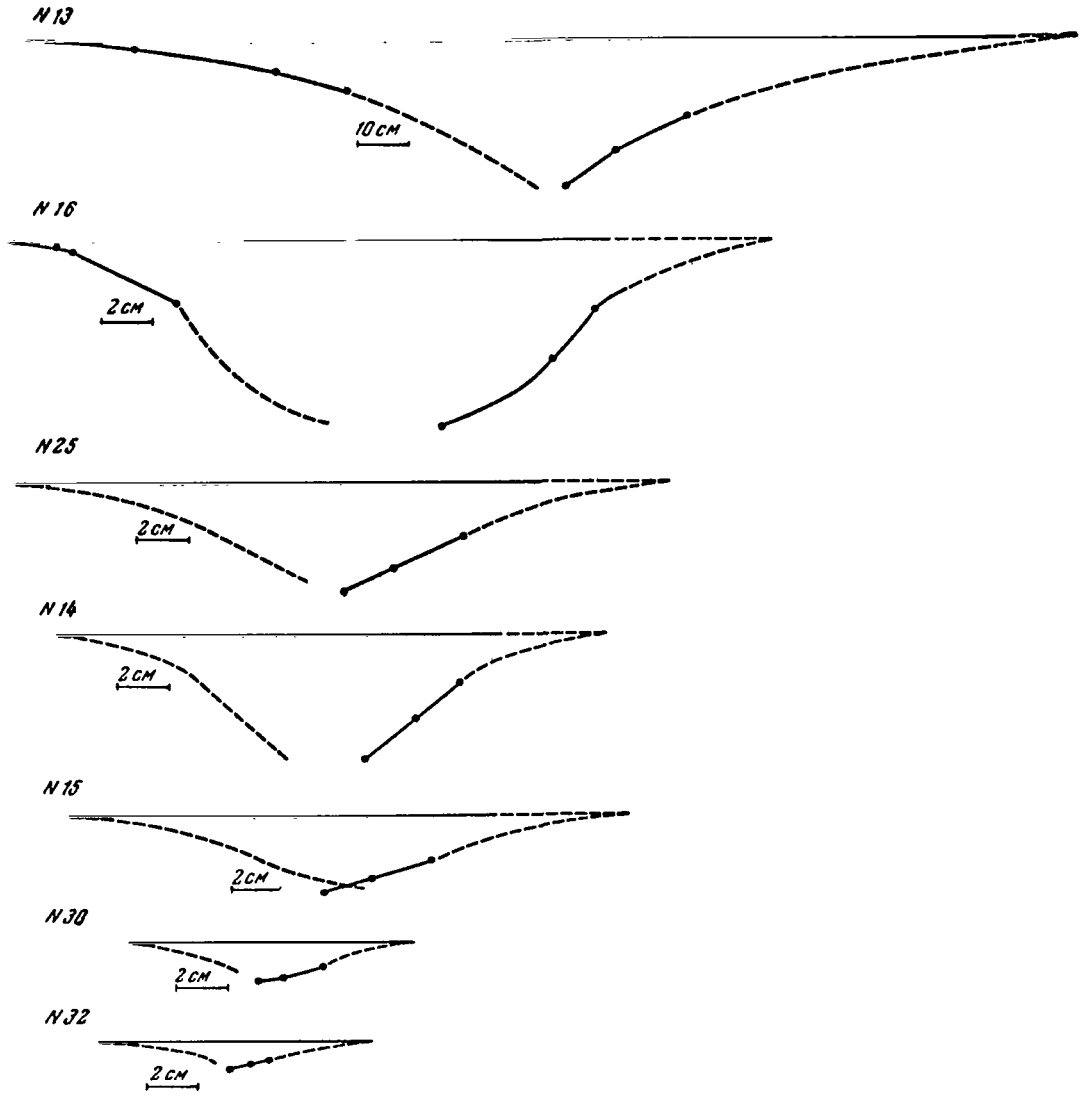

Figure 30. Cross sections of depressions constructed from shadows. Depressions No. 13, 16, 25, 14, 15, 30 and 32.

cellular structure of the lower depression in figure 31f, which is shown in the rectified plan form in figure 31g. Thus, we can distinguish at least two variations of the microsculpture of the bottoms of depressions. In many cases the depression slopes are similar in their sculpture to the surrounding rock. The nature of the structure determining the irregular, ragged edges of the depression, which has a diameter of about 15 cm, is clearly shown in figure 31g.

In a number of cases, ordered structural elements can be examined inside the depressions, which may be connected with either the superposition of two depressions or with peculiarities of the internal structure of the soil. Projecting partitions between craters, which sometimes acquire the character of annular structures, as seen in figure 31d and perhaps in figure 32c, are probably caused by the superposition of two depressions.

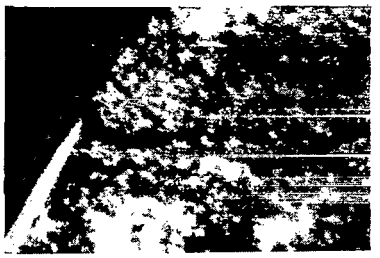

a

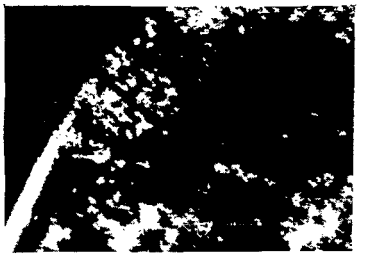

b

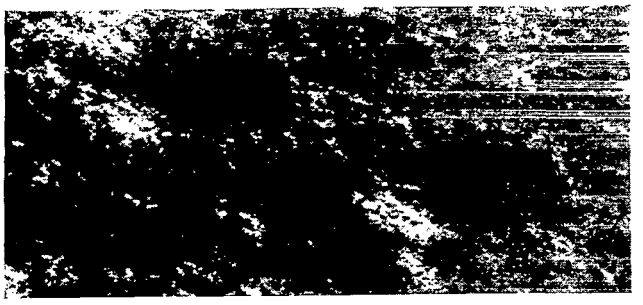

c

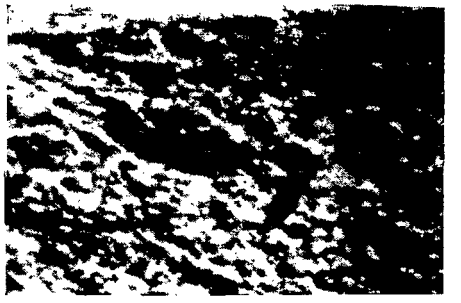

d

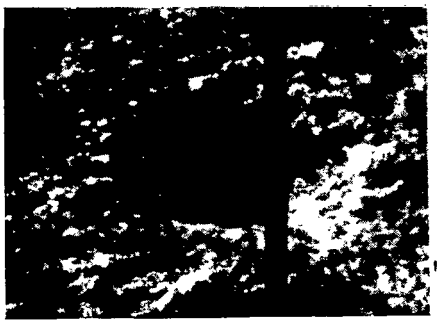

e

Figure 31. Details of the panoramas. a, Panorama III, γ = 10-20°; frame cut parallel to horizon; b, same detail for panorama II; c, panorama II, γ = 40-50°; d, panorama III, γ = 80-90°; e, panorama II, γ = 130-140°; f, panorama III, γ = 80-90°; g, transformed photograph of the same detail.

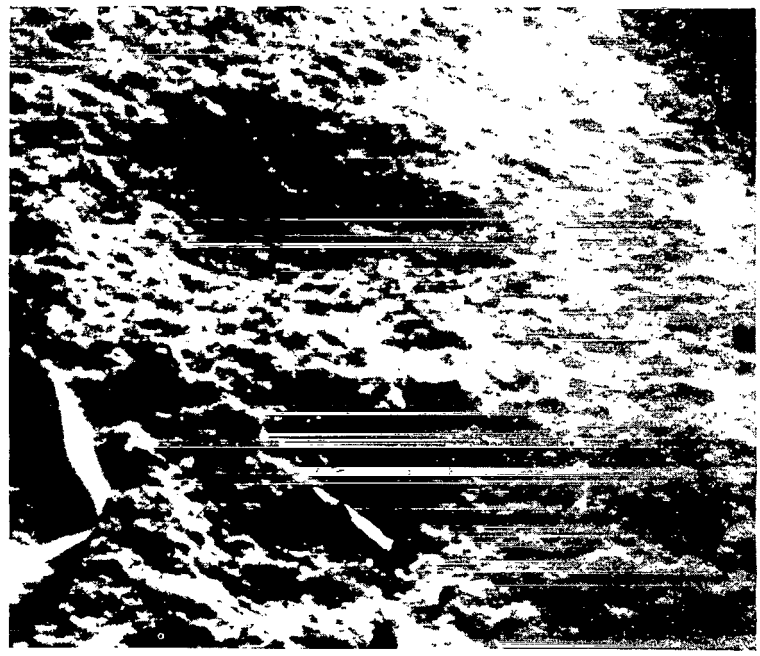

f

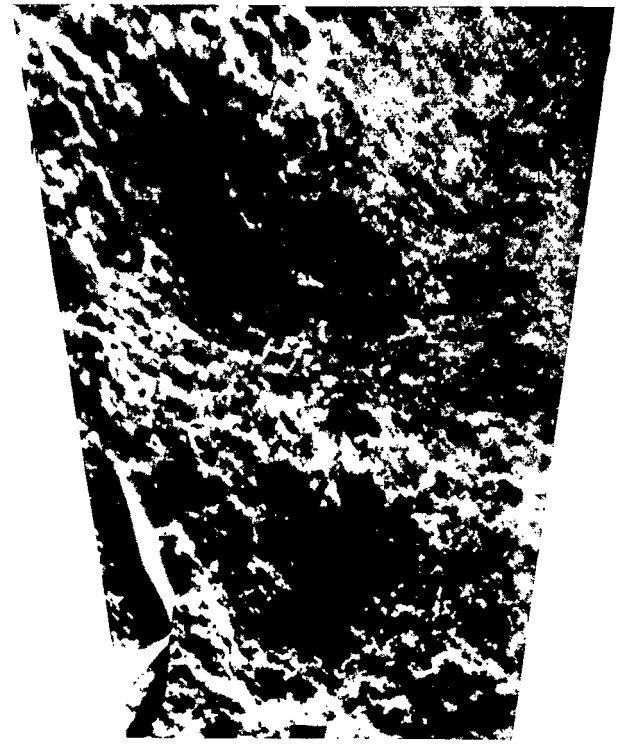

g

Figure 31 (concluded).

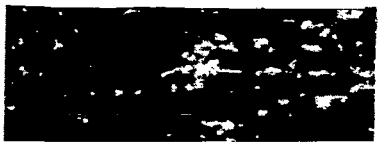

a

b

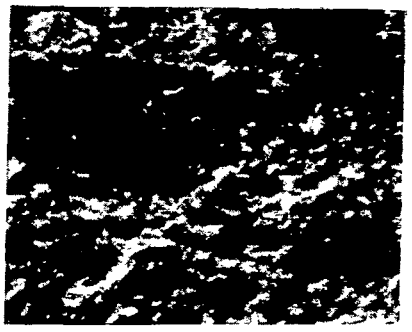

c

d

e

f

Figure 32. Examples of linear structures. a, b, Panorama III, γ = 130-140°; frames of photographs are parallel to structure; c, panorama III, γ = 130-140°; d, transformed photo of the same detail; e, panorama III, γ = 150-160°; f, panorama III, γ = 170-180°; frame of photograph is parallel to "laminar" structure.

Another type of relief that appeared is of a linear nature and is connected with linear structures intersecting the depression. These are described later. Such formations within the bounds of the general contours of depressions can be seen in figures 31a and 31b, partially in figure 31d and in figures 32c and 32d.

Usually the depressions had no clear-cut embankment. These were noted at times by the general illumination of the crater contour and only rarely established with complete reliability as a result of favorable lighting conditions, even when it was slightly developed. For example, an embankment around a crater can be observed in figures 31a and 31e. In the latter case, its lumpy structure can be seen.

Finally, it is necessary to mention several formations, one of which is shown in figures 31f and 31g (in the lower right corner) and the other, similar to it, in figures 32c and 32d (upper left). These are small eminences similar to tumuli, with a depression in the upper part of the tumulus. The depth of the interior outline of the holes was not determined and their structure is still not clear.

It is easy to visualize the dimensions of the entire formation by figure 31f, because a tape 13 mm long lies next to it.

It is remarkable that no traces of a structureless dust layer could be seen anywhere within the limits of the panorama, including the slopes of craters lying in the immediate vicinity of the television head. All visible sections were distinguished by the presence of clear-cut structurally connected formations produced probably by agglutination of fine particles.

2. Linear Structures

The term linear structures here means formations unified by some common characteristic such that a straight line or boundary forms the principal element of their shape. /84

The principal types of linear structures are:

(a) linear sequences of like protuberances forming almost rectilinear structures;

(b) small, practically plane sections ("sides") grouped into three-dimensional structures--complex "polyhedra;" polyhedra reminiscent of parallelopipeds or forming a "serrated structure" are particularly prevalent;

(c) small rayed or forked forms (figs. 32c and 32d) formed in some places by the intersection of linear structures aligned in different directions;

(d) structures whose details are not distinguished; under the given lighting, they appear to be chains.

The discovery of small linear structures is a fundamentally new fact characterizing an important feature of the lunar surface.

Extended rectilinear structures are noticeable on all well-examined sections of the lunar surface close to the station, and are especially clearly apparent between the panoramic longitudes 140-150° (fig. 33; the dashed lines are drawn parallel to the linear structures).

Their small width (on the order of 1 cm) and their small prominence permit the structures to be seen only under certain lighting conditions. They are almost invisible when the Sun is low, because they are covered with long shadows cast by randomly distributed surface irregularities. A different obstacle which hampers reliable tracing of these structures is the eye's natural tendency to combine systems of random points into a single pattern. Thus, in spite of the fact that the actual presence of linear structures has been established with complete reliability and beyond doubt, combining them into some system is not always reliable and is at times subjective to some extent.

One of these possible systems is presented in figure 33 to show how shorter, clear-cut sections of such structures can be combined into a single smooth line passing through an area of doubtful visibility and having a /86
total length of several meters. These lines were studied by stereoscopic effect which enhanced the reliability of tracing them.

Limiting ourselves to the most reliable extended linear structures 20-30 cm long (they were found to number 20), we constructed a vector diagram (rose) of directions. It shows that there are two prevailing azimuthal directions: 0-10° and 40-50° (fig. 34).

Direct measurement of the intersection angles of two clear linear formations on the rectified photographs of the photographic plan (fig. 32d) yields intersection angles of different structures at 40° and 70°. A linear structure intersecting the depression can be seen in the same figure and in figures 32a and 32c. Apparently it is stronger than the surrounding rock.

The relative strength of such structures can be seen particularly clearly in figure 32b. The projecting, thickened part of the structure breaks down here perpendicular to its course to form a system of regular blocks producing clear-cut shadows.

Another type of linear formation can be seen which is similar to the formation in figures 31a and 31b to the left in figure 32e. It resembles a depression similar to a thread-like crack. Figure 32c shows a crevice-like /87
depression with light points along it that project slightly above the general surface of the ground.

Apparently, the linear formations are stronger than the surrounding rock, but separate quite readily into small sections in the transverse direction. These are possible outcrops of tiny veins having higher strength (with surface destruction of the rock).

Figure 33. Dispositions of linear structures in the panorama.

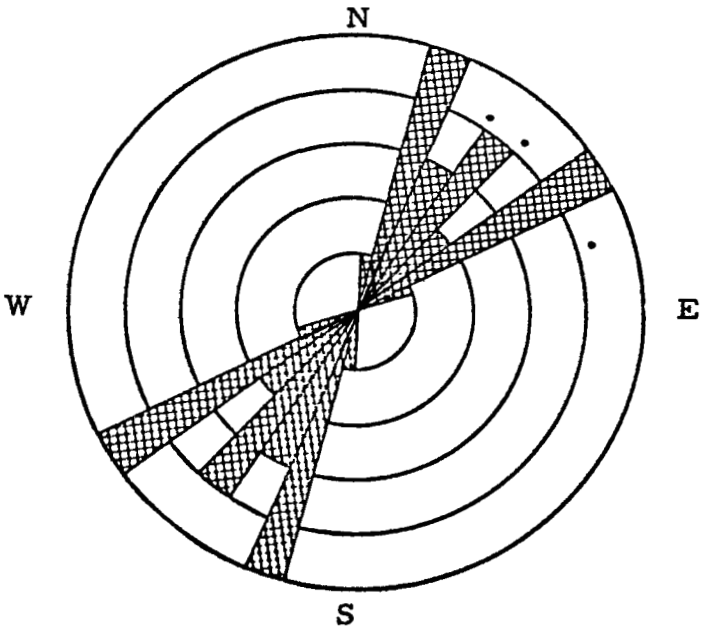

Figure 34. Vector diagram (rose) of linear structures.

3. Stones

We stated previously that the word "stone" was introduced as a provisional term. Since it is too indefinite a term, this word is seldom used in the geological literature, where it is replaced by narrower concepts characterizing the morphological nature of rock fragments. However, it is due to precisely this indefiniteness that this term is convenient for naming formations on the lunar surface that are similar to stones, at least until their nature is more precisely determined.

The horizontal plan of the studied section of the Moon shows 75 stones with dimensions exceeding 2 cm. The plan shows only those objects whose distances have been determined stereoscopically. When counted on the panorama, the number of stones is approximately doubled. For approximate calculation, we should expect to find at least 150 stones of various sizes in an area of /88

about 50 m^2, which corresponds to an average of about three stones per square meter of this type of lunar surface. It seems quite justifiable to call such a surface a stony area.

Dimensions of each stone are characterized by some average taken somewhat provisionally. This is a usual method. The size distribution of stones shown on the horizontal plan is given here:

Sizes, cm	2-5	5-10	10-15	15-20	20-25
Number	32	31	4	6	2

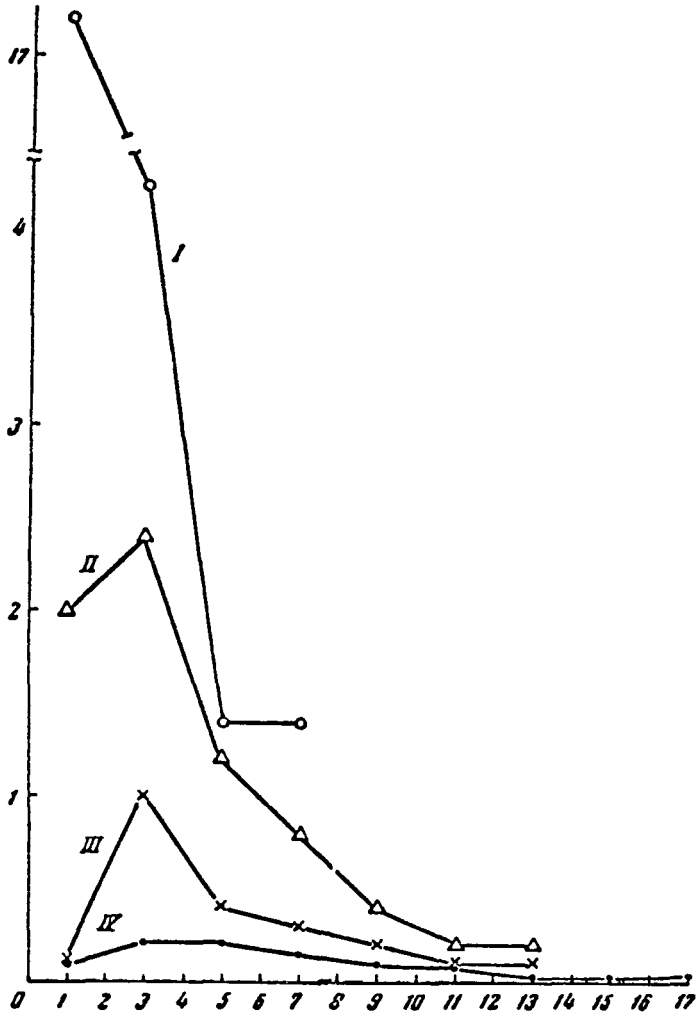

Figure 35. Graph of the number of visible stones versus their size for different zones of the panorama.

It should be remembered that due to visibility conditions in distant sections of the panorama, smaller objects become invisible and the actual distribution curve should tend toward prevalence of smaller stones. Such sizes are considered in the concept of "rock debris" which is understood in geology to mean stones with sizes ranging from 1 to 10 cm. This term should be applied with the restriction that it has a connotation of preservation of the original forms of rock fracture (absence of smoothing and noticeable surface erosion of the fragments), which is not wholly applicable in the given case.

Distribution of visible stones versus their sizes can be seen in the graph of figure 35, where their numbers are given for different zones of panorama III, broken down by concentric ranging circles (fig. 22b) drawn for intervals of

one meter so that the first zone corresponds to a distance of 1 m, the second from 1 to 2 m, the third from 2 to 3 m and the fourth from 3 to 6 m. The average number of stones per square meter for each zone is plotted on the y-axis and stone diameter is on the x-axis.

Single stones lying between craters are dominant in the panorama, but groups are encountered which give the impression of fragments of a single monolith (figs. 36g to 36k). Some chains of stones arranged along a single straight line merit special attention. It is characteristic that the most clear-cut ridge of rocks (190-195°) extends along a direction of about 190°--one of the most typical directions for linear structures (fig. 33). This line is also distinguished by some external features which permit assumption that some denser structure passes through here, reminding us of a destroyed dike or vein.

The observed relief displayed by craters (depressions) of various sizes is possibly of an essentially meteoritic origin. However, it must be assumed that the overwhelming majority of the observed stones cannot be fragments /91 of meteorites. The number of fragments of lunar rocks on the surface should exceed the number of meteorites many times, and discovery of a meteorite in a panorama is very improbable.

In speaking of the way the stones lie on the surface, it must be stated that some of them give an impression of lying freely on the surface (fig. 36, figs. 37a to 37c) and even having rolled into depressions (figs. 31a, 31b, 31f, and 31g), while others are either more tightly bound to the surface or protrude when the ground is destroyed (figs. 36a to 36c, and fig. 37). It may be that the mentioned ridge of stones is the result of outcropping.

The surface of the stones often has a unique, irregular, "pitted" appearance similar to colian weathering or surface dissolution of some terrestrial rocks. As a rule, irregularity of either the active agent or stability of the rock appears in these processes. Figures 37a to 37c show details of the rock surface under different lighting. It is necessary to direct attention to the degree of change in external appearance in this case and ease in erring when estimating its shape. The serrated structure of the stone's crest, seen in all the photographs, is quite curious.

Conchoidal depressions visible on the surfaces of many stones (figs. 36a, 36b, 37d, and 37e) might be traces of impacts of micrometeorites or rock fragments having a vitreous structure.

Figures 37d and 37e show an interesting area by the left base of the stone. It can be considered an accumulation of material strewn from destruction of the rock or an outcropping of large hidden rock fragments uncovered by destruction of the soil.

Figures 36a and 36b show two stones, one of which apparently lies free on the surface and the other somehow merges unnoticeably into the surrounding rock, even in respect to the texture of the surface. This figure and figure 38 show that some stones are elevated, so to speak, on a unique pedestal (as seen

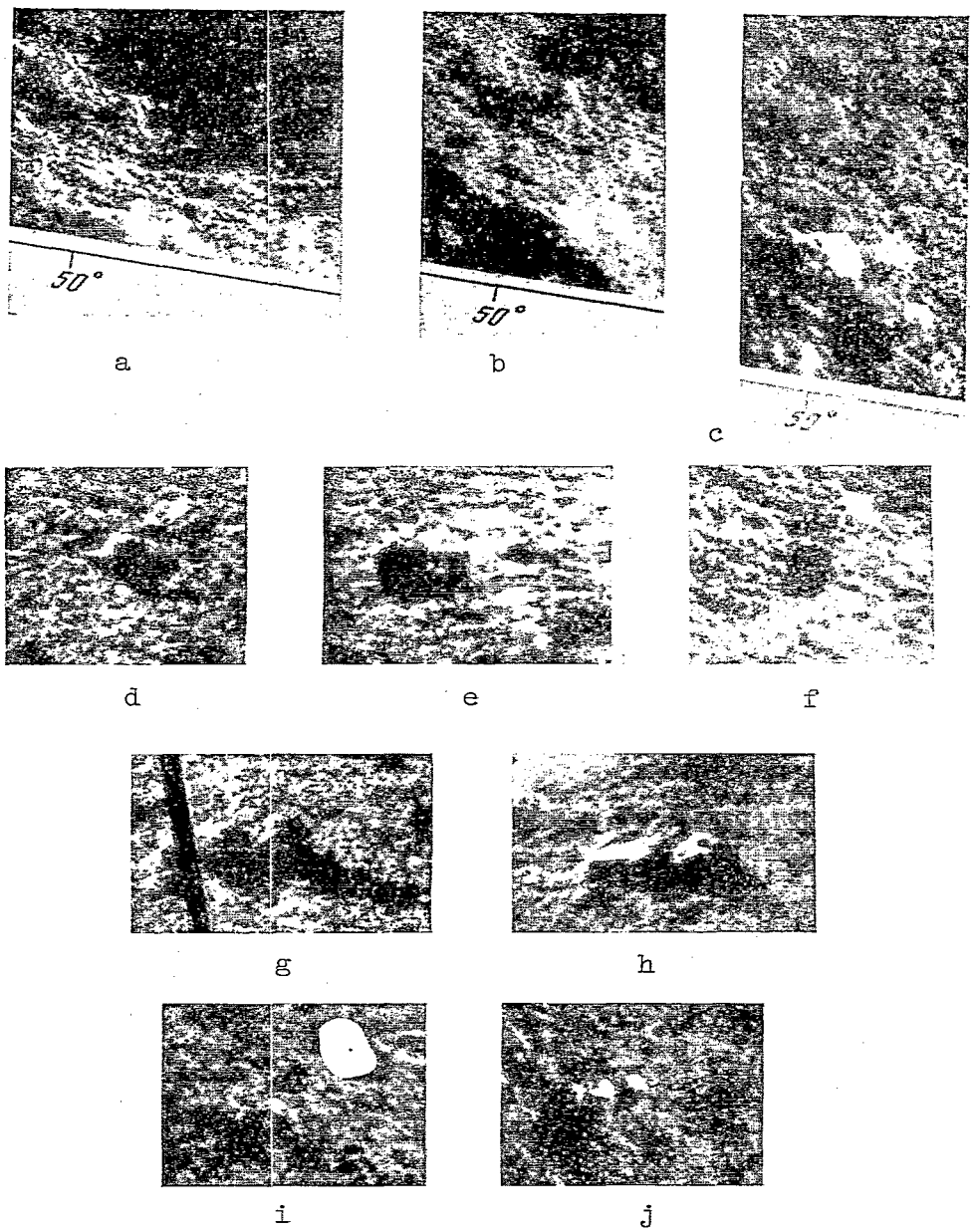

Figure 36. Examples of stones and their groups. a, b, c, Stones at $\gamma = 50^{\circ}$ in various panoramas; fragment frame is parallel to horizon (a, panorama I; b, panorama II; c, panorama III); d, e, f, sharp angle fractures of various stones, panorama III (d, e, $\gamma = 120\text{-}130^{\circ}$; f, $\gamma = 80\text{-}90^{\circ}$); g, h, group of stones, $\gamma = 140^{\circ}$, possibly formed from disintegration of a monolith (g, panorama II; h, panorama II); i, j, groups of stones, panorama III (i, $\gamma = 60\text{-}70^{\circ}$; j, $\gamma = 55\text{-}60^{\circ}$).

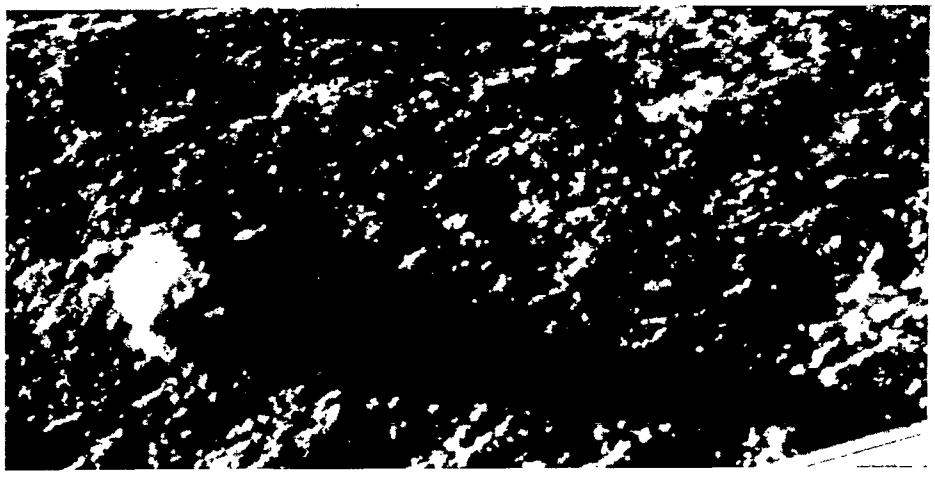

a

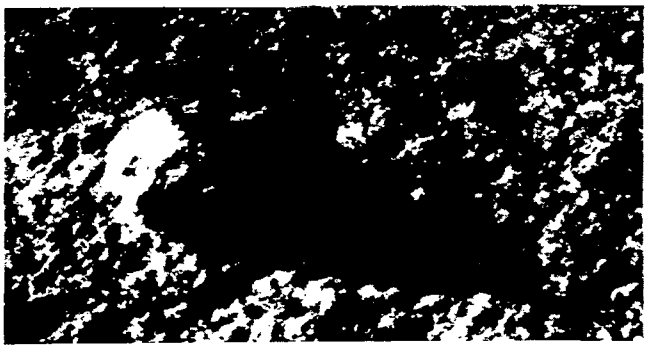

b

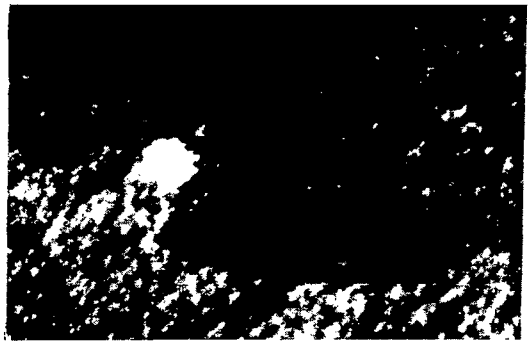

c

d

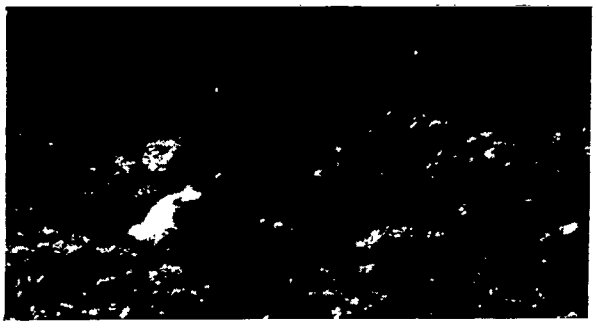

e

f

Figure 37. Morphological peculiarities of stones.
a, b, c, nearby stone at $\gamma = 160^{\circ}$ (a, panorama I; b, panorama II; c, panorama III); d, e, f, shape variation of distant stone at $\gamma = 160^{\circ}$ at various illuminations (d, panorama I; e, panorama II; f, panorama III).

a

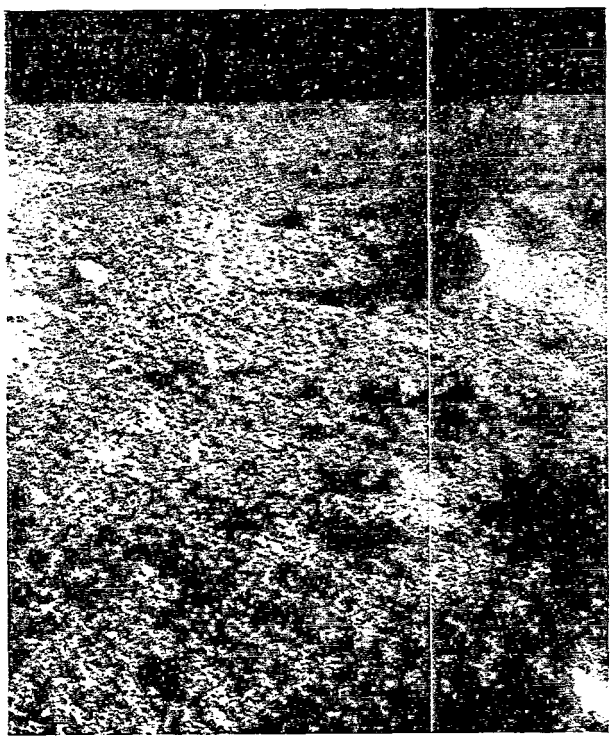

b

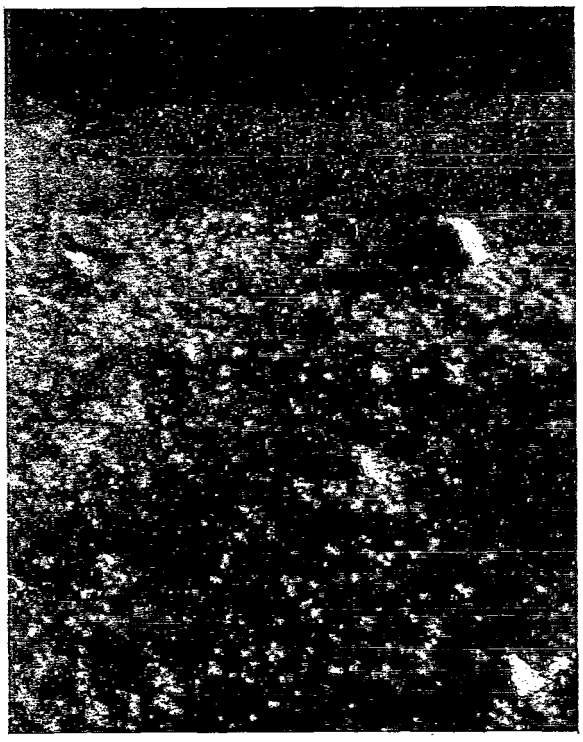

c

Figure 38. Panorama portion 15-30°. Frame parallel to horizon; a, panorama I; b, panorama II; c, panorama III.

in two places in fig. 38). Elevation of a large stone is shown clearly by the curvature of the shadow in figure 38b. This is probably explained by the stone's creating a unique shield against erosion for the ground it lies on. This would permit preservation of the softer surrounding ground by the rock. Returning to figure 36b, we direct attention to the fine cellular structure of the stone which is noticeable on its right side. What appears to be the same structure is seen in figure 37a at the limits of image resolution. It is not at all noticeable at other angles of lighting.

The small stones shown in figures 36d to 36f, with more clear-cut and angular fracture surfaces, have somewhat different surfaces. This is explained by fresh fractures of the surface or by the stones' being relatively durable fragments fallen from linear formations of another petrographic nature. /93

Figures 36g to 36k show examples of stones occurring in groups which are probably strewn fragments of a single monolith.

Some stones are of a smoothed, rounded appearance (fig. 37), even under different lighting. However, after examining the preceding figures (for example, figs. 36g and 36h), we see that fine details of the structure of the surface can be very indiscernable on the lunar surface under contrast lighting.

4. Generalized Model of the Landing Site

As previously stated, the section examined by Luna 9 is small, and to judge the nature of this section, it is essential to find the relation between the appearance of the panorama and those forms of the lunar relief which are observed from the Earth or photographed by other spacecraft. In other words, we must obtain some generalized model of the landing site. There are two obvious ways to construct a generalized model of the site: making use of geodetic processing of the photos transmitted by Luna 9 to average out the heights and thus obtain a smoothed model, or making use of the physical features of the surface section under study and relating them to known morphological characteristics of the lunar relief. The second way has some advantages since reliable determination of the relief by geodetic methods is possible only close to the station, where the stereoscopic effect is noticeable.

When constructing a generalized model, we use the fact that in addition to the true horizon, the panoramas show what might be called a "second horizon" (fig. 39), and both the brightness and amount of small details visible on the landscape changed quite sharply in passing through this horizon. The spherical coordinates of this "second horizon" in the system connected with the station were found to lie on a small circle. If we assume that the plane of this small circle is actually horizontal, then the inclination of the station relative to the local vertical is about 16.5° for the first panorama and about 22.5° for the third.

Knowing the inclination of the station relative to the vertical, we were able to project points located on the second horizon onto the plane /95

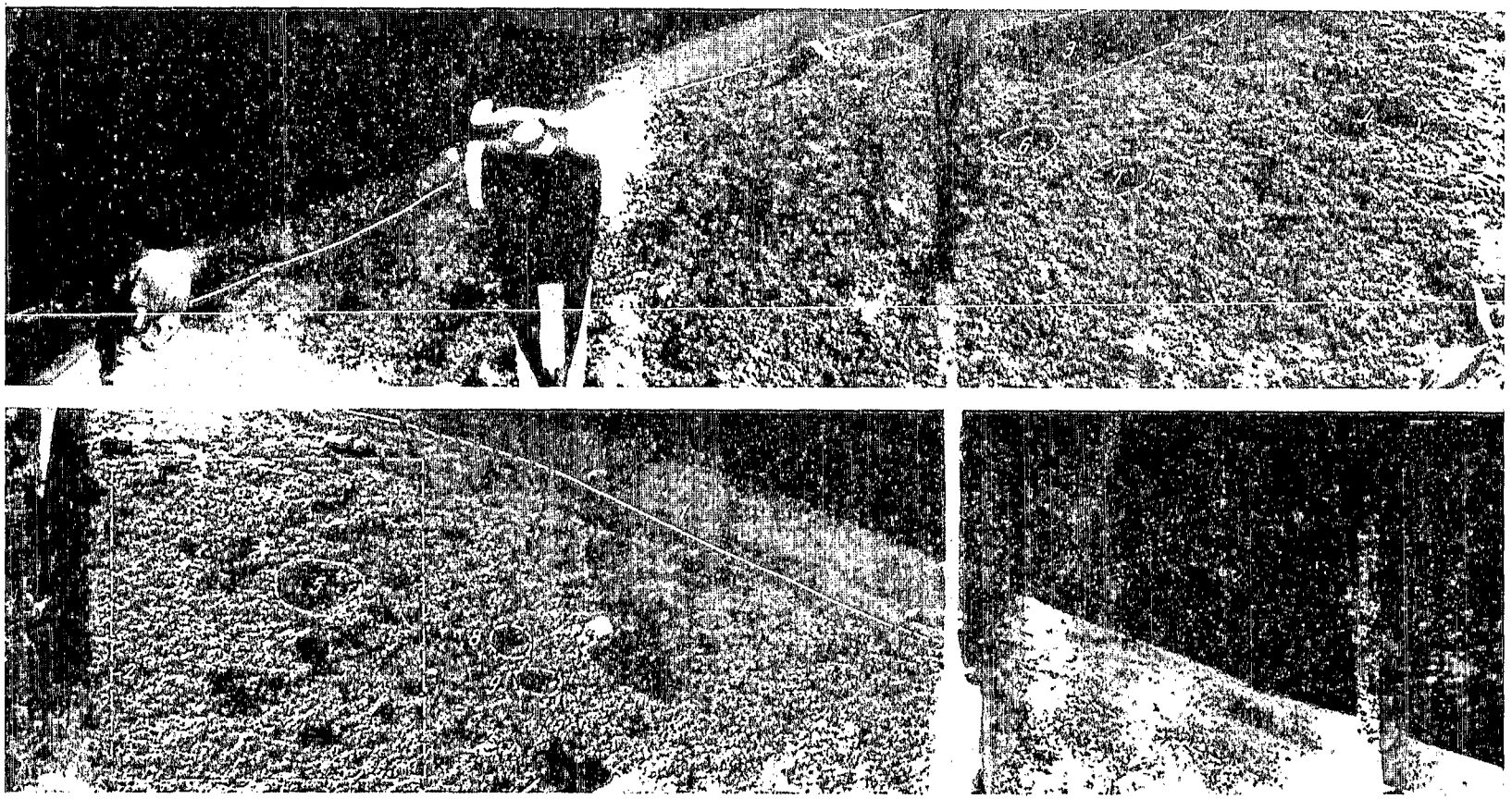

Figure 39. Disposition diagram of relief details. 1, "Brow" of the 15 m crater; 2, region of linear structures; 3-9, craters with profiles made by shadow method.

perpendicular to the vertical, that is, to obtain the plan image of this "second horizon." It is necessary to note, however, that the plan will be dimensionless since the height of the scanning mirror above the projection plane serves as the unit of measurement employed here. An example of the plan obtained in this manner (for panorama I) is given in figure 40. It is easily seen that the points of the "second horizon" in the plan are very satisfactorily represented by a circle whose center lies somewhat north of the plane of inclination of the camera. Considering that an overwhelming predominance of rounded craters is typical of the morphology of the lunar relief with any scales, it seems natural to assume that the station is located on the western slope of a crater and inclined toward its central part, to the east.

To envisage the linear dimensions of this crater, we used stereoscopic images of several sections of the landscape obtained with dihedral mirrors installed in the station.

It was assumed that the crater interior has a shape close to that of a spherical cup. This model was accepted only as a rough representation of the generalized relief and apparently is a satisfactory approximation for the section observed by the station, lying within the crater.

Eleven points were identified by three images in the mirrors, and the position of the center and the radius of the approximating sphere were determined by the least squares method by their coordinates in the system connected with the station. It was assumed that the center of the sphere lay above the center of the crater. The positions of the center and the radius of the approximating sphere were also estimated by 15 points whose distance and the height relative to the center of the station scanning mirror were taken from geodetical or, more precisely, from photogrammetric determinations (refer to the preceding chapter).

It was found that the radius of the approximating sphere is about 25-30 m, and the center of the crater is several meters to the northeast of the station.

Making use of the graph of the "second horizon," it is possible to determine that the depth apparently does not exceed 1 m and the diameter is close to 12-15 m, which agrees with the estimates cited on page 59. It should be noted that unlike the geodetic determinations which used the stereoscopic effect created by the shift in the station during its operation, the determinations described in this section, independent for panoramas I and III, yielded /97 coinciding results and could have been made if the station had not shifted.

The northwestern and southwestern slopes of the crater are also clearly shown on the horizontal plan constructed by photogrammetric methods (refer to part three). The diameter and depth of the crater obtained by geodetic data and those found by morphological characteristics proved to be very close.

As previously stated, it is not known whether the landing site is in a maria or a highland region. Results from photometric determinations of the brightness of the landscape surrounding the station may serve as a criterion for solving this problem. According to preliminary photometric data, the

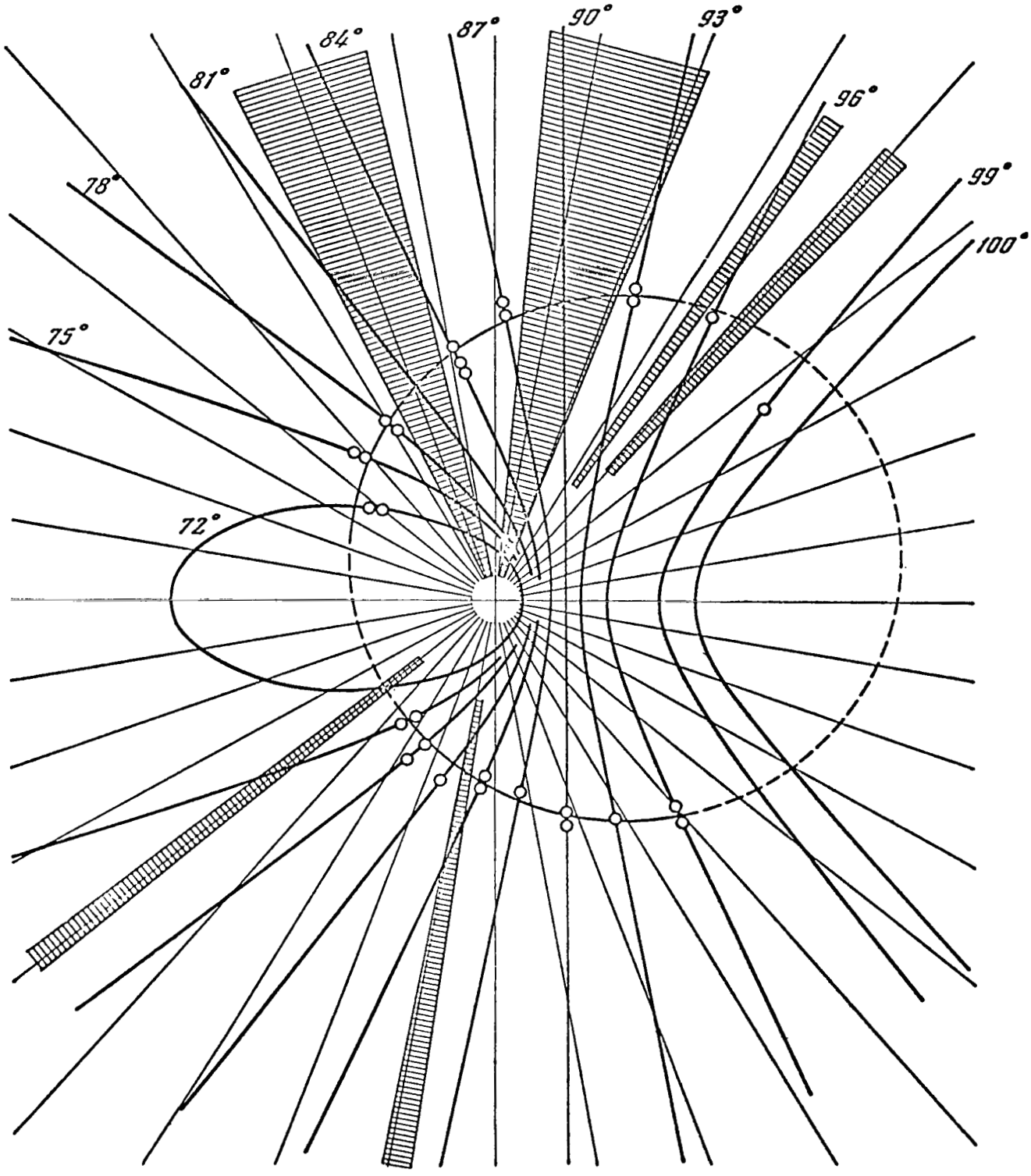

Figure 40. Plan of edge of 15 m crater. Rays correspond to lines of equal azimuths, the hyperbolas to lines of equal heights in the spherical coordinate system fixed with respect to the station. Small circles represent points on the crater edge taken from Panorama I.

interior part of the crater containing the station belongs to the light sections of the lunar surface.

The fact that the horizon seen in the panoramas is not a great circle (refer to fig. 41) provides some additional substantiation for this conclusion. In panorama I, the visible horizon is best represented by a small circle lying above the mathematical by approximately 1.5°. This would indicate that the /98
15 m crater is inside a considerably larger crater, still far smaller than the craters seen in terrestrial optical observations (fig. 42).

We note that the infrared observations conducted by Shorthill and Saari during the total lunar eclipse of 1964 indicated a surface heat conductivity in the Luna 9 site which is high for lunar conditions. During these observations, high heat conductivity (or more precisely, slow cooling of the surface which is connected with the influx of heat from deeper layers and great heat capacity per unit volume of the substance of the surface layer) was also noted for a number of "young" craters whose bottoms appear light in optical observations. It is perhaps natural to assume that the region of increased heat conductivity in the vicinity of the landing site of Luna 9 is due to the presence of a group of "young" craters in this region. It is not excluded that Luna 9 is in one of these craters.

It is generally considered that the bottoms of young craters are characterized by a thin layer of heat-insulating rock and, at times perhaps, by the complete absence of such a layer. In this connection, special attention is drawn by the linear structures clearly visible in the southeastern sector of the panoramas. In many cases, these structures intersect individual depressions and extend to a distance on the order of 1 m. Since depressions with diameters of several decimeters and depths of several centimeters can be seen in the vicinity of linear structures, we apparently must conclude that the depth of the freshly processed layer does not exceed several centimeters, at least in this sector of the panorama. The presence of linear structures opens several possibilities for estimating crater age if we understand age to /99
mean the time interval passed since the linear structures were exposed. This estimate may be substantiated by the fact that craters and smaller sinks occupy not more than 20 percent of the area of the section accessible to observation in the 15 m crater where the station is located.

The external forms of the surface and the details of the microsculpture are connected with erosional exogenic processes in which, in particular, impacts of meteorites of various sizes play an important role. However, in the best observed sections, the average thickness of the layer processed in this manner apparently does not exceed several centimeters. The surface layer has a heavily pitted, spongy structure which generally corresponds well to the presently existing ideas of the nature of the lunar surface. In particular, this is confirmed by the same bell-shaped form characteristic of many craters with depth exceeding several centimeters, marked by accelerated increase in the crater diameter as it approaches the surface. Apparently, this form of crater, as previously stated, is evidence of a change in the vertical rock strength since the crater diameter is ultimately determined on every level by the strength of the rock.

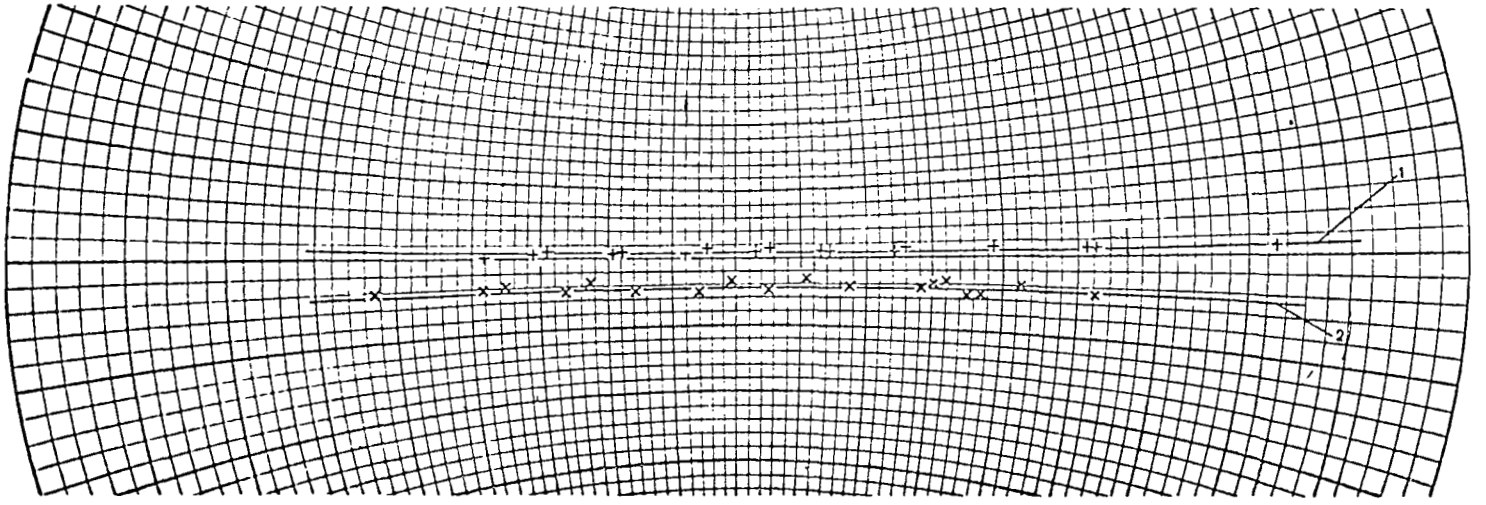

Figure 41. Spherical coordinates of the visible horizon (1) and the edge of the 15 m crater (2) in panorama I. The station axis was inclined to the east 16.5° during panorama transmission.

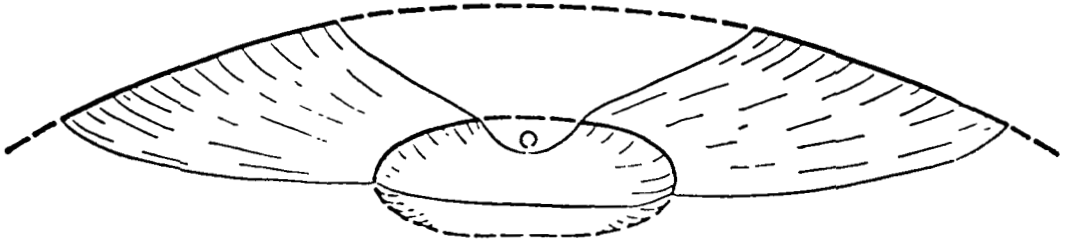

Figure 42. Possible generalized diagram of the relief.

The presence of stones lying on the surface does not contradict the conclusion of low strength of the ground surface layer if we consider that there is rather a negative balance of mass in the observed section. In this case, even stones buried at some depth in the ground should gradually be exposed if they are stronger than the surrounding rock and, so to speak, "float" on the weaker substance surrounding them. It is natural to explain that relatively strong stones are present on the surface by stating that they were ejected from deep parts of the ground when the craters covering the locality were formed.

It is difficult to imagine a process of surface destruction without formation of a dust-like, finely dispersed material. Thus, we may believe that granulated matter forms definite structurally connected aggregates as a result of agglutination, complicating the structure of the surface.

The internal structure of more ancient rock appears in the process of /100
destruction. In the latter, denser linear formations having the nature of veins intersecting at different angles are to be found within the less stable basic mass. The presence of thicker destroyed veins or dikes may be displayed in the linear arrangement of individual ridges of stones.

Of course, the foregoing is insufficient to judge whether Luna 9 is on bedrock "sprinkled" by a thin layer of ground processed as a result of destruction, or on an accumulation of large fragments with crushed rock strewn over it. It is also not clear how typical this picture is for the Moon as a whole. It is possible that the situation considered here is not very rare. Then, with radio astronomical data as a basis, the idea of a large buried fragment layer whose density increases slowly with depth is sufficient to ensure low heat conductivity and heat capacity of the surface layers.

The fact that linear structures are observed on only a limited part of the surface possibly favors the last proposition.

Even examination of a small section of the Moon shows the simultaneity of formation of different elements in the surface and a certain complexity of its geological history which could scarcely lead to a single process. It is possible to propose a number of processes as having created the present lunar surface in a combination unknown under terrestrial conditions. Their analogy must be sought in entirely different geological formations or in specific laboratory processes.

Translated for the National Aeronautics and Space Administration by
John F. Holman and Co. Inc.

PART III. PANORAMIC PHOTOGRAPHS OF LUNAR SURFACE

Panorama I Fragments 1-9
Panorama II Fragments 1-6
Panorama III Fragments 1-7
Transformed Photographs
Stereopairs 1-12
Panoramas I-III
Topographic Plan of Landing Site
Topographic Diagram of Landing Site

Panorama I, fragment 1

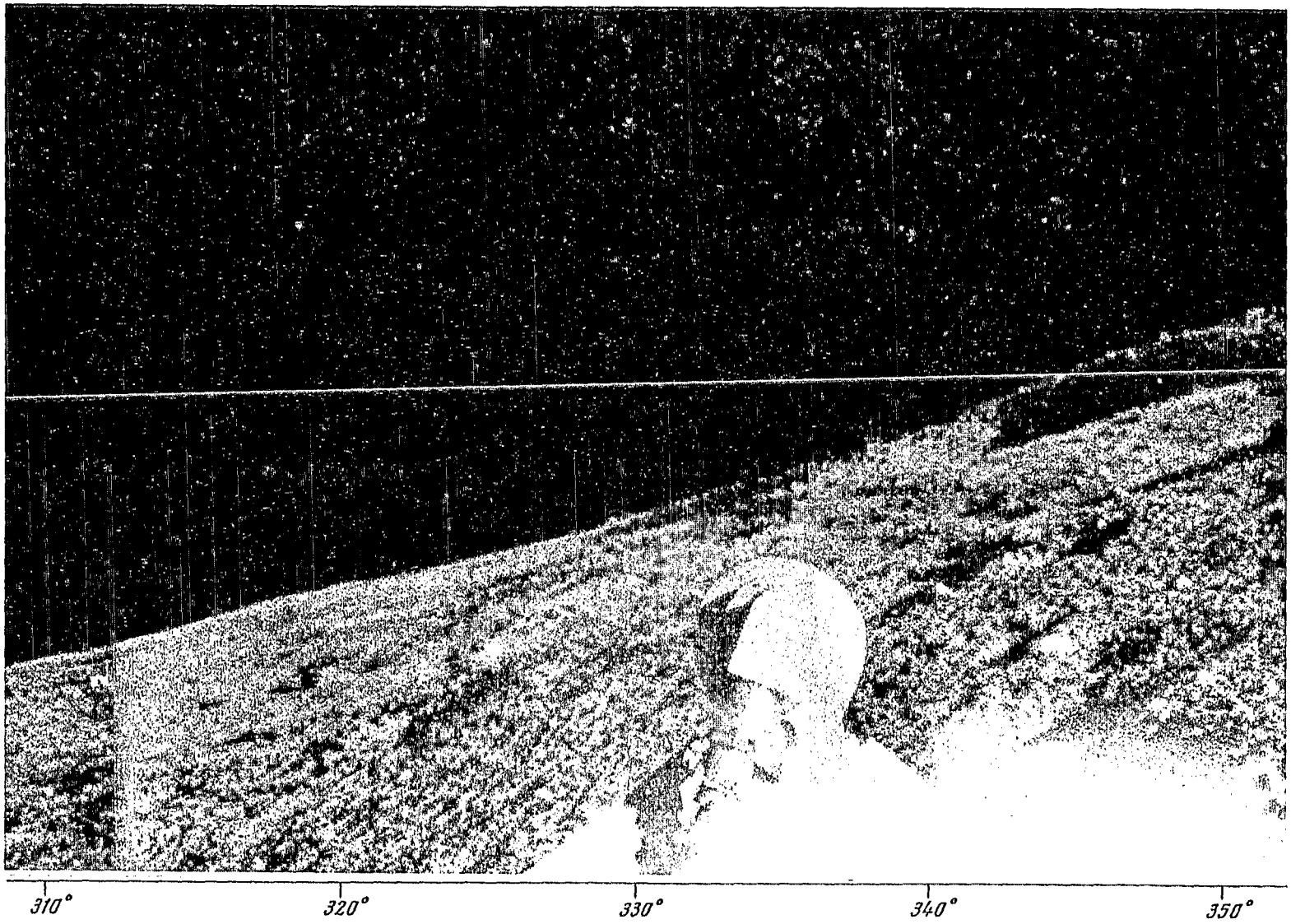

Panorama I, fragment 2

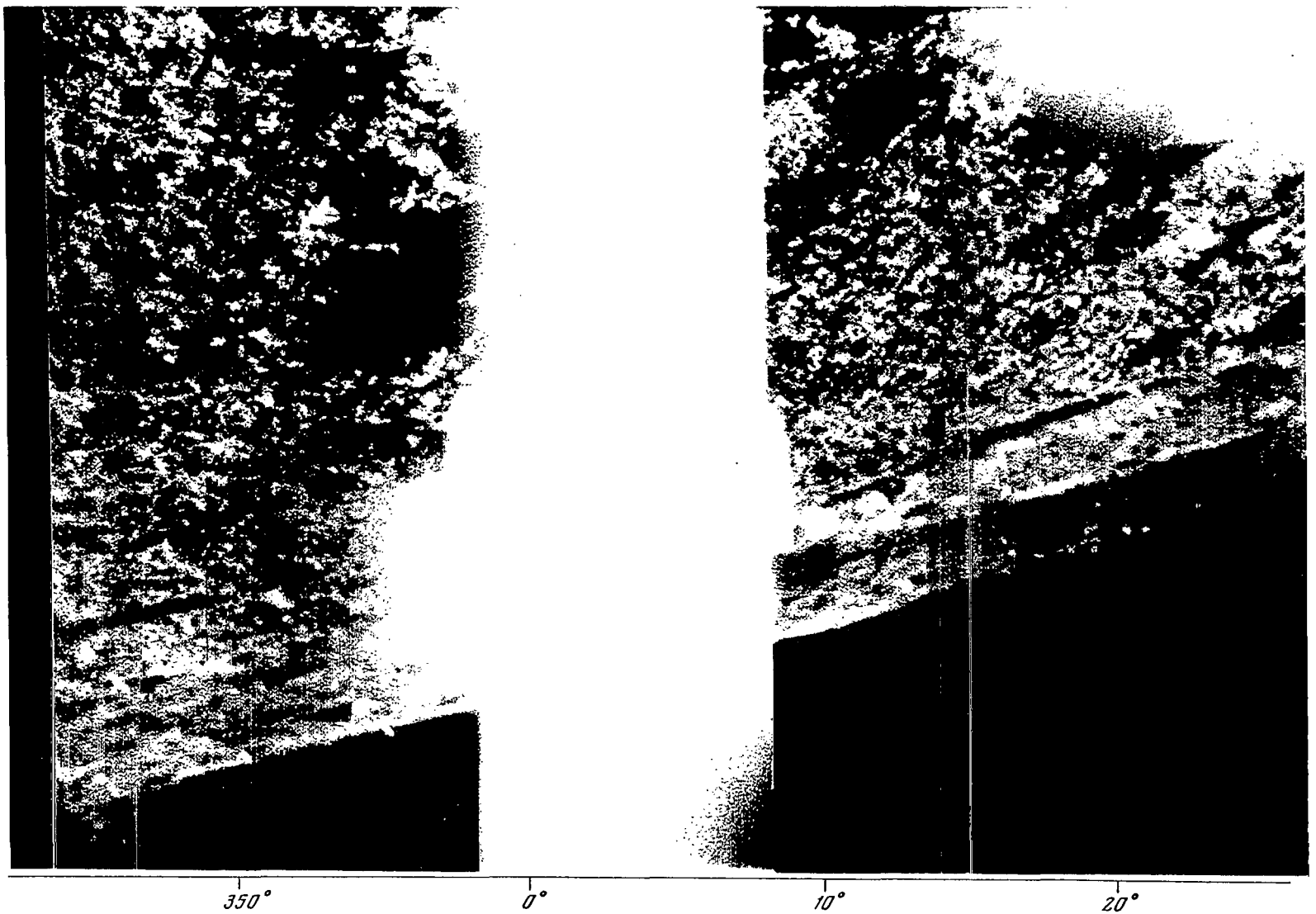

Panorama I, fragment 3

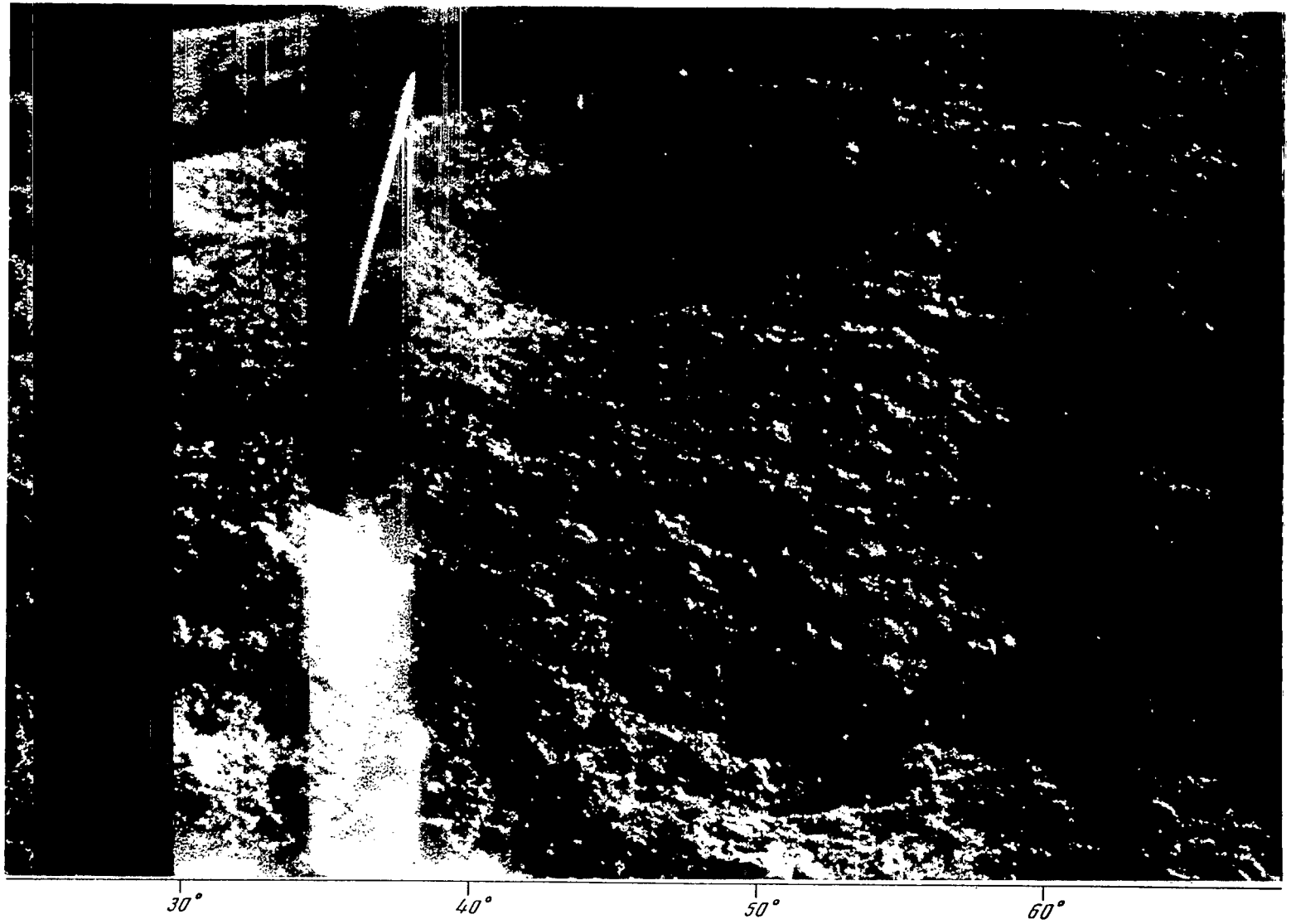

Panorama I, fragment 4

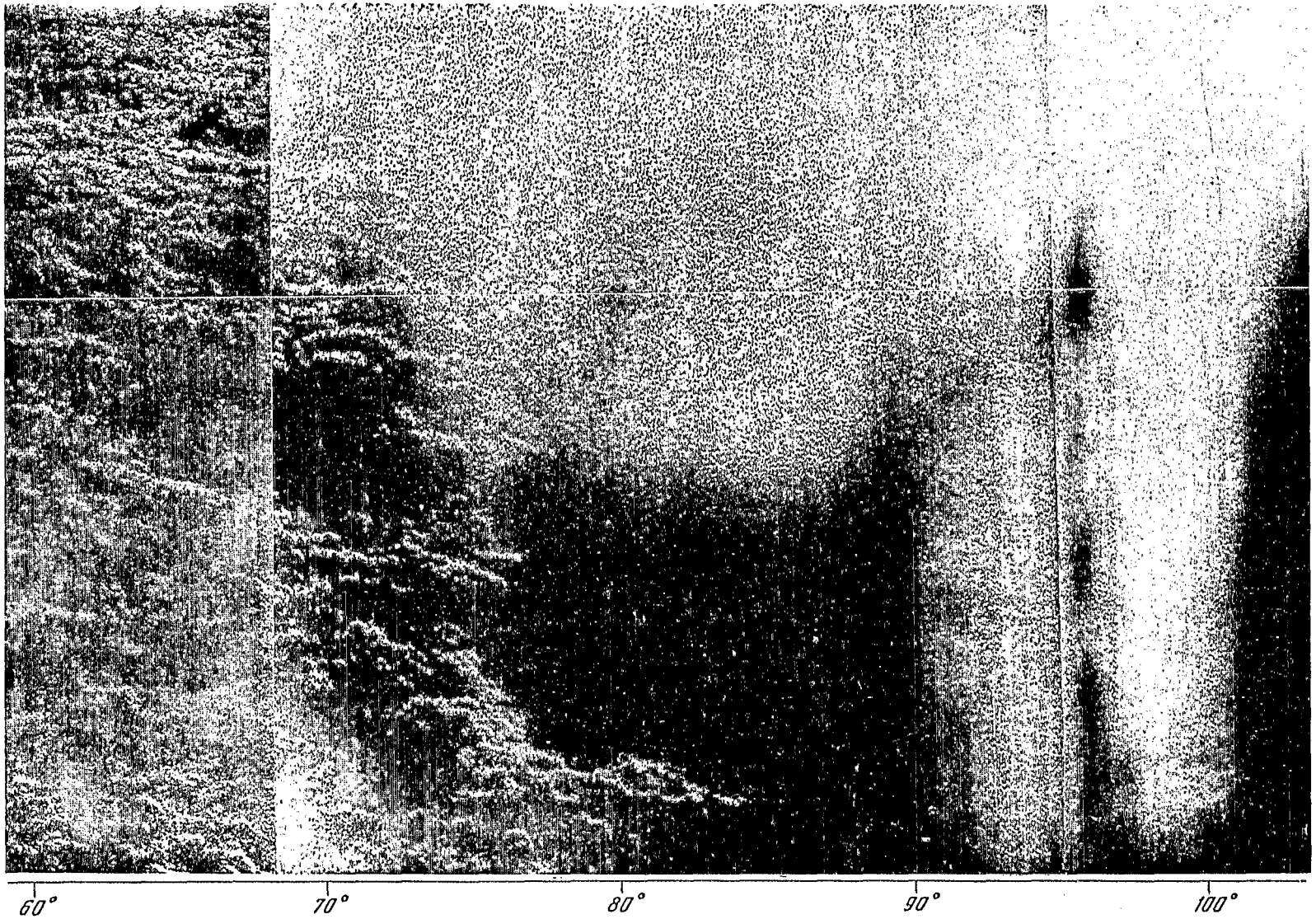

Panorama I, fragment 5

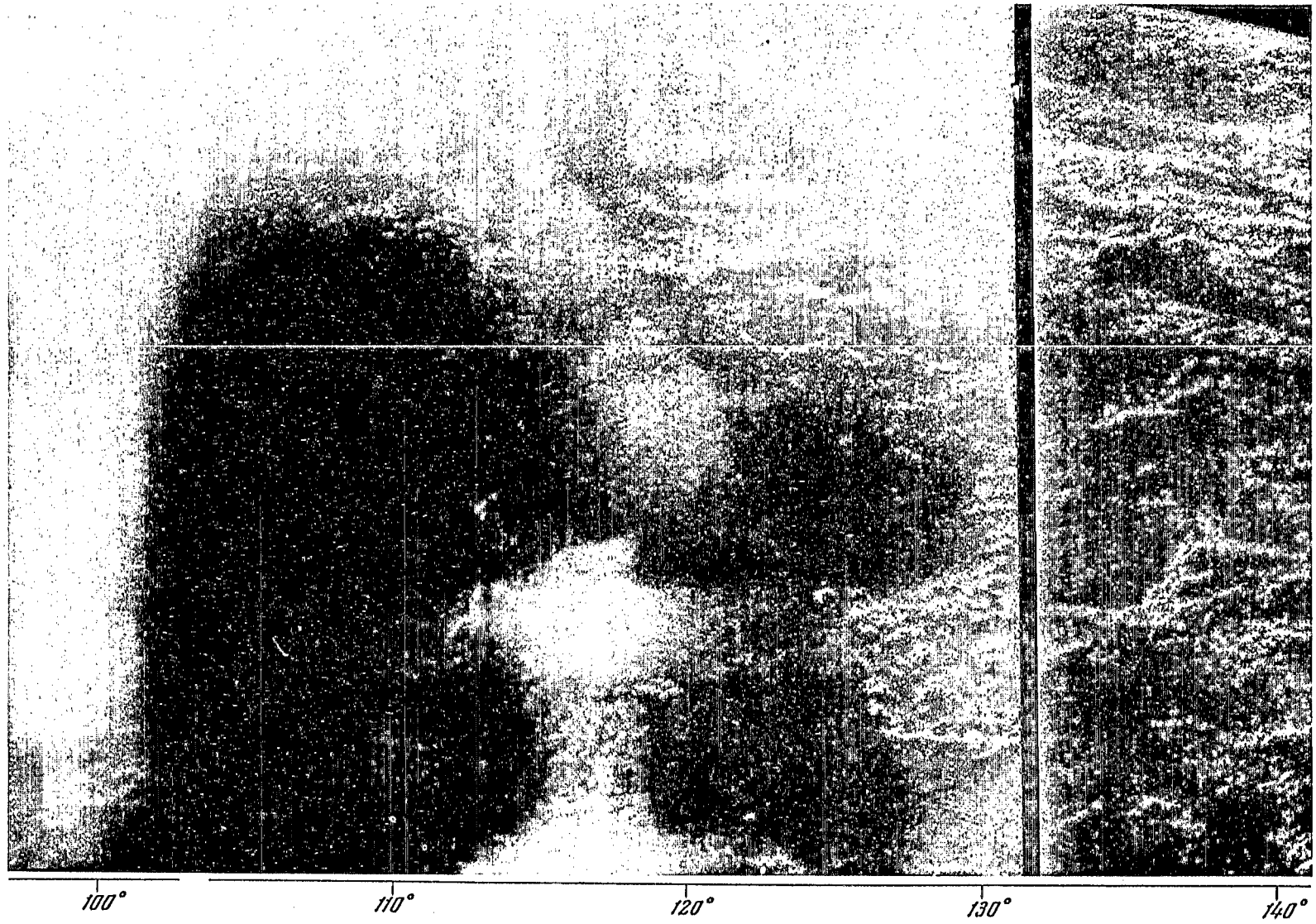

Panorama I, fragment 6

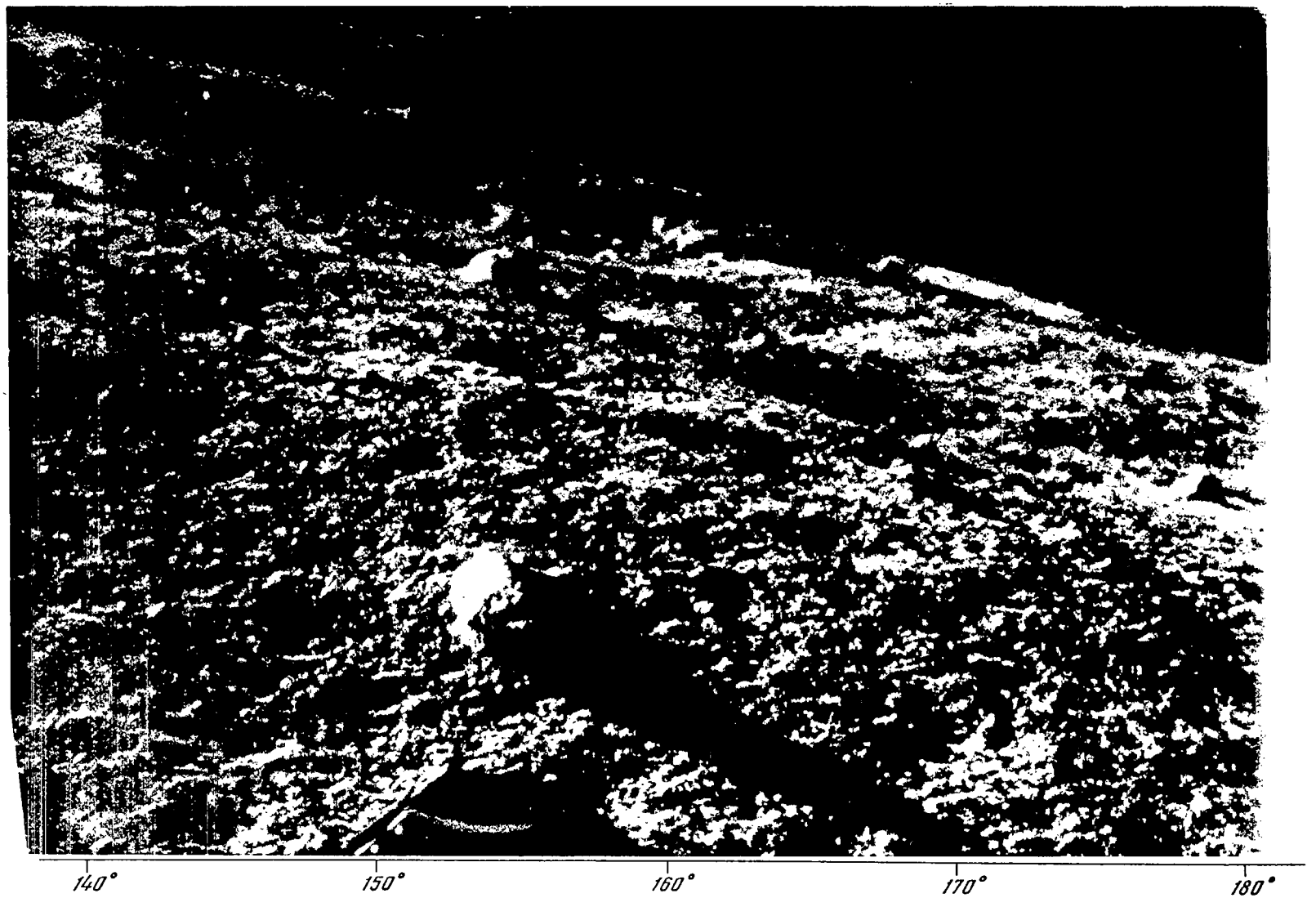

Panorama I, fragment 7

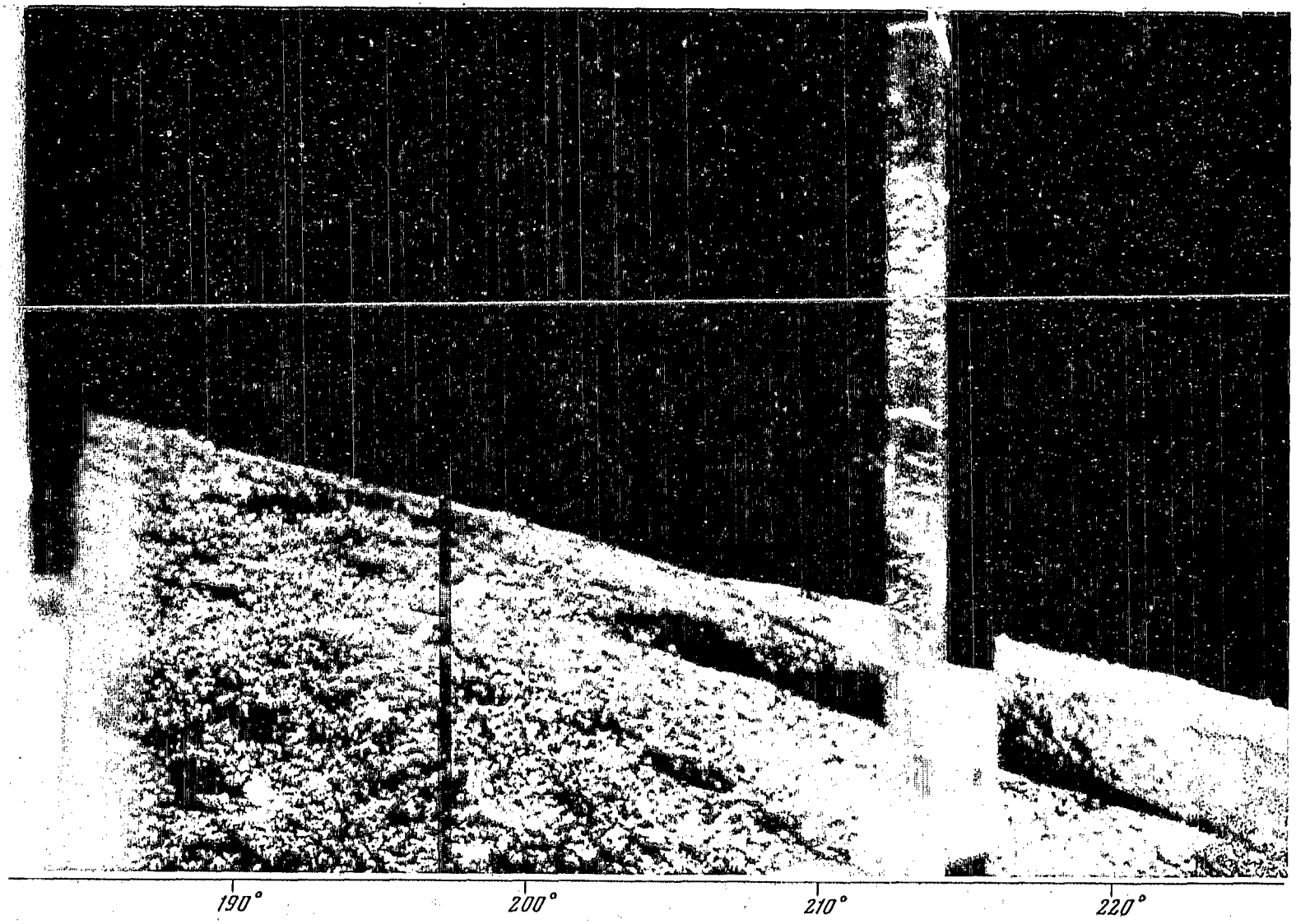

Panorama I, fragment 8

Panorama I, fragment 9

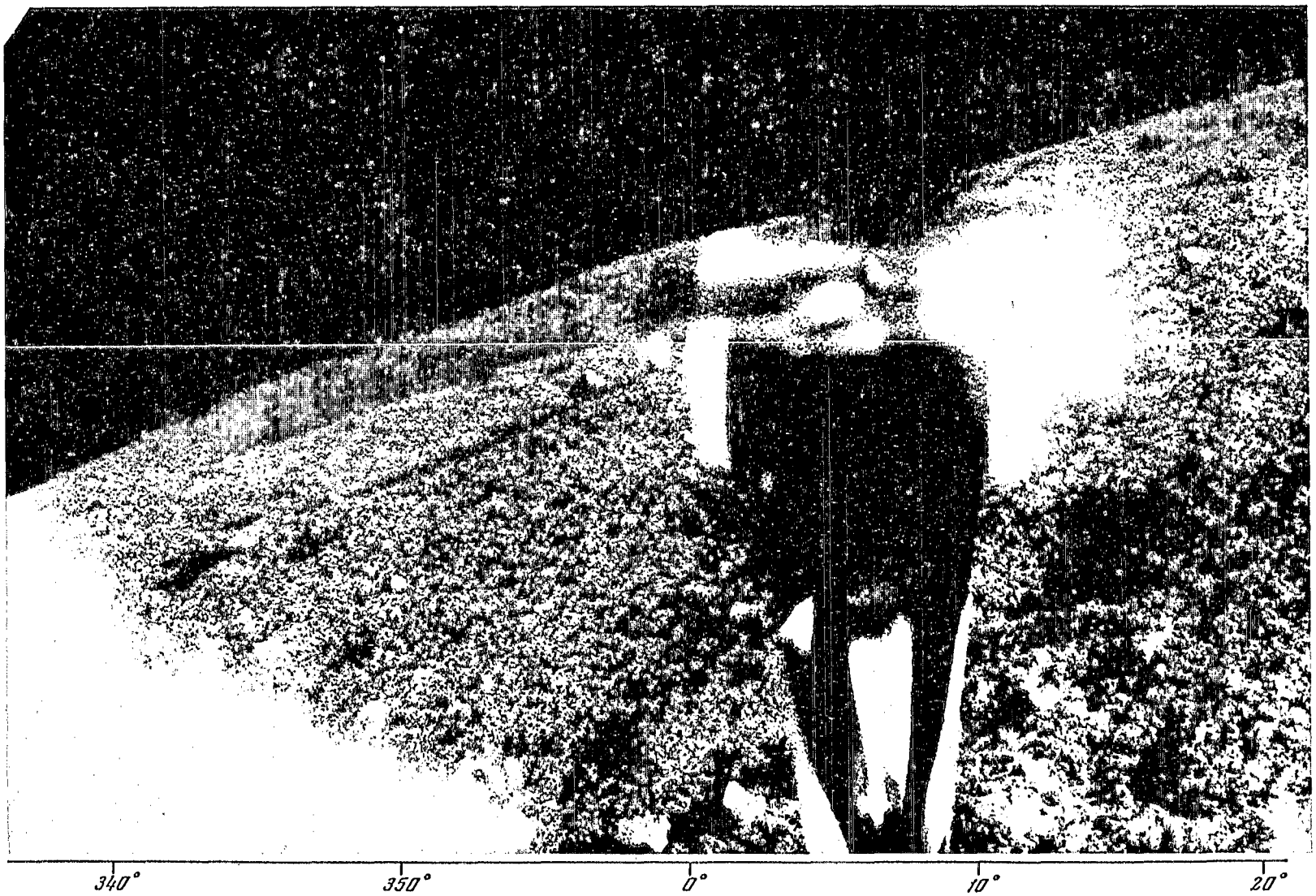

Panorama II, fragment 1

Panorama II, fragment 2

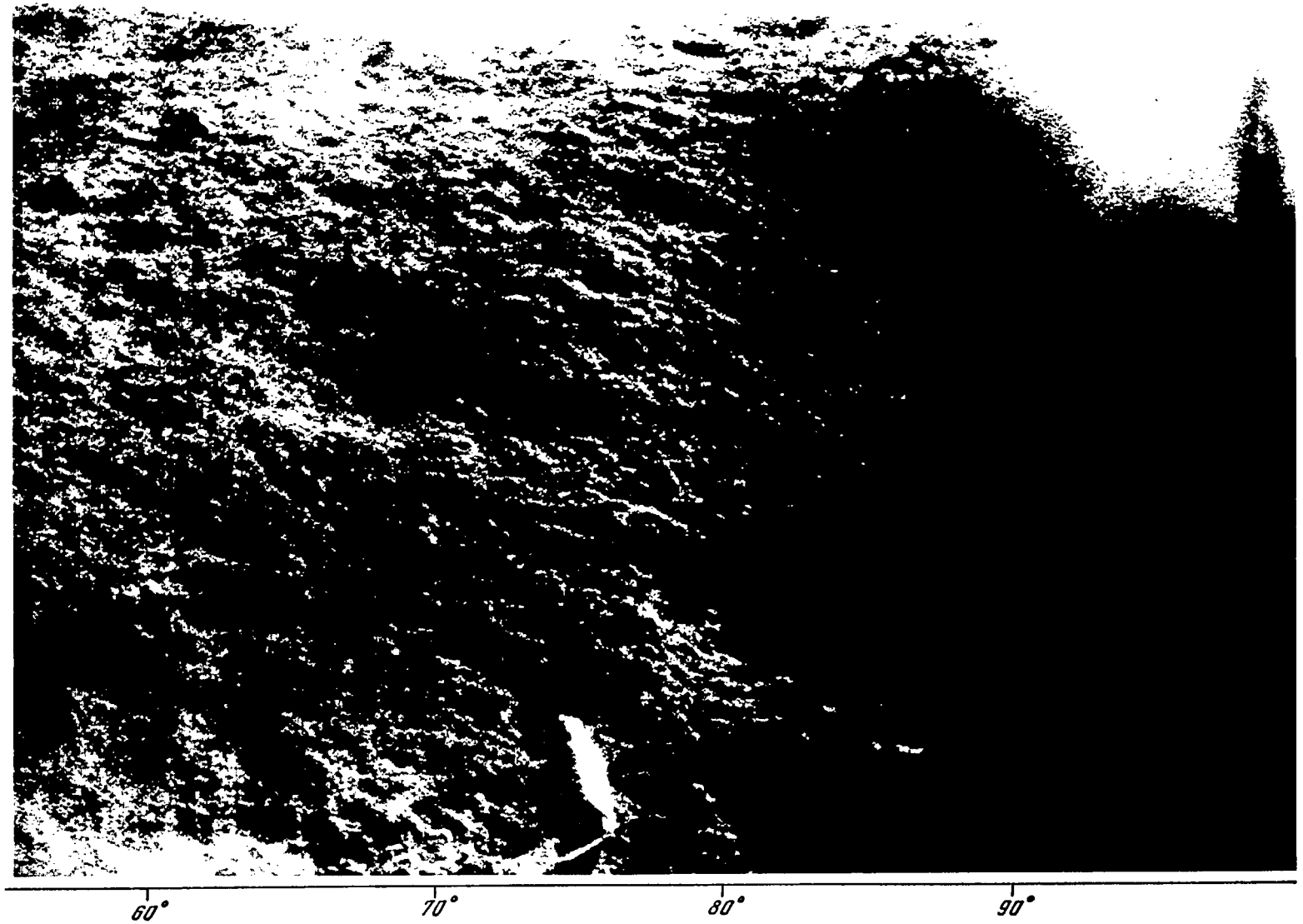

Panorama II, fragment 3

Panorama II, fragment 4

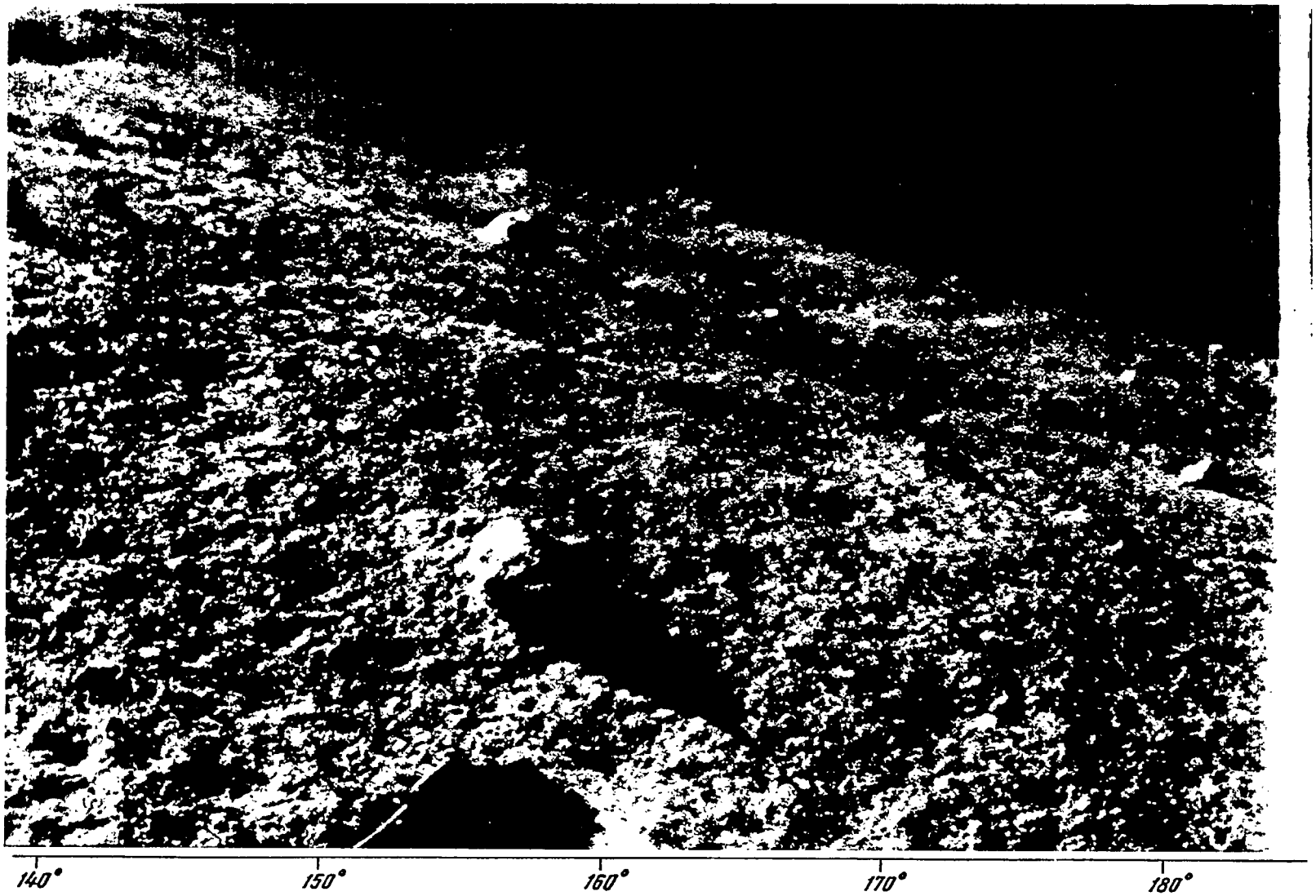

Panorama II, fragment 5

Panorama II, fragment 6

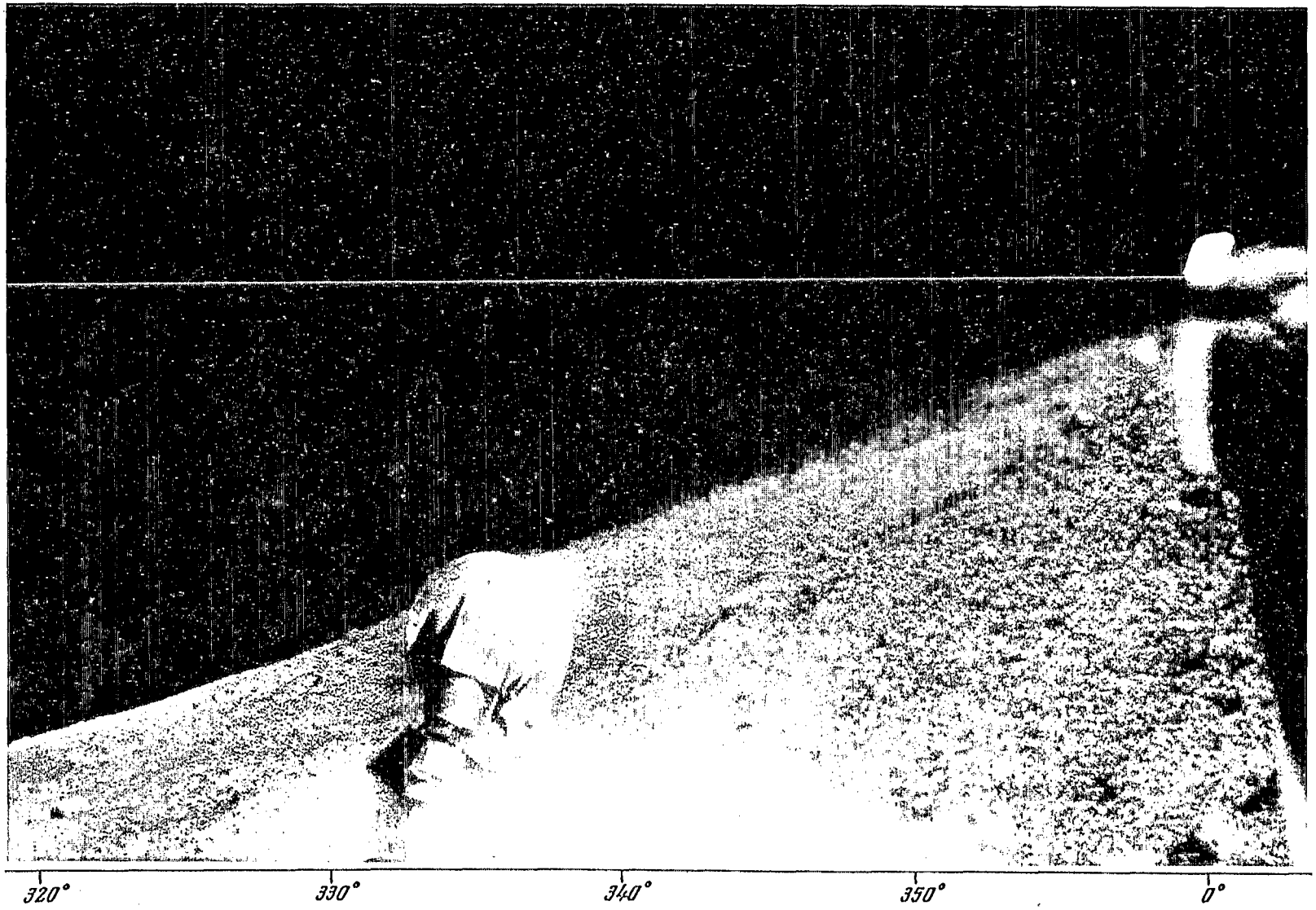

Panorama III, fragment 1

Panorama III, fragment 2

Panorama III, fragment 3

Panorama III, fragment 4

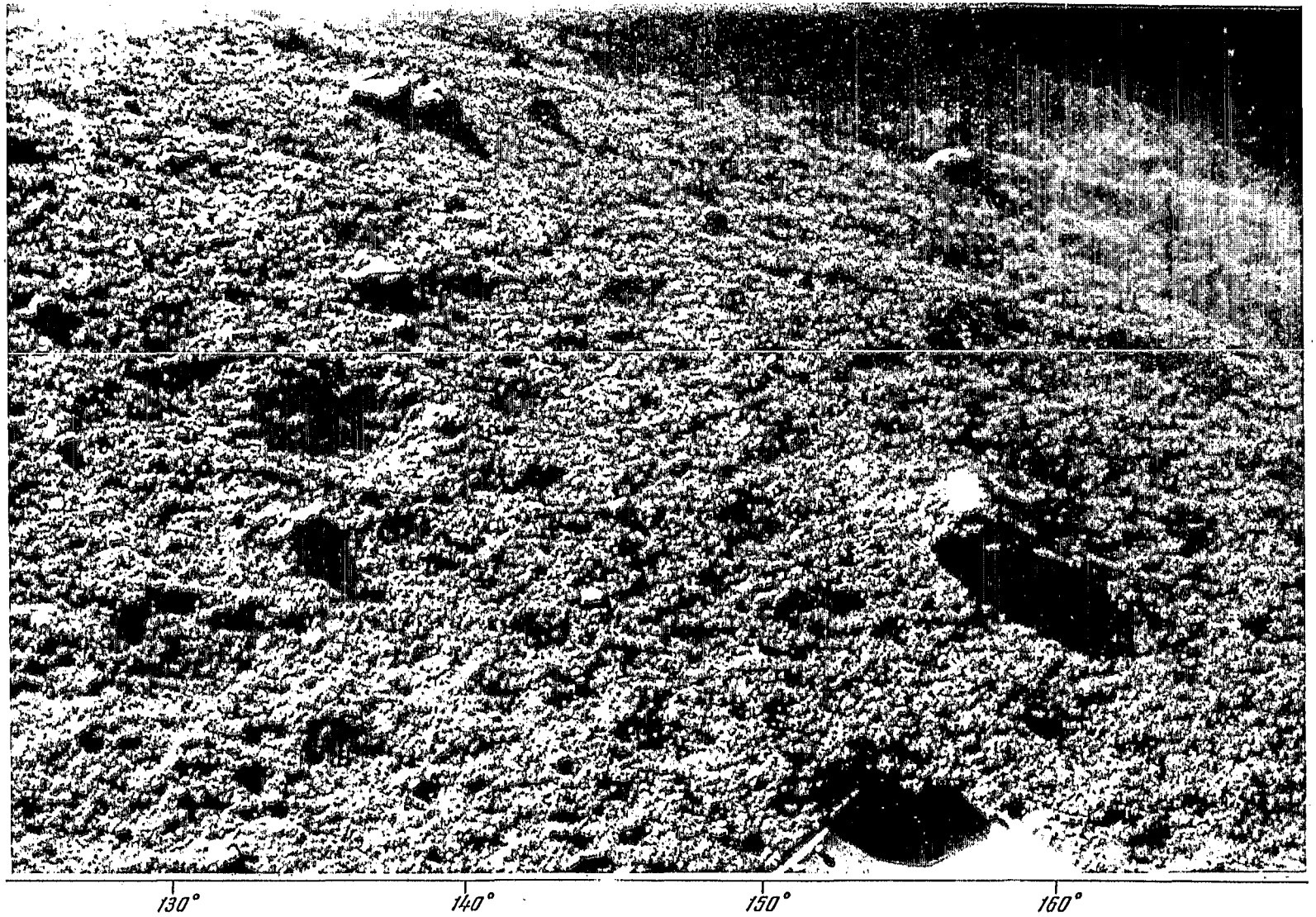

Panorama III, fragment 5

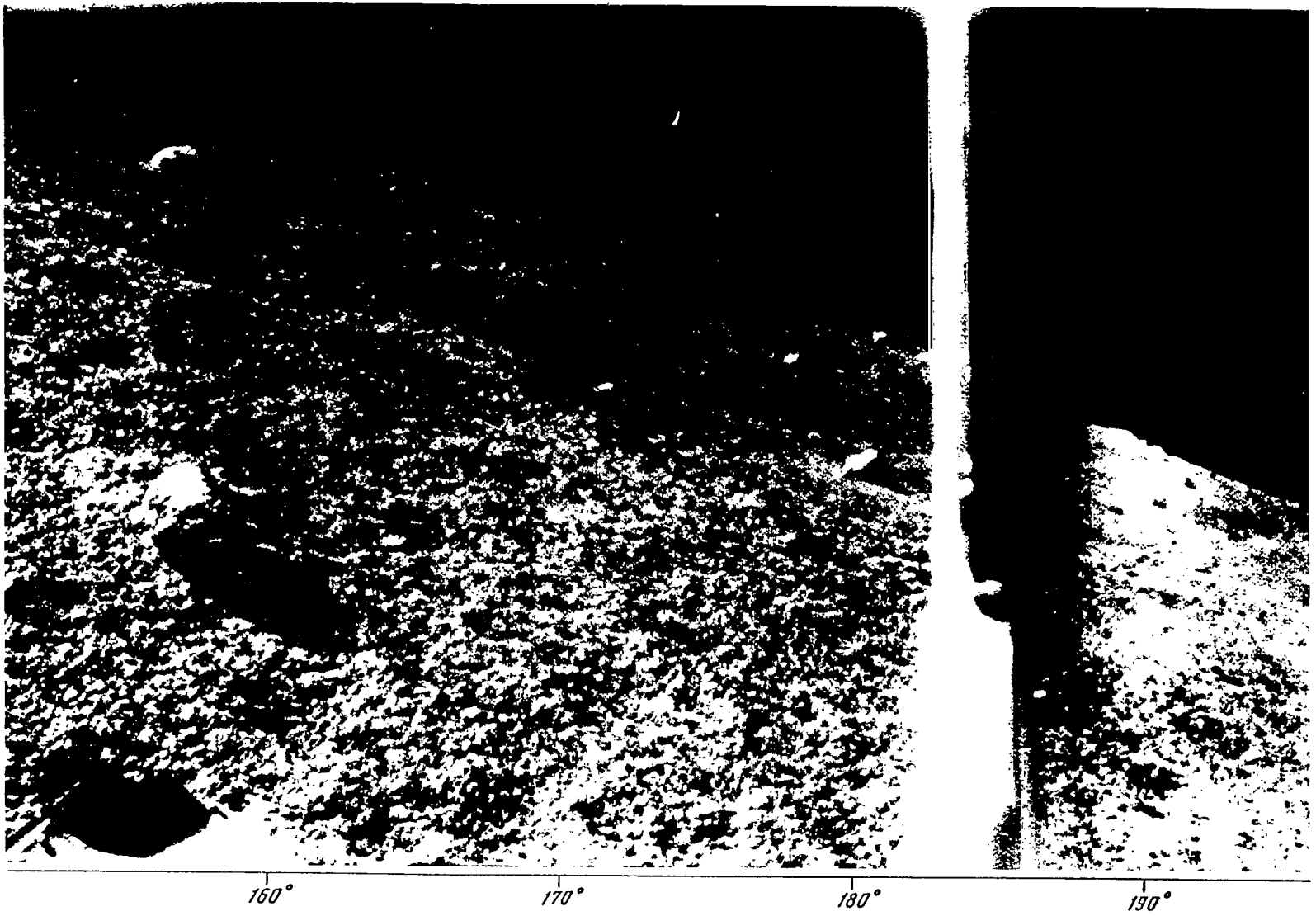

Panorama III, fragment 6

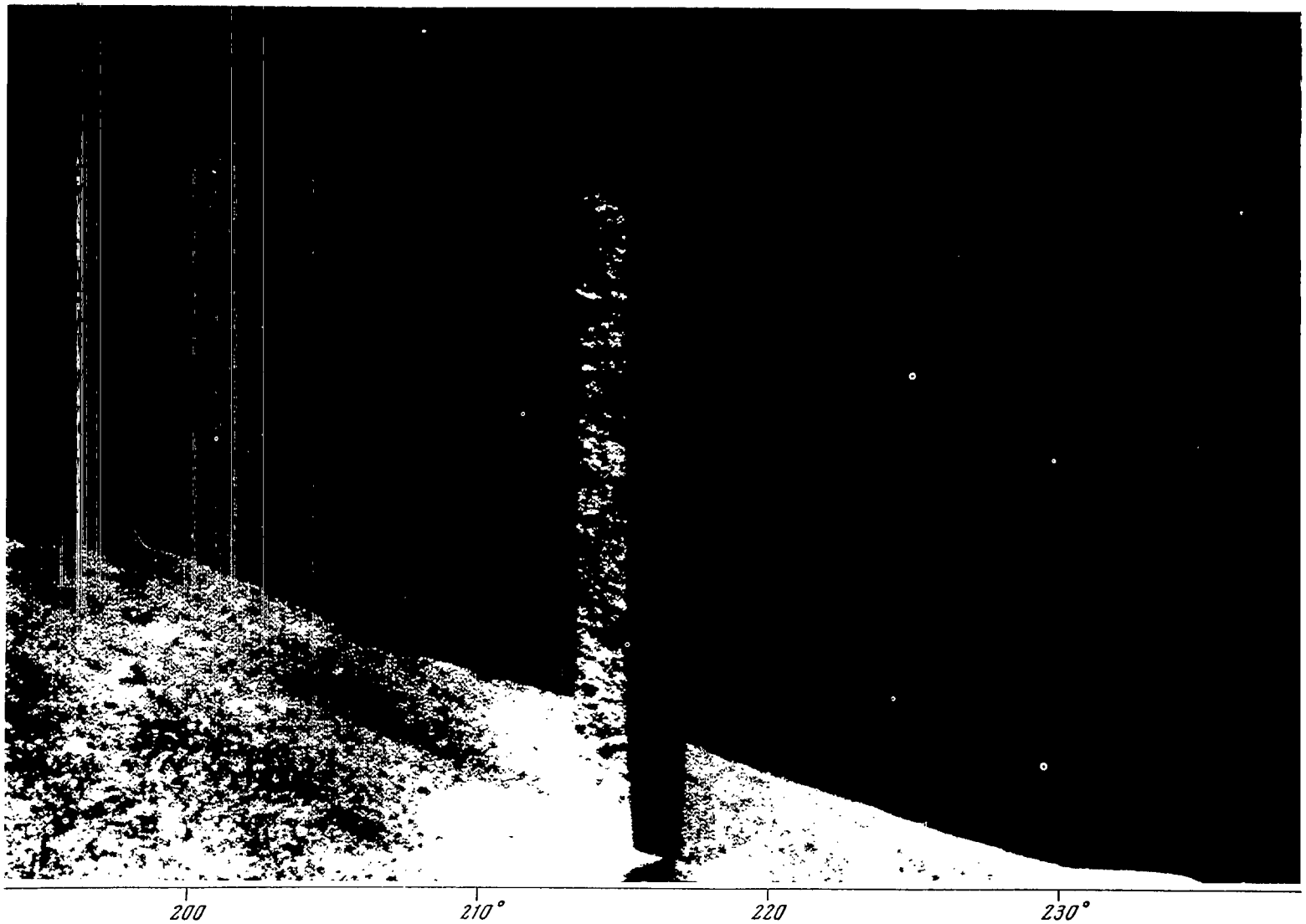

Panorama III, fragment 7

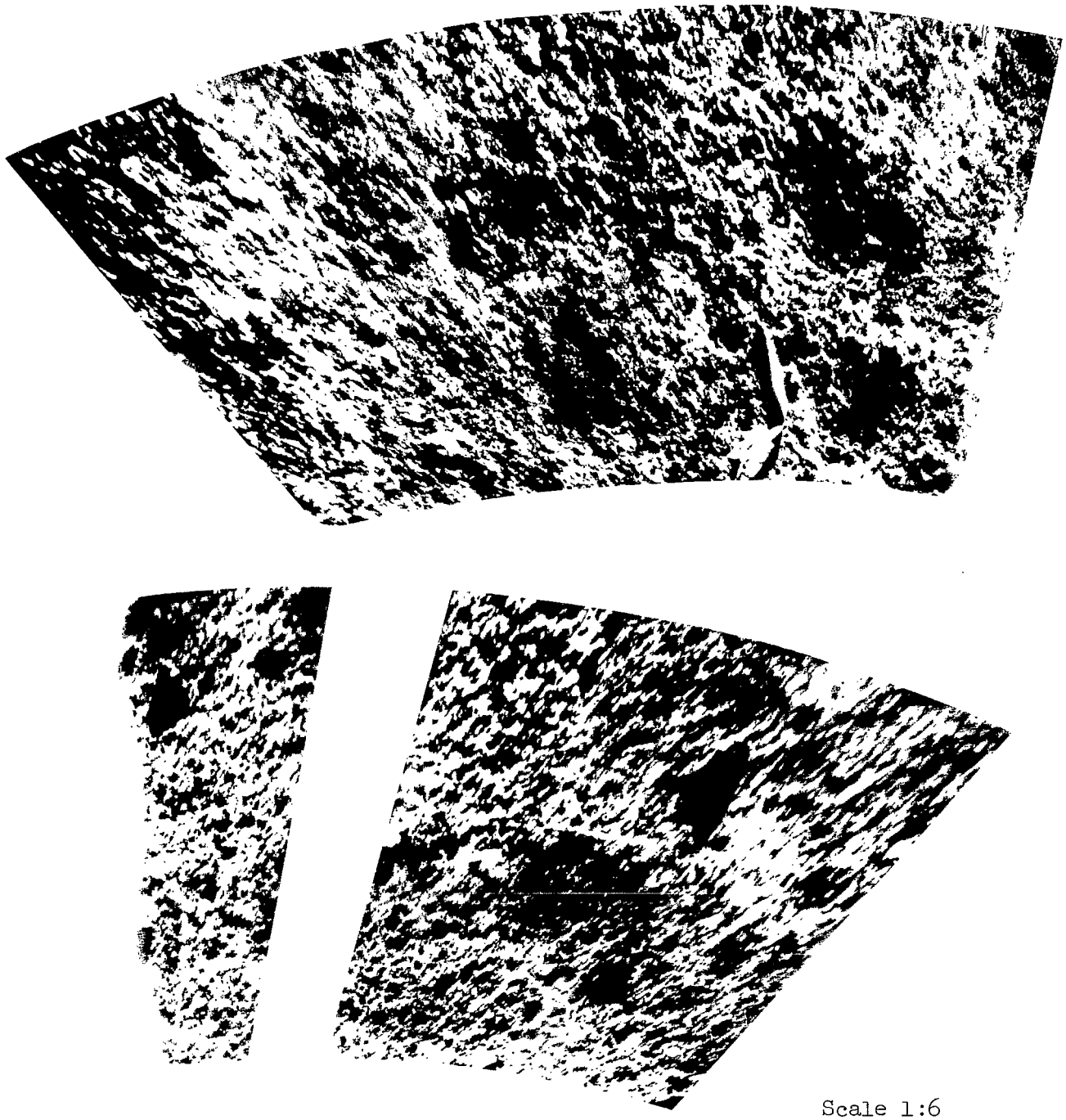

Scale 1:6

Transformed Photographs

Stereopair 1

Panorama II

Panorama III

Stereopair 2

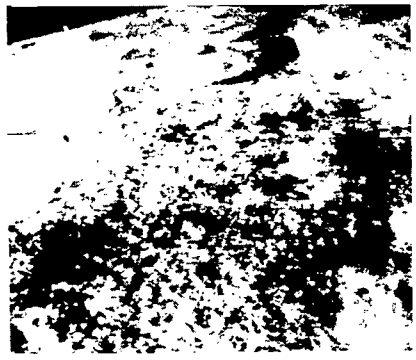

Panorama II

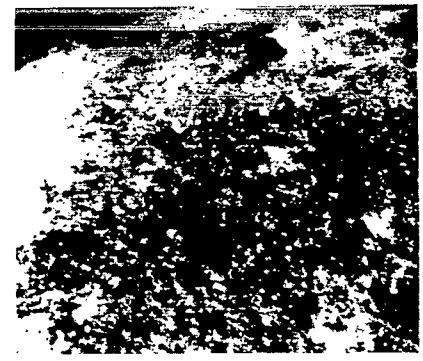

Panorama III

Stereopair 3

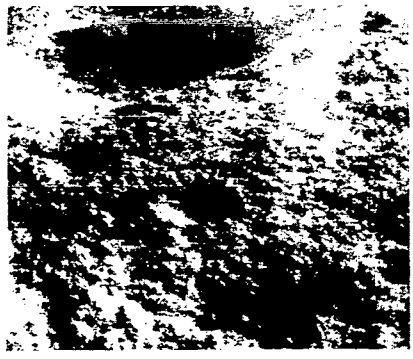

Panorama II

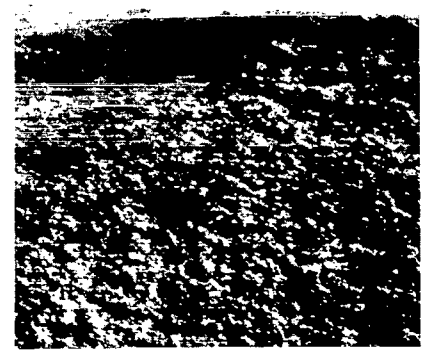

Panorama III

Stereopair 4

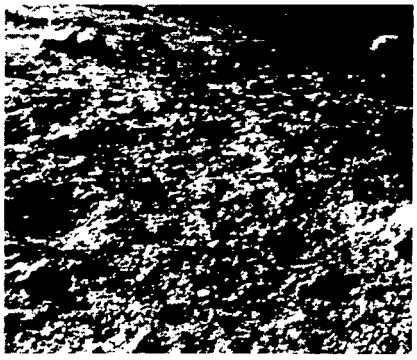

Panorama III

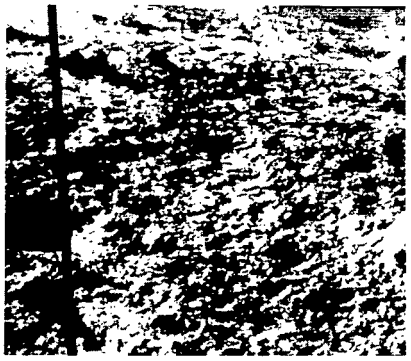

Panorama II

Stereopair 5

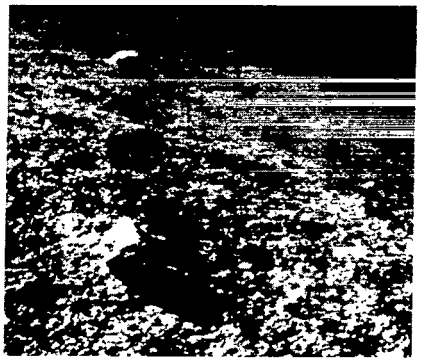

Panorama III

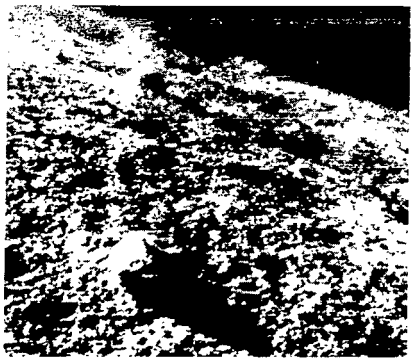

Panorama II

Stereopair 6

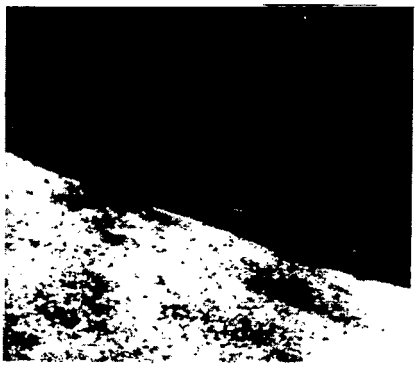

Panorama III

Panorama II

Stereopair 7

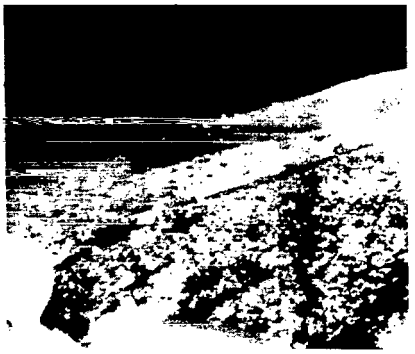

Panorama I

Panorama III

Stereopair 8

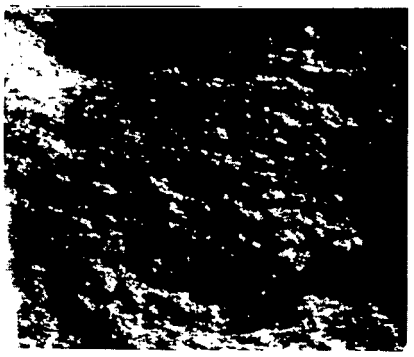

Panorama I

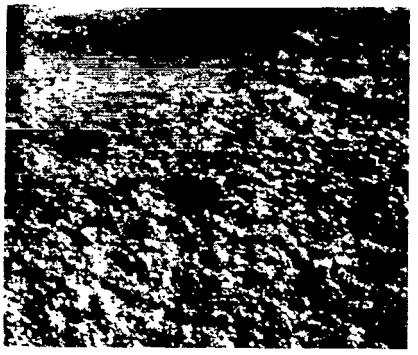

Panorama III

Stereopair 9

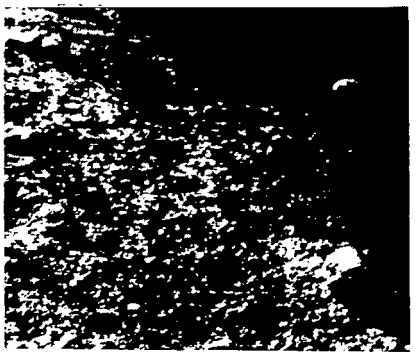

Panorama III

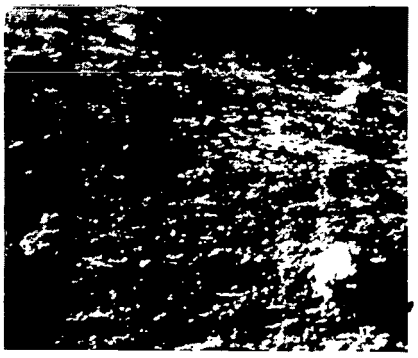

Panorama I

Stereopair 10

Panorama III

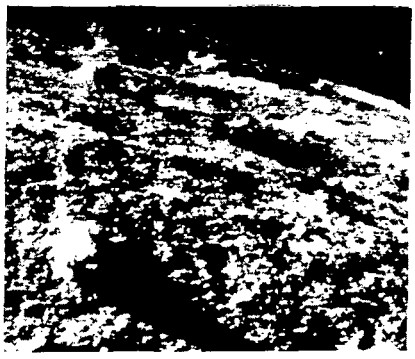

Panorama I

Stereopair 11

Panorama III

Panorama I

Stereopair 12

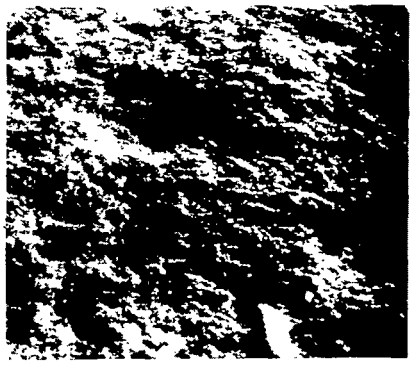

Panorama II

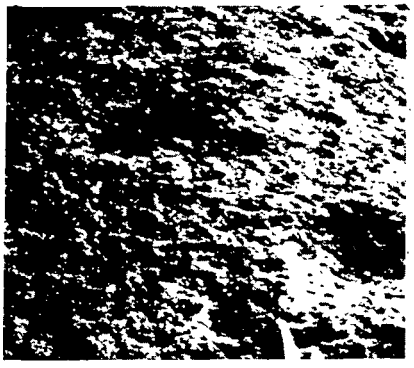

Panorama III

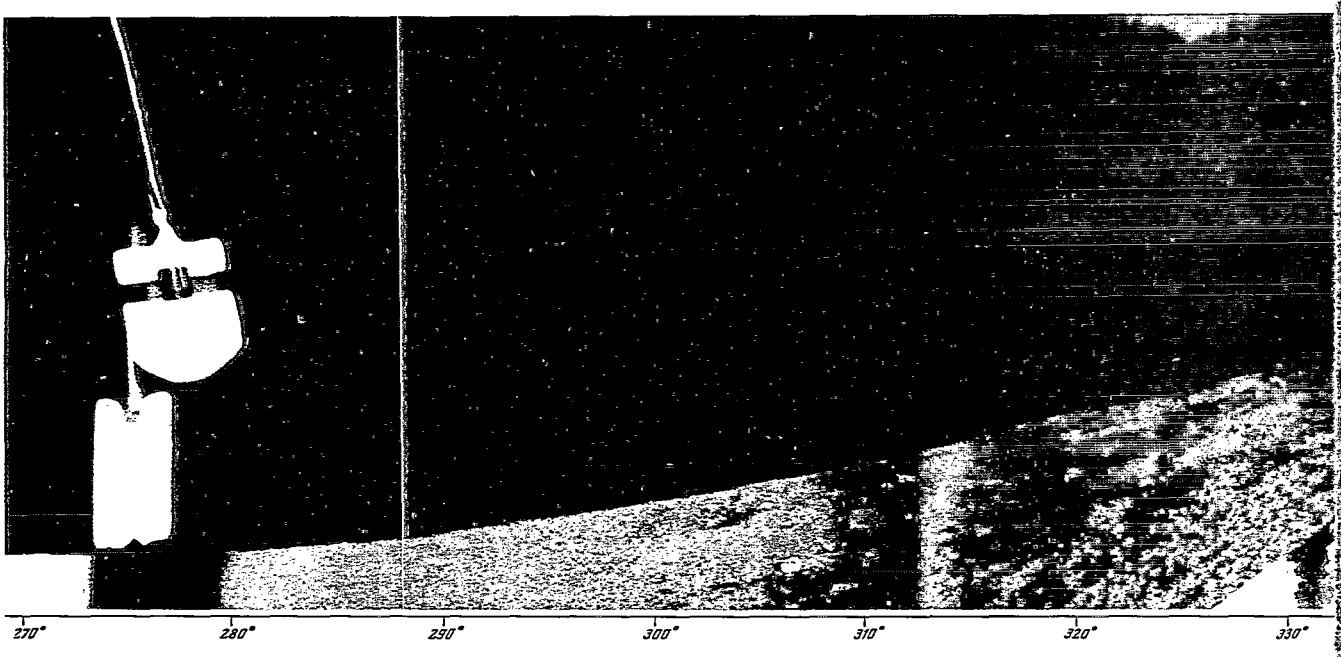

Panorama I

Panorama I

Panorama III

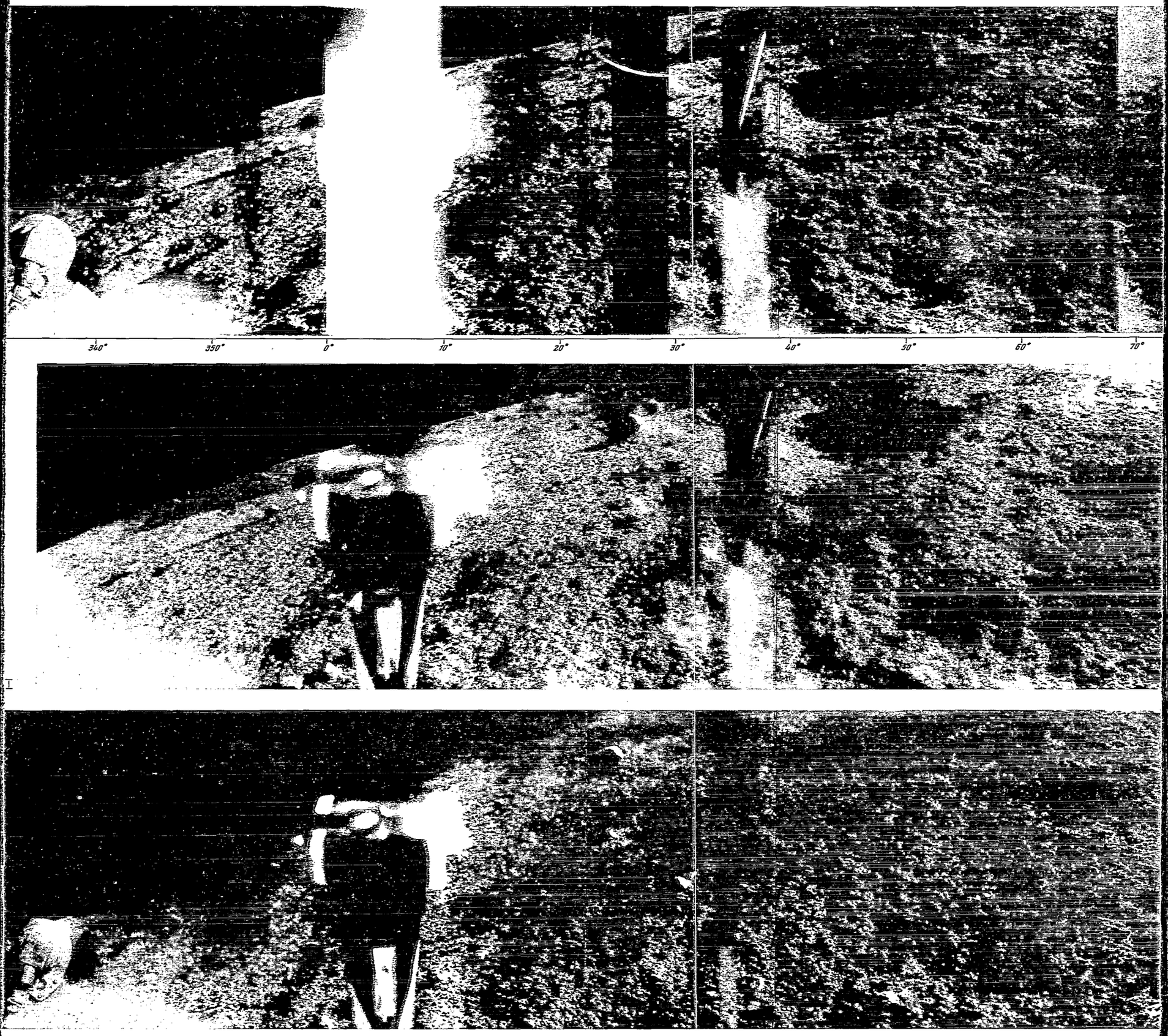
340°
350°
0°
10°
20°
30°
40°
50°
60°
70°

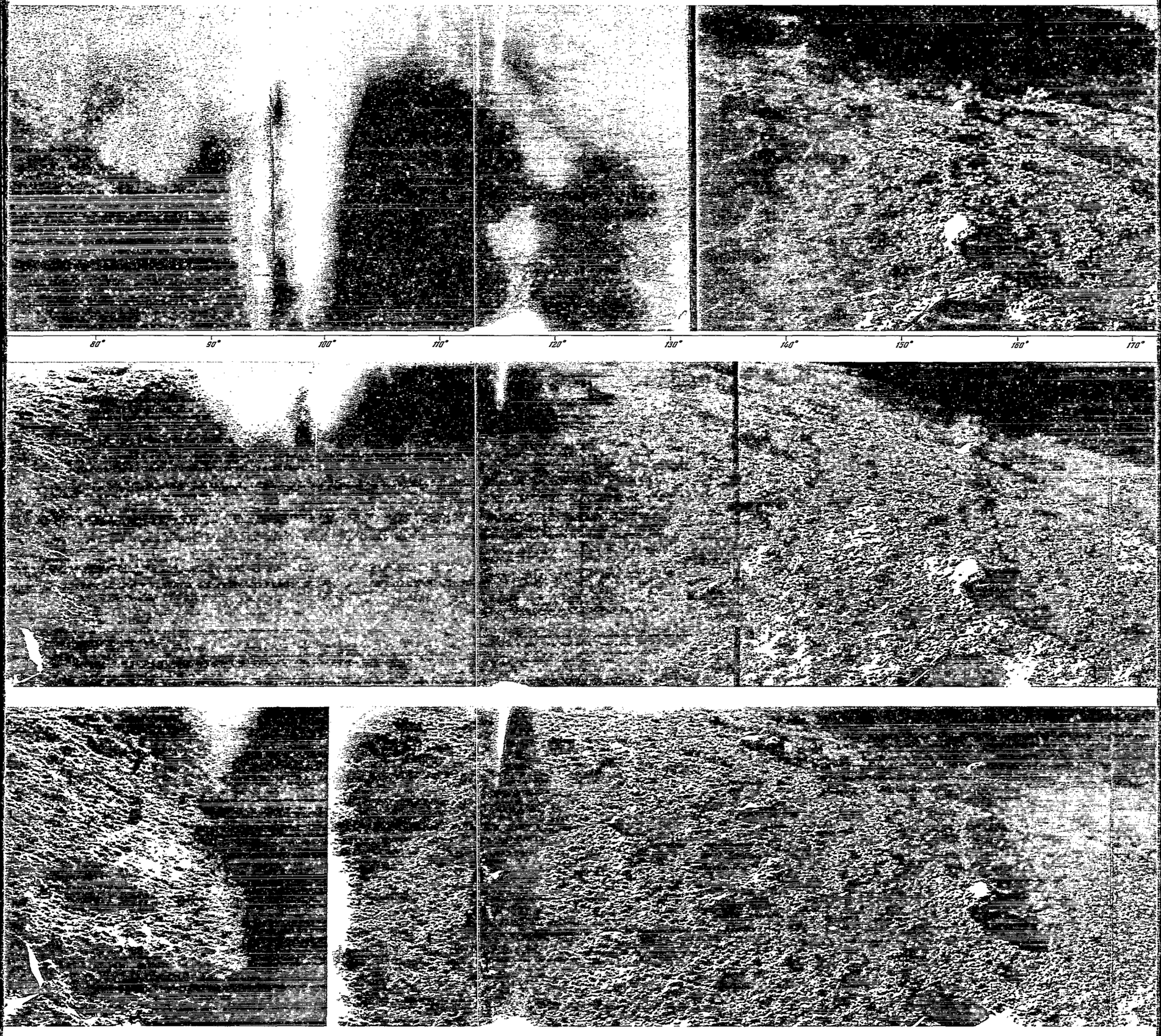
80°
90°
100°
110°
120°
130°
140°
150°
160°
170°

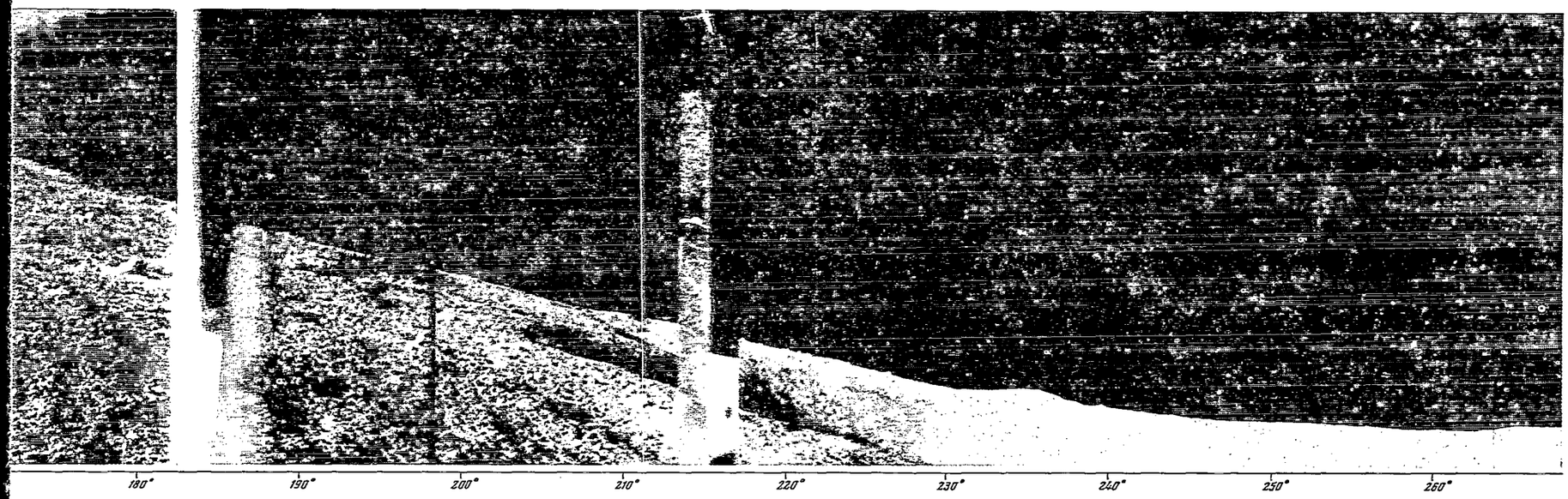
180°
190°
200°
210°
220°
230°
240°
250°
260°

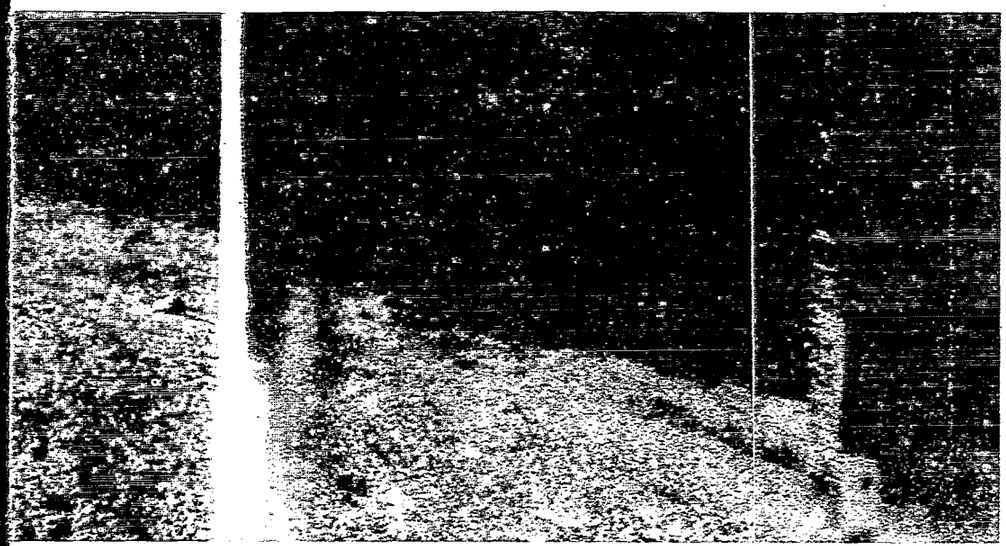

TOPOGRAPHIC PLAN OF LUNA 9 LANDING SITE

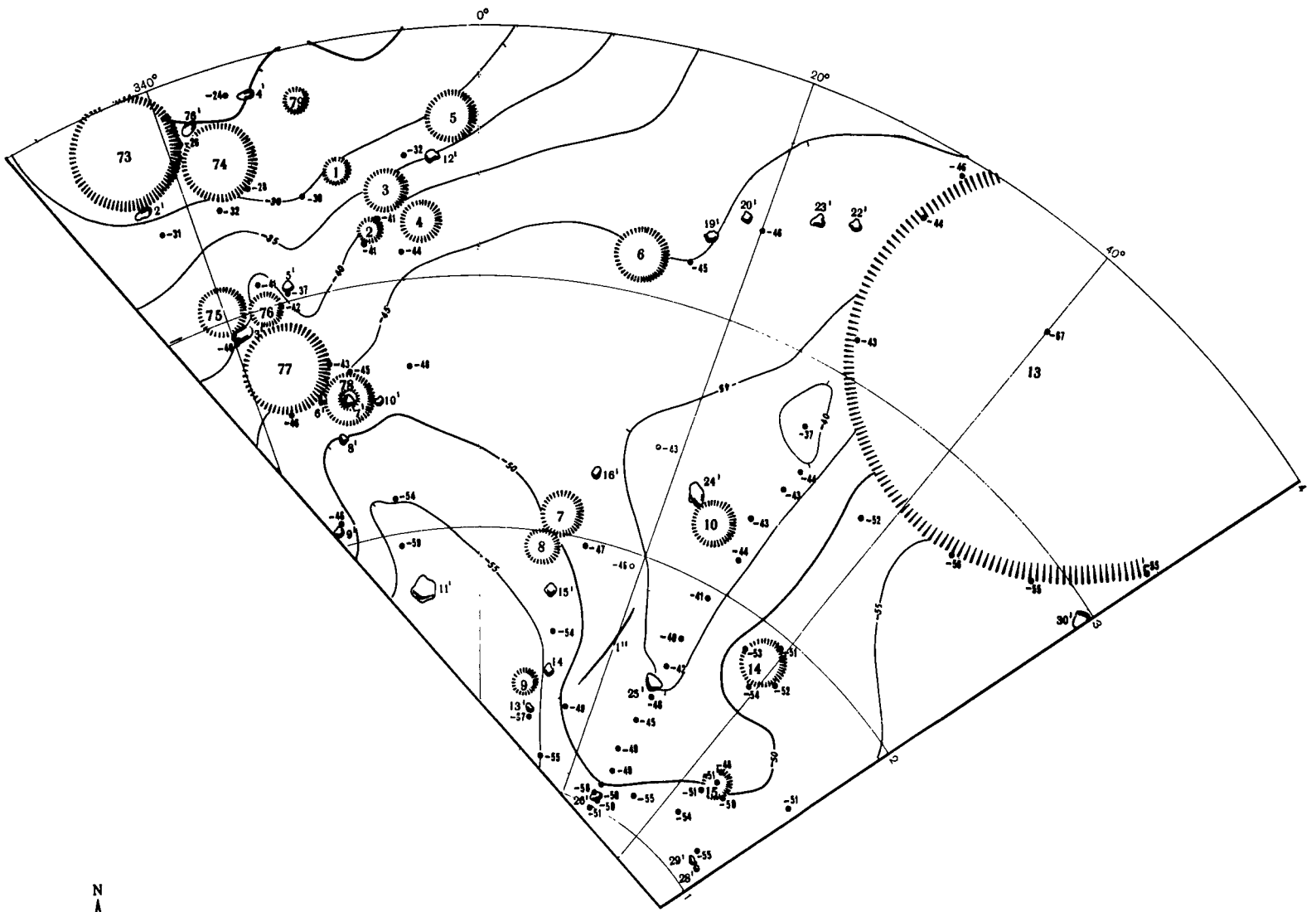

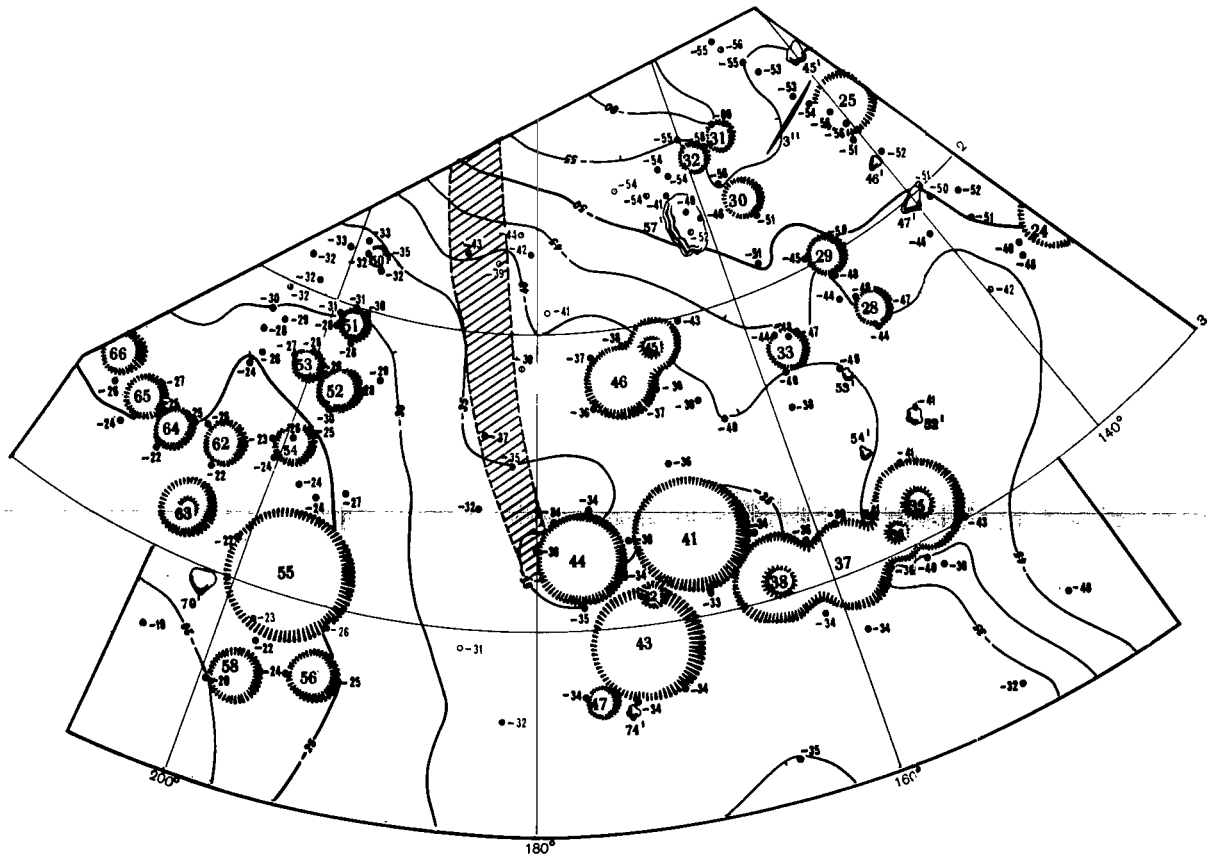

Symbols

- height (cm)
- horizontals
- craters
- rocks
- linear forms, microstratum
- distance lines (m)
- azimuth lines

Scale 1:20

0.5 0 0.5 1.0 m

Relief section for 5 cm
Altitude indications given
relative to center of
third panorama

Topographic plan constructed by Moscow Institute of Geodetic, Aerial Photographic and Cartographic Engineers in 1966 from materials obtained from Soviet automatic station Luna 9
4-5 February 1966

TOPOGRAPHIC DIAGRAM OF LUNA 9 LANDING SITE

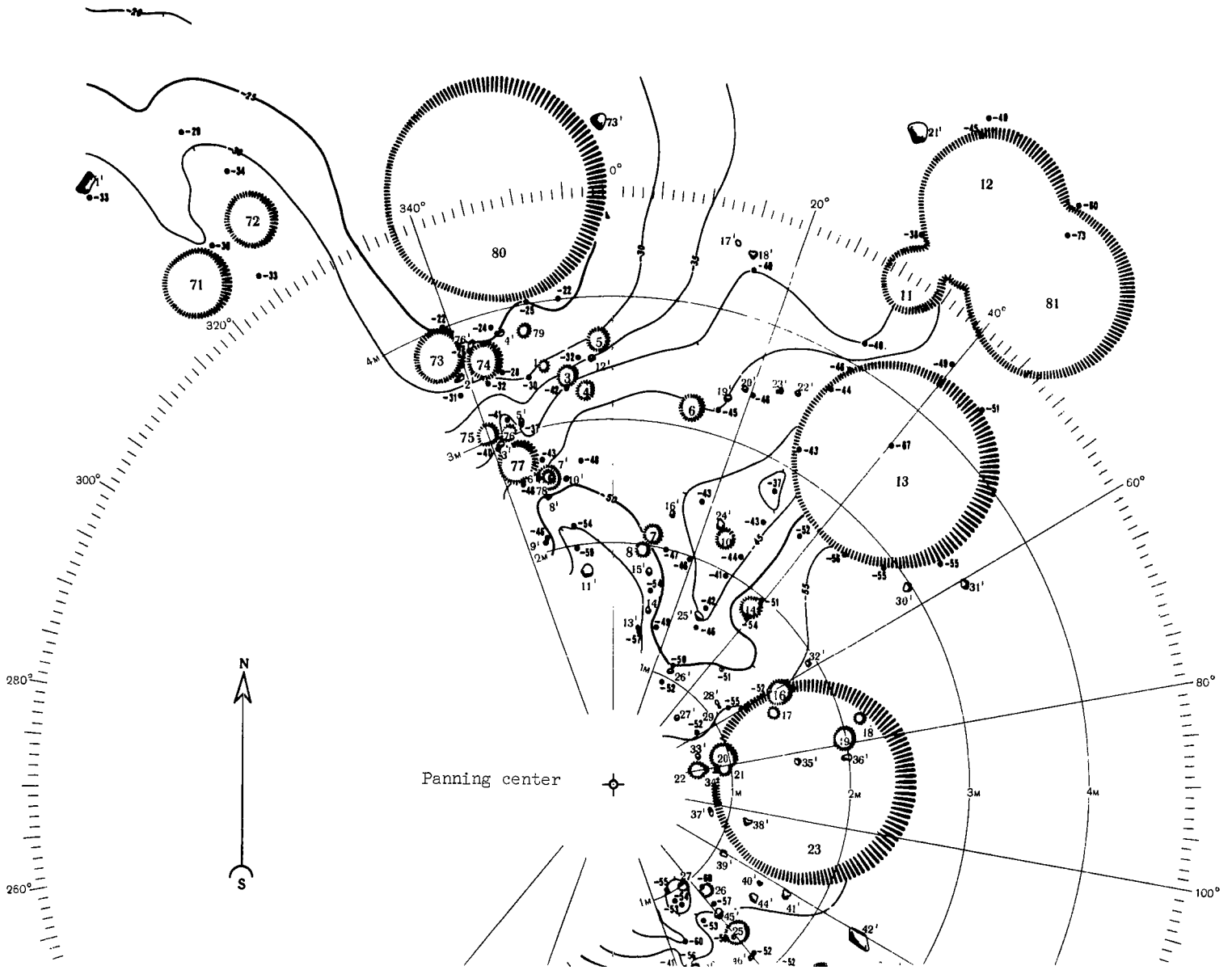

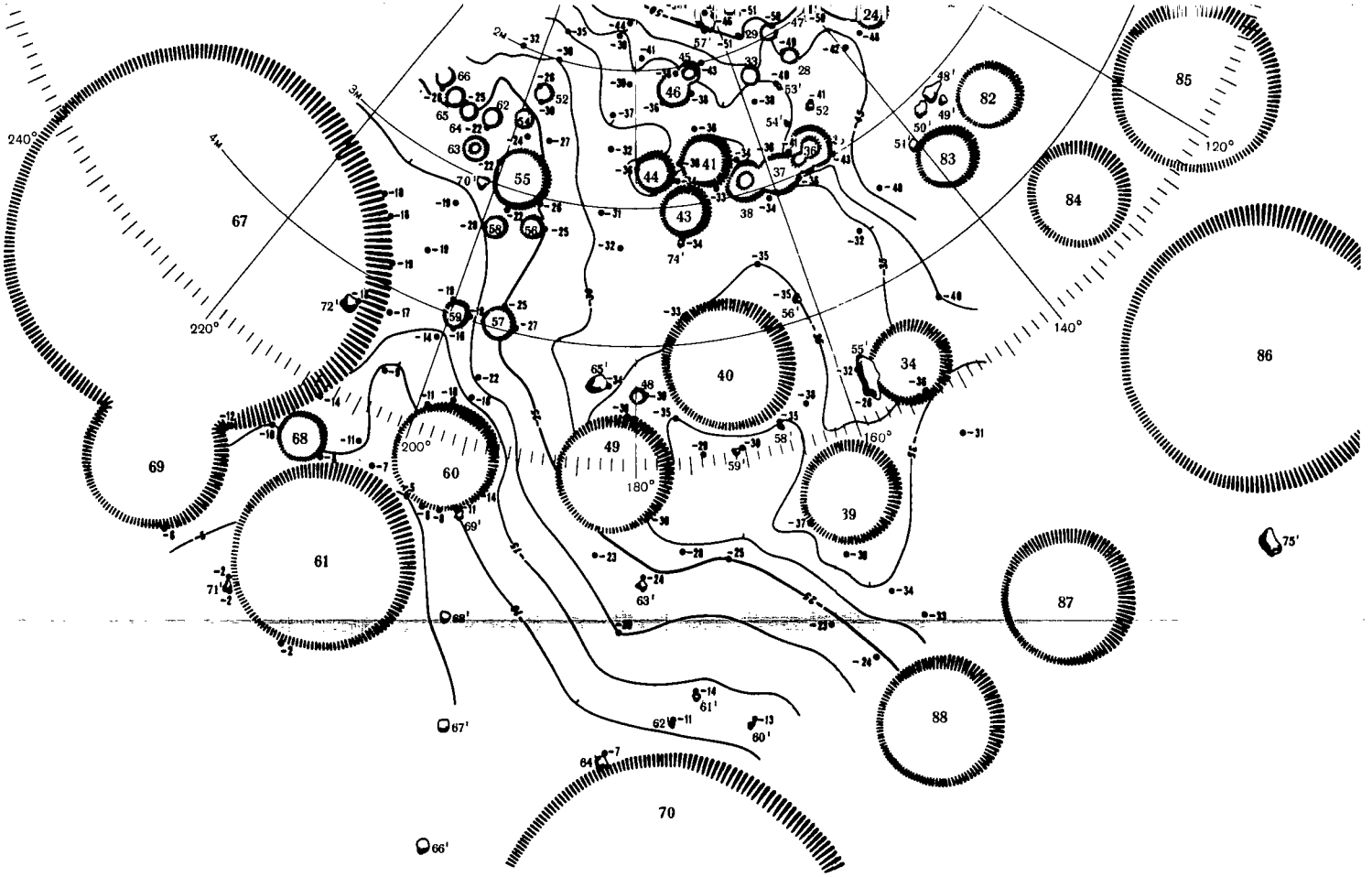

Symbols

- height (cm)
- horizontals
- craters
- rocks
- distance lines (m)
- azimuth lines

Scale 1:40

1 0 1 2 м

Relief section for 5 cm
Altitude indications given
relative to center of
third panorama

Diagram constructed by Moscow Institute of Geodetic, Aerial Photographic and Cartographic Engineers in 1966 from materials obtained from Soviet automatic station Luna 9 4-5 February 1966

"The aeronautical and space activities of the United States shall be conducted so as to contribute . . . to the expansion of human knowledge of phenomena in the atmosphere and space. The Administration shall provide for the widest practicable and appropriate dissemination of information concerning its activities and the results thereof."

—NATIONAL AERONAUTICS AND SPACE ACT OF 1958

NASA SCIENTIFIC AND TECHNICAL PUBLICATIONS

TECHNICAL REPORTS: Scientific and technical information considered important, complete, and a lasting contribution to existing knowledge.

TECHNICAL NOTES: Information less broad in scope but nevertheless of importance as a contribution to existing knowledge.

TECHNICAL MEMORANDUMS: Information receiving limited distribution because of preliminary data, security classification, or other reasons.

CONTRACTOR REPORTS: Technical information generated in connection with a NASA contract or grant and released under NASA auspices.

TECHNICAL TRANSLATIONS: Information published in a foreign language considered to merit NASA distribution in English.

SPECIAL PUBLICATIONS: Information derived from or of value to NASA activities. Publications include conference proceedings, monographs, data compilations, handbooks, sourcebooks, and special bibliographies.

TECHNOLOGY UTILIZATION PUBLICATIONS: Information on technology used by NASA that may be of particular interest in commercial and other nonaerospace applications. Publications include Tech Briefs; Technology Utilization Reports and Notes; and Technology Surveys.

Details on the availability of these publications may be obtained from:

SCIENTIFIC AND TECHNICAL INFORMATION DIVISION

NATIONAL AERONAUTICS AND SPACE ADMINISTRATION

Washington, D.C. 20546